

AD-A102 364

NAVAL RESEARCH LAB WASHINGTON DC  
NON-REAL TIME STRESS TESTS OF THE ANDVT HF MODEM. (U)  
AUG 81 W M JEWETT, R COLE  
UNCLASSIFIED

NRL-MR-4574

F/6 17/2

1 or 1  
AD A  
100-684



NI

END  
DATE FILMED  
9-81  
DTIC

AD 1100000004

111-10-11  
SECURITY CLASSIFICATION OF THIS PAGE (When Data Entered)

REPORT DOCUMENTATION PAGE		READ INSTRUCTIONS BEFORE COMPLETING FORM
1. REPORT NUMBER NRL Memorandum Report 4574	2. GOVT ACCESSION NO. AD-A 102 364	3. RECIPIENT'S CATALOG NUMBER
4. TITLE (and Subtitle) NON-REAL TIME STRESS TESTS OF THE ANDVT HF MODEM		5. TYPE OF REPORT & PERIOD COVERED Interim report on a continuing NRL problem.
6. AUTHOR(s) W. M. Jewett and R. Cole, Jr.		7. PERFORMING ORG. REPORT NUMBER
8. PERFORMING ORGANIZATION NAME AND ADDRESS Naval Research Laboratory Washington, DC 20375		9. PROGRAM ELEMENT PROJECT, TASK AREA & WORK UNIT NUMBERS 33401N; X0736-CC; 75-0126-0-1
10. CONTROLLING OFFICE NAME AND ADDRESS Naval Electronic Systems Command Washington, DC 20360		11. REPORT DATE August 1981
12. NUMBER OF PAGES 90		13. SECURITY CLASS. (of this report) UNCLASSIFIED
14. MONITORING AGENCY NAME & ADDRESS (if different from Controlling Office) 100 X 100 21 100 X 100 21		15a. DECLASSIFICATION/DOWNGRADING SCHEDULE
16. DISTRIBUTION STATEMENT (of this Report) Approved for public release; distribution unlimited.		
17. DISTRIBUTION STATEMENT (of the abstract entered in Block 20, if different from Report)		
18. SUPPLEMENTARY NOTES		
19. KEY WORDS (Continue on reverse side if necessary and identify by block number) ANDVT HF modems HF channels DPSK modulation Channel simulation		
20. ABSTRACT (Continue on reverse side if necessary and identify by block number) The performance of the signal design for the ANDVT HF modem was investigated for a large variety of Rayleigh fading channel conditions. The tests included the simulation of standard test channels proposed by CCIR, as well as a variety of tonal interference conditions. Data are presented on the performance obtained with error correction coding on a portion of the information in addition to the results for the uncoded information.		

DD FORM 1 JAN 73 1473 EDITION OF 1 NOV 65 IS OBSOLETE  
S/N 0102-014-6601

SECURITY CLASSIFICATION OF THIS PAGE (When Data Entered)

251900 34

## CONTENTS

1.0 INTRODUCTION .....	1
2.0 REVIEW OF ANDVT HF MODEM SIGNAL DESIGN .....	1
3.0 DESCRIPTION OF TESTS .....	3
4.0 TEST RESULTS .....	4
4.1 Effects of Peak Clipping .....	5
4.2 Bandpass Filtering .....	6
4.3 Tonal Interference with Gaussian Noise .....	6
4.4 Preamble Acquisition .....	8
4.5 Effects of Multipath Conditions .....	9
4.6 Performance on CCIR Channels .....	12
4.7 Performance on Consortium Channel .....	13
4.8 Performance on Rician Channel .....	14
5.0 CONCLUSIONS .....	14
REFERENCES .....	15

Accession For	
NTIS GRA&I <input checked="" type="checkbox"/>	
DTIC TAB <input type="checkbox"/>	
Unannounced <input type="checkbox"/>	
Justification	
By _____	
Distribution/ _____	
Availability Codes	
Dist	Avail and/or Special
A	

## NON-REAL TIME STRESS TESTS OF THE ANDVT HF MODEM

### 1.0 INTRODUCTION

Tests have been performed on a non-real time FORTRAN version of the high frequency (hf) modulator/demodulator (modem) [1, 2] for the Advanced Narrowband Digital Voice Terminal (ANDVT). The tests were performed using another FORTRAN program [3] designed to stress an hf modem over a wide range of propagation conditions, interference levels, transmission equipment characteristics, and operational scenarios.

The tests were limited to the operation of the ANDVT modem in the digital voice mode. In that mode, the hf modem design is tailored to the requirements of transmitting the encrypted data of a 2400 bit per second (bps) linear predictive encoder voice processor (LPC-10) in a half duplex, push-to-talk, hf net. The modem protects the most sensitive portions of the LPC data by applying a one-half rate error correction code to 44% of the data. The remaining 56% of the LPC data are transmitted without coding for error control.

Results are presented on the performance of the modem for a wide range of multiplicative forms of distortion (characteristic of Rayleigh fading multipath channels) and additive distortion produced by Gaussian noise and tonal interference (frequently encountered on hf channels). The modem was tested over specific simulated channels corresponding to the test channels recommended by the international CCIR organization [4], as well as other specific channels which have been used previously by the Naval Research Laboratory (NRL) [5, 6, 7]. All tests were performed with all functions in the demodulator active. These functions include the doppler and synchronization acquisition using the preamble and doppler and synchronization tracking using the data tones.

### 2.0 REVIEW OF ANDVT HF MODEM SIGNAL DESIGN

The following is a brief description of the ANDVT hf modem signal design as specified for the tactical terminal (CV-3591). This equipment will provide a secure voice capability to military users who must operate over bandwidth-limited circuits. The standard operational mode is half duplex hf net operations, where several parties transmit and receive on a common rf assignment and use a common COMSEC key variable for encryption. In the net mode, each transmission is preceded by a modem preamble and a COMSEC system preamble or message indicator (MI). Thus, the hf modem signal consists of three principal parts which are transmitted sequentially with each transmission, as shown in figure 1.

The purpose of the modem preamble is to establish the synchronization and frequency adjustments necessary to permit half duplex communications between two independent stations using single sideband hf radio equipment. In addition, the modem preamble establishes an epoch denoting the beginning of the system preamble.

Following the modem preamble, there is the transmission of the MI plus a mode control word. The unencrypted mode control word is used by the modem receiver to identify the informational mode; i.e., digital voice or one of the special data modes.

Manuscript submitted April 14, 1981.

The third principal part of each transmission is the digital voice message.

The hf modem preamble is divided into three parts as shown in figure 2. Part one consists of the transmission of four unmodulated tones that are spaced 675 Hz apart. This signal is used by the modem receiver for initial frequency/doppler correction. The transmission lasts for 24 frame periods at 75 frames/second, which is 0.32 seconds. Four tones are transmitted for the doppler preamble to provide for operation in a frequency selective fading channel. The transmitted signal permits an unambiguous frequency correction for frequency errors less than  $\pm 168.75$  Hz.

The doppler tones are followed by a transmission of three tones which are also spaced 675 Hz apart. These tones are biphase modulated ( $\pm\pi/2$ ) at the 75 baud frame rate. They are used by the modem receiver to acquire frame synchronization. The transmission lasts for eight frame periods, which is approximately 0.107 seconds. The three tones provide redundancy for operation in a frequency selective fading channel. They are interleaved between the four doppler tone assignments to provide maximum frequency diversity.

The last part of the modem preamble consists of the transmission of a 240 bit PN sequence by biphase modulating 16 tones which are spaced 112.5 Hz apart. This 240 bit sequence comprises 16 repetitions of a 15 bit PN sequence. The transmission of the 240 bits requires 15 frame periods. It is preceded by one frame with random phases on the 16 tones to serve as a phase reference for DPSK demodulation of the first frame of the PN sequence. The PN sequence is used by the modem receiver to identify the start of the COMSEC system preamble.

The COMSEC system preamble consists of a four-bit mode control word plus the MI, which can have a maximum length of 124 bits. These data are combined into one 128 bit word which is encoded for error control with a (252, 128) BCH code. That is a (255, 131) BCH code that has been shortened by three bits. The 252 bit code word is transmitted eight times; therefore, the total transmission is 2016 bits. The modem format is the same 16 tones that were used for the PN sequence, but the modulation is 4-phase DPSK. The transmission lasts for 63 frame periods, which is 0.84 seconds. The eight order diversity is a combination of both time diversity and in-band frequency diversity, as each pair of bits (dibits) is transmitted on eight separate DPSK tones with each transmission separated in time by eight frame periods (approximately 0.107 seconds).

The hf modem modulation format for digital voice is four-phase DPSK on 39 tones which are spaced 56.25 Hz apart. The frame rate is 44.444 frames/second, corresponding to the frame rate of the LPC-10. With four-phase modulation on 39 tones at 44.444 frames/second, the transmission rate 3466.666 bps. This is 1066.666 bps in excess of the 2400 bps information rate of the voice processor. This redundancy is inserted into the transmitted signal by the modem after encryption to protect the most sensitive data bits.

The redundancy is obtained by selecting 24 bits out of each encrypted 54 bit LPC-10 frame and encoding them with a (24, 12) error correction code. The (24, 12) code is the (23, 12) Golay code with an overall parity bit. Figure 3 shows which bits in each frame are selected for coding.

Two Golay code words are formed and they are combined to produce 24 dibits. The remaining 30 information bits, which are not coded, are formed into 15 dibits. Thus, in each frame period, there are 24 dibits of coded information and 15 dibits of uncoded information, which are used to phase modulate 39 tones. Figure 4 illustrates this division of data into coded and uncoded bits and their assignment to selected tones. Each frame period, the assignment of tones to dibits is permuted to spread the effects of narrowband frequency selective fading, narrowband interference, and poor frequency response of transmission filters. The permutation rule is an addition of five (modulo 39) to each tone/dabit assignment.

The decoding capabilities of the Golay code are increased by using a soft decision decoding algorithm [8]. The algorithm consists of making multiple trials at decoding the received information, using estimates of the most likely error patterns.

The hf modem remains in the digital voice net mode until it detects loss of signal for five successive frames. At that time it reverts back to a search for modem preamble. There is no recovery from a loss of signal for a period longer than five frame periods (0.1125 seconds).

Figure 5 is a summary of the principal characteristics of the hf modem in the digital voice mode.

### 3.0 DESCRIPTION OF TESTS

Non-real time stress tests of the hf modem were performed in three steps as depicted in figure 6. In step one a FORTRAN version of the hf modulator was used to generate a digital file of the sampled output of the modulator for the condition that the input data was a 2047 bit pseudo-random noise (PN) sequence. The sampling rate was 7200 Hz. In step two the stress program operated on that data file to generate a second file representing the sampled received audio signal. The final step was the demodulation of the received signal and the analysis of the demodulator performance.

Figure 7 is a simplified block diagram of the functions performed by the stress program. The stress condition for a particular test was established by a table of variables, which could be modified easily prior to the starting of each test. The normal order in which the stress functions were performed is shown in figure 7, although it was possible to bypass any of the functions. Tests to date have not involved the simulation of pulse noise nor the simulation of a receiver automatic gain control (AGC).

The range of propagation conditions which were simulated consisted of:

- Four CCIR skywave channel models, representing good, moderate, poor, and flutter fading conditions [4].
- One U.S. Secure Voice Consortium skywave channel model, representing a perturbed condition [5].
- Extreme skywave channel models which stress the modem with multipath differential time delays up to 7.0 ms and doppler frequency spreads up to 5.0 Hz.

- A combined skywave and groundwave model (Rician), representing operation at extended line-of-sight (ELOS) ranges.
- A groundwave channel model consisting of a non-fading signal with additive noise and non-fading interference.

The types of noise and interference that were simulated consisted of:

- Gaussian noise, white over 3600 Hz bandwidth.
- Wideband frequency shift keyed (FSK) interference, representing a single 75 baud randomly keyed signal with an 850 Hz frequency shift.
- Narrowband FSK interference, representing either one or sixteen 75 baud randomly keyed signals, spaced 170 Hz apart, with 85 Hz frequency shift.
- Narrowband differential phase shift keyed (DPSK) interference, representing sixteen 75 baud randomly keyed tones with four phase modulation.
- A continuous wave (CW) unkeyed tone.
- A CW tone swept with a sawtooth wave, with the frequency range and sweep rate independently specified.

Extreme transmission equipment characteristics were simulated by selection of transmitter and receiver filters which provided severe attenuation at the band edges of the hf modem signal set, and by introducing frequency translation errors representing a radio frequency equipment with poor frequency control.

#### 4.0 TEST RESULTS

The test results reported here are divided into two general categories. First, results are presented on the performance of the modem as a function of a given parameter. Those parameters may be summarized as:

- Gaussian noise level
- use of peak clipping at the modulator output
- use of extreme filtering of the modem signal
- tonal interference, with Gaussian noise
- doppler acquisition for different frequency translation errors, with Gaussian noise
- performance of modem preamble and COMSEC system preamble with Gaussian noise
- effects of a wide range of multipath propagation conditions where

the variables are the number of paths, relative amplitudes of the paths, and doppler frequency spread.

The second category of test results are the modem performance for specific "Standard" channel conditions, i.e., the CCIR channel models, the consortium channel model, and a Rician channel model. Data are presented for the performance of the modem on these channels, both with and without tonal interference.

#### 4.1 Effects of Peak Clipping

The hf modem signal design is based on the simultaneous transmission of multiple tones. The number of tones may be either 3, 4, 16, or 39 depending on the operational state. The result is that the composite waveform from the modulator may vary considerable in its peak voltage and rms voltage characteristics. Therefore, some peak clipping of the 16 tone signal and the 39 tone signal is done prior to the digital-to-analog conversion in order to generate signals that have nearly uniform peak-to-rms voltage characteristics.

Table 1 shows the rms signal level and the peak-to-rms ratios for each of the four signal states, for clipping levels of 0, 8, and 9.5 dB. No clipping is applied to the 3 tone and 4 tone signals. The result is that with 8 dB of clipping on the 16 tone signal and 9.5 dB of clipping on the 39 tone signal, the composite waveform for all four states have relatively uniform peak-to-rms characteristics.

The disadvantage of peak clipping of the data tones is that it produces noise within the signal bandwidth. The result is a degradation in performance for a given S/N ratio, where S includes the noise due to the distortion products and N is the external additive noise. This is shown in figure 8, which is a plot of the bit error rate in the 39 tones versus the signal-to-noise density ratio ( $P/N_0$ ). P is the total power of the signal and distortion products and  $N_0$  is the noise density of the additive Gaussian noise. Data are shown for the case where no clipping is used and where the 39 tones are clipped 9.5 dB. The data are further divided to show the bit error rate on the 30 bits of uncoded data and the bit error rate on the 24 bits of coded data. It may be seen from these data that 9.5 dB of peak clipping results in approximately a one dB degradation in the bit error rate of the coded data at an error rate of  $1 \times 10^{-3}$ , and a degradation of approximately 2 dB on the uncoded data for the same bit error rate.

Peak clipping is advantageous when the modulator must work into a peak power limited amplifier, such as normally encountered in single sideband hf transmitters. Figure 9 shows the same comparison as was shown in figure 8, except that now the signal with peak clipping has the same peak power as the signal without clipping. It may be readily seen from these data that, for the bit error rates of interest for digital voice, peak clipping provides a significant advantage. In order to maintain that advantage it is necessary that the filters in the equipments between the digital-to-analog converter and the rf power amplifier have good phase response. A non-linear phase response will result in an increase in the peak-to-rms ratio of the signal, thus reducing the advantage sought.

In the remaining data of this report the 16 tone signal has been clipped 8.0 dB and the 39 tone signal has been clipped 9.5 dB. If these data are used to compare with any other data it must be done on the basis of equal peak power. Reference [9] is a separate report on the peak clipping problem.

#### 4.2 Bandpass Filtering

Two separate, simple, non-recursive, digital filters were selected to apply extreme filtering to the ANDVT modem signal. The equation for filter one was:

$$Y_0 = 0.6 X_0 - 0.5 X_{-2} - 0.1 X_{-4}$$

Filter two was a cascade of four of these filters. The amplitude and phase response of the two filters are given in table 2, and the amplitude responses are plotted in figures 10 and 11. In figure 10 the abscissa indicates frequency relative to the Nyquist frequency (3600 Hz). In figure 11 the abscissa is Hertz, with the frequency range of the 39 tone hf modem indicated by dashed lines. Filter number one provided approximately 3 dB attenuation at the frequency of the lowest data tone in the voice mode (675 Hz). Filter two provided approximately 12 dB attenuation at that same frequency.

It was the purpose of these tests to show to what extent the modem performance gracefully degraded as the signal passband was decreased. Figure 12 shows the bit error rate on the 39 tone signal versus  $P/N_0$  with and without stress filter number one. Identical filters were simulated for both the transmit and the receive filters, thus the total attenuation was equal to twice the values shown in table 2 and figures 10 and 11. That is, at the lower band edge (675 Hz) the total attenuation was 6 dB. This resulted in approximately a one dB degradation in performance on both the coded and uncoded data bits.

Figure 13 is a similar plot for the condition that the transmit and receive filters had the characteristics described for stress filter number two. For this condition the total attenuation at 675 Hz was 24 dB. This resulted in a degradation of approximately 6 dB for the uncoded data at a bit error rate of  $1 \times 10^{-2}$ . The degradation on the coded bits was approximately 2 dB.

The conclusion reached from these data is that quite severe limiting of the frequency passband may be imposed with relatively little effect on the coded bits, which control the overall performance of the LPC-10.

#### 4.3 Tonal Interference with Gaussian Noise

Two separate wideband FSK signals were used as inband tonal interference, representing other users in the common 3 kHz frequency spectrum. Both FSK signals were modulated at a 75 baud rate with 850 Hz shift. Both were standard FSK signals. One FSK signal was centered at 2000 Hz, and the other was centered at 2550 Hz. Keying was random with continuous phase at the transitions. The FSK signals were not filtered as they might be by bandpass filters in the interference modulator and/or transmitter. The interfering signals were keyed at a modulation rate identical to that used for transmitting the ANDVT modem preamble and message indicator (MI). The FSK transitions occurred approximately one-half of a baud period away from the transitions in the undelayed ANDVT preamble, a worst case condition. Figure 14 is a diagram of the location of the wideband FSK shift

frequencies relative to the ANDVT tone assignments.

The vertical dotted lines in figure 14 represent the FSK shift frequencies. The doppler tones are the four tones transmitted at the beginning of the preamble to facilitate doppler acquisition. The sync tones are the three biphase modulated tones transmitted next in the preamble which help establish synchronization and timing. Tone library No. 1 is the 39 tone signal set used for the transmission of digital voice; library No. 2 is the 16 tone signal set used for transmission of the epoch and the MI, the final portion of the modem preamble.

Three narrowband FSK signals were used as tonal interference to the ANDVT modem signal. Each was modulated at 75 baud with 85 Hz shift. One was a single FSK subchannel corresponding to channel number 9 of the AN/UCC-1 ship-board telegraph terminal equipment [10]. That channel has a center frequency of 1785 Hz. The second narrowband FSK interference signal corresponded to channel number 15 of the AN/UCC-1 equipment. Its center frequency was at 2805 Hz. The third interference signal consisted of all 16 subchannels of the AN/UCC-1 equipment. These FSK signals are spaced 170 Hz apart with carrier frequencies ranging from 425 Hz to 2975 Hz. Modulation conditions for the narrowband FSK interference were identical to those described for the wideband FSK interference signals. Figure 15 is a diagram of the location of the two single channel FSK signals relative to the ANDVT modem tone assignments.

A third form of tonal interference was a simulation of the standard 16 tone, 2400 bps, four-phase DPSK signal. The 16 tones were spaced 110 Hz apart from 935 Hz to 2585 Hz. The modulation was random data at a 75 baud rate. The optional unmodulated doppler tracking tone at 605 Hz was not transmitted.

A continuous unmodulated tone (CW) was used as a fourth form of inband interference. The frequency of the tone was either 675 Hz, 787.5 Hz, or 900 Hz. Figure 16 is a diagram of the location of the CW tones relative to the ANDVT modem tone assignments.

The final form of tonal interference was a CW tone which was swept between 500 Hz and 3000 Hz by a sawtooth wave having a period of 0.5 second. That corresponded to a sweep rate of 5000 Hz which resulted in the interference moving through a 112.5 cycle range in a period equal to the modem frame time in the voice mode (0.0225 seconds). A range of 112.5 cycles was equivalent to the spacing between three consecutive orthogonal tones for the 39 tone hf modem.

The performance of the 39 tone demodulator/decoder was tested for the condition that the  $P/N_0$  of the desired signal was held constant and an interference signal was added at various levels. Figures 17 through 27 show the bit error rate on the 39 tone versus interference level (in dBm) for the condition that  $P/N_0$  was equal to 42 dB with no interference present. For each of these tests the composite signal level ( $P$ ) was equal to -0.6 dBm as previously shown in table 1. Thus, the power per tone of each of the 39 tones was equal to:

$$\begin{aligned} \text{power per tone} &= -0.6 \text{ dBm} - 10 \log (39) \\ &= -0.6 - 15.9 \\ &= -16.5 \text{ dBm} \end{aligned}$$

Therefore, when the interference level was at -16.5 dBm, its total power was equal to the power of each of the desired data tones.

Figures 17 and 18 are the results with the two wideband FSK signals as interference. The first wideband FSK signal, centered at 2000 Hz, was slightly more damaging than the signal centered at 2550 Hz. This was undoubtedly due to the fact that both shift frequencies were within the bandwidth of the 39 tone library.

Figures 19, 20, and 21 show similar data for the three narrowband FSK interference signals. Figure 22 is the results for the 16 tone DPSK signal, and figure 23 compares the results with the 16 tone DPSK signal to the results shown previously in figure 21 for the 16 tone FSK interference signal. For the same interference level, the FSK signal was more damaging than the DPSK signal, because it covered a wider bandwidth.

Figures 24, 25, and 26 show the results when the interference signal is one of the three CW tones while figure 27 is the result of using a swept tone interference.

All of the data shown in figures 17 through 27 show relatively uniform results independent of the exact nature of the tonal interference. The uncoded bit error rate was controlled by the low  $P/N_0$  value of 42 dB that was selected. The interference had relatively little effect on these data. For the coded bits, a bit error rate of  $1 \times 10^{-3}$  was reached for interference levels between -12 dBm and -18 dBm, depending on the type of interference. At an interference level of -6 dBm the coded bits had nearly a constant error rate independent of the interference type. Data are not shown for interference levels higher than -6 dBm because for those conditions the performance of the preambles started to become unreliable.

The terminal will operate under conditions where the interference is higher than -6 dBm if the desired  $P/N_0$  is increased. Figure 28 is an example with the desired  $P/N_0$  increased to 49.4 dB, which was a 7.4 dB increase over the signal level used for the data shown in figures 17 through 27. The interference signal was the swept tone. It may be seen from figure 28 that the reliable operating point was moved up to -3 dBm for the interference level.

The conclusion reached in these tests with tonal interference were that at a modest  $P/N_0$  of 42 dB, the interference would begin to have an effect on the LPC-10 when the interference levels were between -12 dBm and -18 dBm. The preambles would be effected when the interference level exceeded -6 dBm. Furthermore, these levels will be shifted to higher values if the desired signal-to-noise level were increased, but it is not a one-for-one relationship.

#### 4.4 Preamble Acquisition

The first portion of the modem preamble consists of four unmodulated tones which provide a means for the modem receiver to estimate any frequency translation or doppler error. The four tones are spaced 675 Hz apart to provide frequency diversity in a fading channel.

Tests of the doppler acquisition algorithm were made for various Gaussian noise levels and for various known frequency offsets. The doppler acquisition

algorithm provides for making an estimate of the frequency error in either a 3 dB bandwidth of approximately 270 Hz or a bandwidth of 45 Hz about each of the four tone assignments. The algorithm makes energy measurements in adjacent tone slots to determine whether to make a wideband frequency estimate/correction or a narrowband estimate/correction. During the 24 frame period of the doppler signal, it is possible to make either one to four wideband estimates, or one wideband estimate plus one narrowband estimate, or one narrowband estimate.

Figure 29 is a plot of the absolute value of the error in the doppler estimate versus  $P/N_0$  for the condition that the input signal was not off frequency. For this condition only a single narrowband estimate was performed. Figures 30 through 33 are similar data for the conditions that the input signal was translated in frequency by either 50, 62.5, 75, or 112.5 Hz, respectively. For these conditions the preamble detector performed a wideband estimate followed by a narrowband estimate of the frequency offset. Figure 34 contains the results for the condition that the input signal was shifted by 150 Hz. Two wideband frequency estimates were performed.

The results of these tests indicate that the two-step doppler detection algorithm will estimate the frequency with an accuracy of one Hz or less for  $P/N_0$  greater than 38 dB for frequency errors up to 112.5 Hz.

The synchronization aspects of the preamble are concerned with the detection of the framing epoch (240 bit PN sequence) and the correct demodulation and decoding of the message indicator. Figure 35 shows the probability of detecting the epoch and message indicator as a function of the  $P/N_0$  for Gaussian noise conditions. The epoch detection algorithm is the most robust portion of the modem signal design. It has a 99% probability of detecting a valid PN sequence for a  $P/N_0$  of 33.1 dB. The message indicator requires a  $P/N_0$  of approximately 34.4 dB for a 99% probability of correct detection.

#### 4.5 Effects of Multipath Conditions

The multiplicative effects of a fading multipath form of a propagation channel were simulated by a tapped delay line concept of the ionosphere. The input parameters were the number of paths, their delay, and their relative amplitudes, plus the mean frequency offset and doppler spread for each path. Figure 36 is a diagram of the general concept, which is the principle of many real-time channel simulators. The complex gain values for each tap on the delay line were generated by linearly combining 20 complex sinusoids spread over a frequency range equal to two times the specified doppler spread. Each of the 20 frequencies were chosen randomly such that one sinusoid was located in each of 20 equal increments in the total spread of  $\pm 5$  Hz. This is depicted in the diagram in figure 37. Table 3 is an example of the random tones selection for a spread of one Hz. The results of combining the 20 sinusoids are the complex tap gain values which exhibit Rayleigh fading characteristics and uniform phase, as shown in figures 38 and 39. The tap gain values were generated at 1/100 the modem sampling rate or at a 72 Hz rate, and linear interpolation was used between samples.

Figure 40 is a plot of the fade rate versus doppler frequency spread for one path. Fade rate was defined as the average number of fades per minute. A fade was defined to start when the amplitude of the signal decreased to 6 dB below the mean value. A fade ended when the amplitude of the signal rose to

5 dB below the mean value. That one dB difference in thresholds between the start and end of a fade period was selected to minimize the probability of interpreting a very small change in signal level as a very rapid fade. Figure 41 is a plot of the median fade duration versus frequency spread for a one-path model. A frequency spread of one Hz resulted in a fade rate of 45.6 fades per minute, and the median fade period was 0.22 seconds. Table 4 is a comparison of the fade rates measured with this method of generating complex tap gain values versus the fade rates promulgated by CCIR for the four standard CCIR values for doppler frequency spread. Fade rates were measured on the envelope of an unmodulated tone.

Tests were performed to determine the performance of the modem as a function of the multipath delay, doppler frequency spread, number of paths, and their relative amplitudes. The CCIR document [4] states that, in general, modem behavior can be adequately assessed using two multipath components of equal mean strength. These tests demonstrate that this is generally true for a DPSK modem without coding, but it is not true for a modem that incorporates coding in the frequency domain similar to the ANDVT modem.

Figure 42 is a plot of the measured bit error rate versus multipath delay for the case of a two-path channel model with one Hz frequency spread on each path. Both paths were of equal amplitude and the  $P/N_0$  was 49.4 dB. Data are presented on the bit error rate for both the coded and the uncoded data for differential delays up to 7 ms. These data show that the uncoded bits were relatively insensitive to the amount of delay for delay values of 3 ms or less. Above 3 ms there was a gradual degradation in the bit error rate of the uncoded data. The degradation was due to the fact that the time guard band of the modem was only 4.7 ms; thus, the delayed signal was causing a phase transition during this integration period.

For the coded data the optimum performance was obtained for a delay of approximately 3 ms. For values greater than 3 ms the time guard problem existed. For values less than 3 ms the fading became less frequency selective. (With no delay the performance would be identical to a one-path model which exhibits frequency flat fading.) With frequency-flat fading the advantage of coding in the frequency domain is lost.

Figure 43 shows the bit error rate as a function of doppler spread for two equal paths with a relative delay of one ms. The  $P/N_0$  was 49.4 dB. For frequency spreads between 0.5 ms to 5.0 ms there was a linear relationship to the bit error rate for the uncoded data. This was not true for the coded data, although the slope of the curve approaches that of the uncoded data for frequency spreads greater than 3 Hz. For frequency spreads less than 0.5 Hz, the bit error rates of both the coded and uncoded data must approach those of the non-fading Gaussian channel.

The data in figures 42 and 43 were for two paths of equal amplitudes. Figure 44 shows the bit error rate as a function of the relative amplitudes of two paths with 1 ms delay and 1 Hz spread on each path. Again, the  $P/N_0$  was 49.4 dB. These data show that for the uncoded case the bit error rate was essentially independent of the amplitude of the second path. This was not true for the coded data. Best performance was obtained when the two paths were of equal amplitude. Under those conditions the fading was more frequency selective than when one path was attenuated. When the second path was 18 dB below the amplitude of the first path, the fading characteristics approached those of a

single path with frequency flat fading and the error rate of the coded bits approached that of the uncoded bits.

The next test in this series obtained the bit error rate as a function of the number of paths. All paths had equal amplitudes and one Hz doppler frequency spread. The relative delays of the paths were as follows:

<u>Path No.</u>	<u>Delay (ms)</u>
1	0
2	2.0
3	1.5
4	0.9
5	0.7
6	0.35

The results of this test for a  $P/N_0$  of 44.4 dB are shown in figure 45. The uncoded data were relatively insensitive to the number of paths. The error rate was determined by the  $P/N_0$  and the fading on a single path. The bit error rate for the coded data improved as the number of paths increased. The bit error rate decreased by a factor of 3.3 when the number of paths increased from two to six. Some results from these same tests are presented in figure 46 as the percent of frames with error versus the number of paths. These data show that for the uncoded data the distribution of errors changed with the number of paths. With only one path the frequency flat fading produces bursts of errors. Adding extra paths made the distribution more random but had little effect on the average error rate. The data in figures 45 and 46 are for a  $P/N_0$  of 44.4 dB rather than 49.4 dB as was used for the previous tests in this series. The lower  $P/N_0$  value was used because it showed the tendency for the curve to flatten out at six paths for a bit error rate that was easily measured. Figure 47 shows the bit error rate versus number of paths for  $P/N_0$  equal 49.4 dB. This shows the dramatic improvement in error rate as the number of paths increased, with a bit error rate less than  $1 \times 10^{-4}$  for four paths.

Some interesting conclusions may be drawn from this series of tests. They relate to the selection of frequency assignments for secure voice operation with the ANDVT modem. Our present methods for channel selection are based on experience with clear voice transmission and point-to-point teletype. With non-diversity, clear voice operation experience has shown that best operation is obtained if one attempts to minimize multipath and maximize S/N by operating just below the maximum usable frequency (MUF). That would represent a single propagation path with slow, frequency flat fading. The non-continuous nature of the clear voice transmission easily bridges the fades on such a path. For point-to-point teletype operation, using continuous transmissions of standard FSK or DPSK signals, best operation is again obtained by working just below the MUF. The fading may be counteracted by use of rf or antenna diversity.

Secure voice nets are generally operated non-diversity; thus, if channels are selected in the same manner, to be just below the MUF, the frequency flat fading will not be to the advantage of the ANDVT coding. Therefore, consideration should be given to selecting operating frequencies that are lower in frequency relative to the MUF and exhibit more multipath components. Strong multipath components are preferred to weak ones, as demonstrated in figure 44. This must be balanced against the fact that S/N generally decreases at the lower frequencies.

#### 4.6 Performance on CCIR Channels

Table 5 lists the characteristics of the four CCIR Channel models. All four models consisted of two propagation paths with equal attenuation and equal doppler frequency spread on each path. The variables were the differential delay between the two paths and the doppler frequency spread. The value of these variables ranged from 0.5 ms delay with 0.1 Hz spread for a good channel to 3.0 ms delay with 2.0 Hz spread for a flutter fading channel. The spread was defined as the double-sided bandwidth of the fading spectra. Figure 48 is a plot of the CCIR channel parameters; i.e., doppler spread versus differential delay. The fact that the data points in figure 48 can be seen to lie on a smooth curve implies that the four channel models were selected from a larger model which describes the behavior of the ionosphere.

The bit error rate versus  $P/N_0$  for the four CCIR channels are shown in figures 49, 50, 51, and 52 respectively. Separate curves are given for the coded and uncoded data bits. These data indicate that the uncoded data bits are relatively independent of the fading conditions for  $P/N_0$  values of 55 dB or less. That is illustrated in figure 53 which give the uncoded bit error rates for the CCIR Number 1 channel and the CCIR Number 4 channel. The differences between these two extreme channel conditions is very much greater for the coded data bits as shown in figure 54.

Figures 55 and 56 show bit error rate versus channel number for two  $P/N_0$  values. The abscissa in these graphs should be viewed as a continuous range of channel conditions from good to perturbed. Viewed in that manner, those curves show the relative effects of working in good to poor conditions.

Figure 57 is a plot of  $P/N_0$  versus CCIR channel number for the condition that the coded bit error rate is  $1 \times 10^{-3}$ . That is the condition where the uncorrected errors on the most sensitive data begins to be discernable on the synthesized speech. There is approximately a 10 dB range between channel Number 1 and channel Number 4 for that condition.

In references [6, 7] data were presented on the performance of the ANDVT signal design on a two-path and a six-path channel model. The two-path channel model was for equal amplitude paths, 1 Hz spread on each path, and a delay of 1 ms. The results are shown in figure 58. Figures 59 and 60 compare those results with results obtained for the CCIR Number 3 channel. The differences may be considered slight, and are due to the differences in delay and the different channel simulation techniques.

Figures 61 through 64 show the effect of adding the wideband FSK Number 1 interference signal to the signal perturbed by CCIR Number 1, Number 2, Number 3, and Number 4, respectively. Figures 65 and 66 show similar data for CCIR Number 1 and Number 2 with the 16 tone DPSK interference signal. The  $P/N_0$  for each of the tests was 49.4 dB. These data are not dissimilar from the data presented for the Gaussian channel case; the difference being in the higher  $P/N_0$  values required for the fading signal. The interference was non-fading in these latter tests.

An interesting fact due to the simulation technique was observed when simulating channels with very low doppler frequency spread, such as the CCIR Number 1 channel with a spread of 0.1 Hz and a delay of 0.5 ms. For such low frequency spreads the effect is that the nulls in the frequency band do not circulate through the entire 3000 Hz band. This is illustrated in figure 67 which shows the bit error rate on the uncoded bits versus tone number in the 39 tone modem, where tone one is at 675 Hz. The  $P/N_0$  was 45.4 dB. This fact has been observed also with the simulation of the same channel with a real-time channel simulator implemented in the CSP-30 signal processor [11]. The effect is believed to be due to the fact that both simulators use a digital implementation where everything is tied to one common time base, thus for very low frequency spread the positions of the nulls in the frequency domain do not on an average depart far from their original position at the start of a test. Figure 68 shows bit error rate versus tone number for a modified CCIR Number 1 channel in which one path has been given a small (0.1 Hz) mean frequency offset in addition to the normal 0.1 Hz doppler spread. The result is that the nulls do get distributed across the entire frequency band and the error rates are uniform across the band. This also resulted in a very small decrease in the uncoded bit error rate and about a 2/1 decrease in the coded error rate.

#### 4.7 Performance on Consortium Channel

In 1975 a consortium of U.S. Department of Defense laboratories and agencies conducted extensive testing of narrowband digital voice processors. That work included tests by NRL on hf channels. The consortium hf channel model, selected by NRL for those tests, was based on measurements made on a perturbed propagation path between Washington, DC and Cheyenne, Wyoming. Table 6 lists the characteristics of that channel model. It consisted of four paths with a maximum differential delay of 2.2 ms. Each path had separately specified relative amplitude, mean frequency offset, and doppler frequency spread. In general, the relative amplitudes of a path decreased as a function of the delay, and the mean frequency offset and doppler spread each increased as a function of the delay. These relationships are depicted in figures 69, 70 and 71.

Tests similar to those performed for the CCIR channel models were done using the four-path consortium channel model. The results are shown in figure 72. This channel model was defined as a perturbed channel as was the CCIR No. 4 channel. A third definition of a perturbed channel was the 6 path channel model described in references [6, 7]. The results previously obtained on that channel model are shown in figure 73. Figures 74 and 75 compare the results obtained on these three definitions of a perturbed channel. Figure 74 is for the uncoded data; figure 75 is for the coded data. There was a very small difference in the performance over these three channels for the uncoded data at  $P/N_0$  values less than 55 dB. There

was a significant difference in the performance for the coded data. The data clearly separates out the three channels in regard to the amount of frequency selective fading that was present. The modem performed the worst on the CCIR Number 4 channel which has relatively little frequency selective fading. This again illustrates the possibility of successfully working ANDVT on channels that normally would be avoided; that is, those channels that have several multipath components.

#### 4.8 Performance on a Rician Channel

A fading channel with a spectral component was simulated for the combined skywave and groundwave model representing operation at ELOS ranges. Table 7 lists the characteristics for that channel model, a two-path model with the fading skywave component delayed 2.2 ms relative to the non-fading groundwave component. The root-mean square (rms) level of the skywave signal was six dB higher than the rms of the groundwave signal. The doppler spread on the fading signal was 1.0 Hz. The characteristics of the delayed path were essentially equivalent to the delayed path of the two-path CCIR Number 3 channel, where the delay was 2.0 ms and the spread was 1 Hz. The results on the Rician channel are shown in figure 76 which may be compared to the data in figure 51. From that data it may be concluded that the performance was controlled in both cases by the fading spectra on one path and it mattered little whether the second path was fading. In both cases the combination of the two paths produced similar frequency selective fading characteristics, as determined by the bit error rates obtained on the coded data.

#### 5.0 Conclusions

Extensive non-real time testing of a FORTRAN implementation of the ANDVT hf modem has been performed for operation in the digital voice mode. The tests have included measurement of the modem performance on both Gaussian and Rayleigh fading channels. Specific channels of interest to the international community and to the U.S. Secure Voice Speech Consortium have been simulated. Tests have been performed with a wide range of tonal interference, as well as with extreme filtering of the transmitted signal. Tests were performed to determine the modems sensitivity to a wide range of parameters for multipath operations.

The results clearly indicate that the signal design for this modem, which includes forward-error-correction coding in the frequency domain, will provide significant protection to the most sensitive bits of the LPC-10 speech analyzer. In addition, the range of propagation conditions and interference conditions for which satisfactory operation may be expected is expanded dramatically.

## REFERENCES

1. "The HF Modem for the ANDVT TACTERM (CV-3591)", Wayne M. Jewett and Raymond Cole, Jr., NRL Memo Report in preparation.
2. "A Non-Real Time Implementation of the ANDVT HF Modem, Net Voice Mode" NRL Report in preparation.
3. "Additive and Multiplicative Distortion Simulator for Non-Real Time Testing of HF Modems" NRL Report in preparation.
4. "HF Ionospheric Channel Simulators", Report 549 in Volume III of the CCIR Xiii Plenary Assembly, Geneva, Switzerland, 1974.
5. "Report of Narrowband Secure Voice Consortium, Appendix A", 1975.
6. "HF Modem Design for the Advanced Narrowband Digital Voice Terminal", CNR Final Report, November 1977.
7. "HF Modem Evaluations for the Advanced Narrowband Digital Voice Terminal (ANDVT)", CNR Final Report, November 1978.
8. "A Class of Algorithms for Decoding Block Codes with Channel Measurement Information", David Chase, IEEE Transactions on Information Theory, Vol. IT-18, No. 1, January 1972.
9. "Performance of ANDVT HF Modem with Peak Clipping", Wayne M. Jewett and Raymond Cole, Jr., NRL Memo Report 4374, October 30, 1980.
10. Technical Manual for Telegraph Terminal AN/UCC-1D(V), NAVSHIPS 0967-239-4010, 27 April 1967.
11. "A Programmable Real-Time HF Channel Simulator", R. Cole, W. M. Jewett, and J. W. Linnehan, Sixth Conference on Modeling and Simulation, Instrument Society of America, Pittsburgh, Pennsylvania, Part 1, pp. 256-266, April 1975.

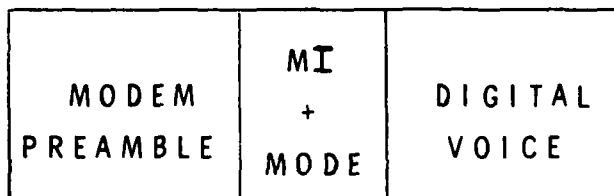


Fig. 1 — Sequence of transmissions

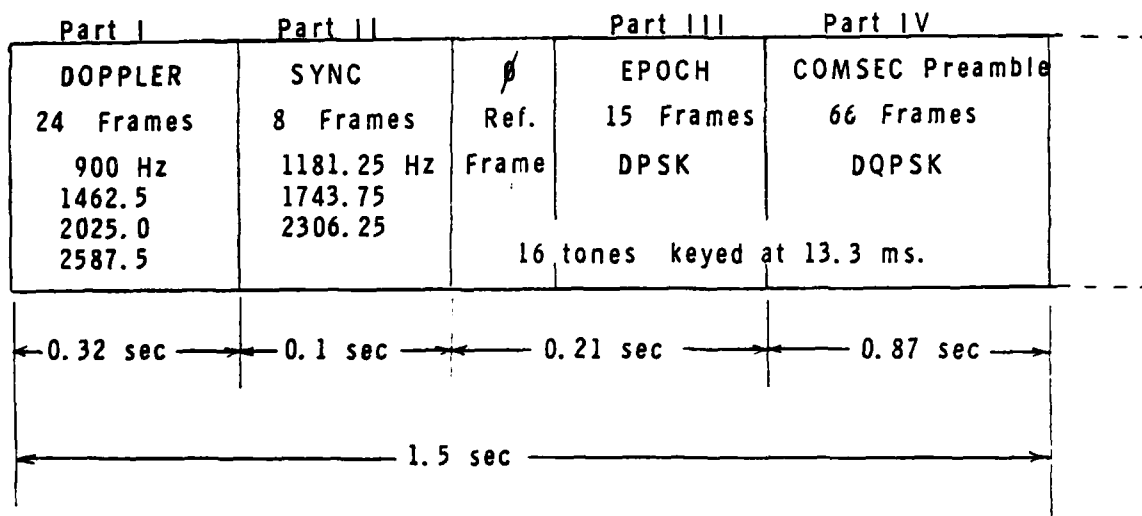


Fig. 2 — Preamble design

MSB

PCM	1	2	3	4	5	6	7
PITCH	G	G	G	G	G	G	
RMS	G	G	G	G			
R1	G	G	G	G			
R2	G	G	G	G			
R3	G	G	G				
R4	G	G					
R5							
R6							
R7							
R8							
R9							
R10							
SYNC	G						

G = PROTECTED WITH  
GOLAY CODE

Fig. 3 — Coding in modem on LPC-10 data  
(voiced frames)

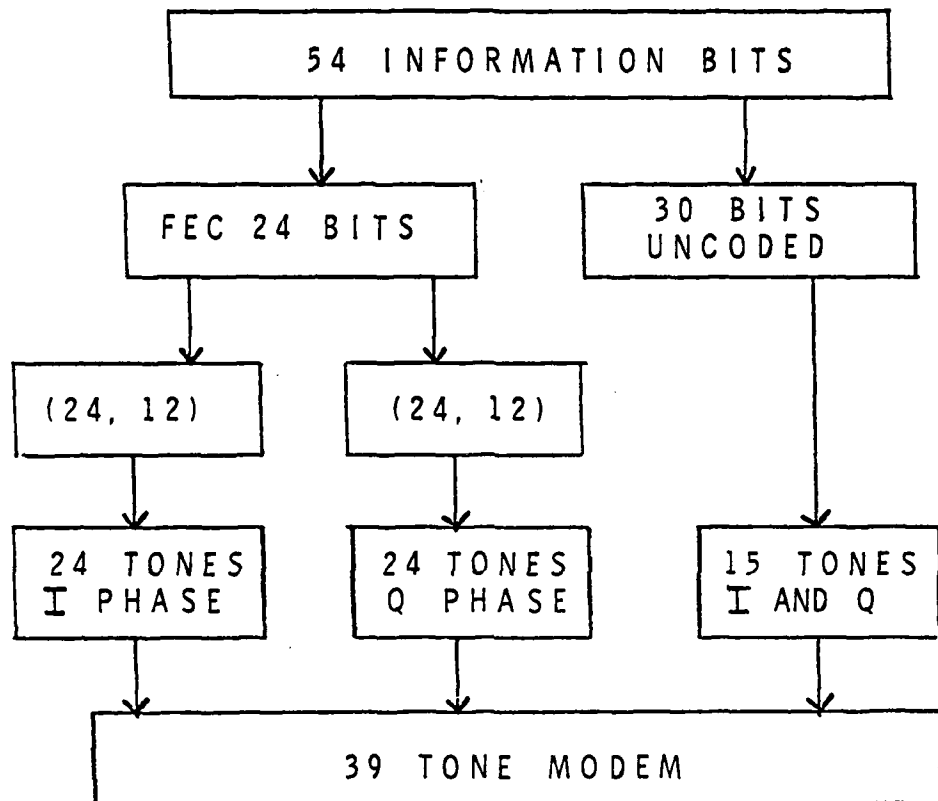
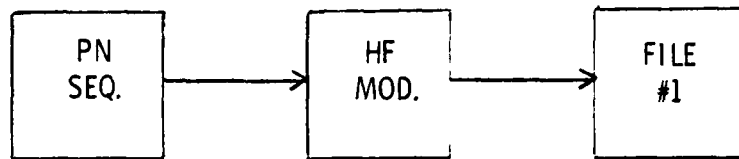


Fig. 4 — Modulation format for digital voice

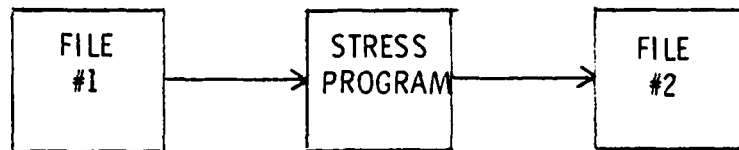
- 39 TONES
- 4-PHASE DPSK
- 44.44 FRAMES/SEC (22.5 MSEC)
- INF. RATE - 2400 bps
- TX. RATE - 3466.66 bps
- $\Delta F$  - 56.25 Hz
- BANDWIDTH - 2193.75 Hz
- DOPPLER TRACKING FROM DATA TONES
- SLOT SYNC TRACKING
- TIME GUARD - 4.7 MSEC
- SAMPLING RATE - 7200 Hz
- FFT SIZE - 128

Fig. 5 - HF modem characteristics, voice mode

1. GENERATE TRANSMIT SIGNAL



2. TRANSMIT THROUGH STRESS CHANNEL



3. DEMODULATE

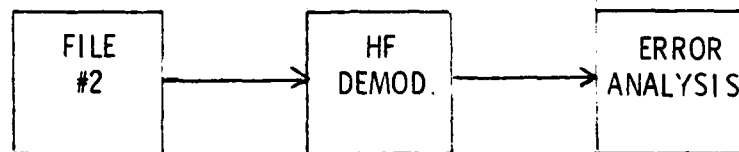


Fig. 6 — Non-real-time testing sequence of events

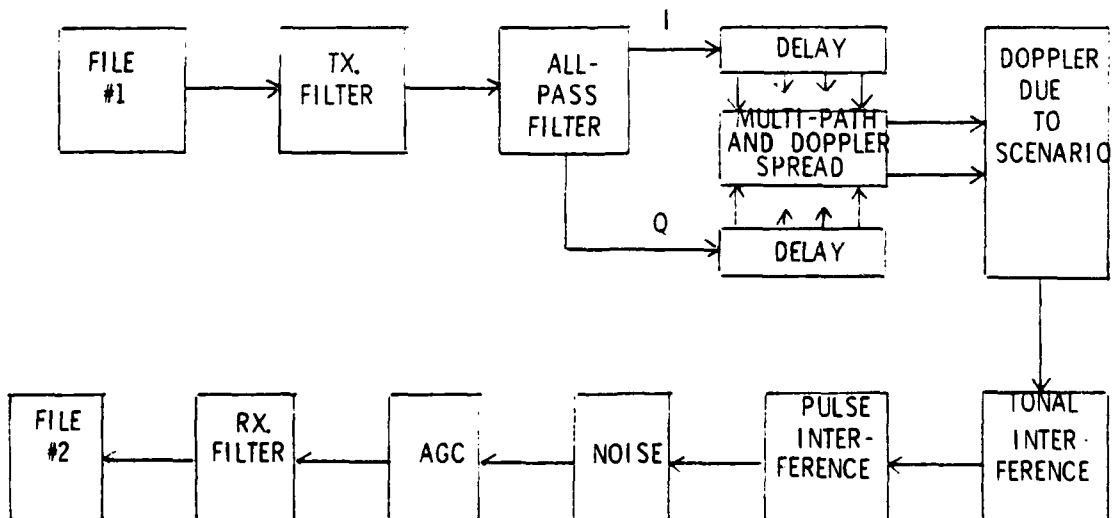


Fig. 7 — Non-real-time stress program

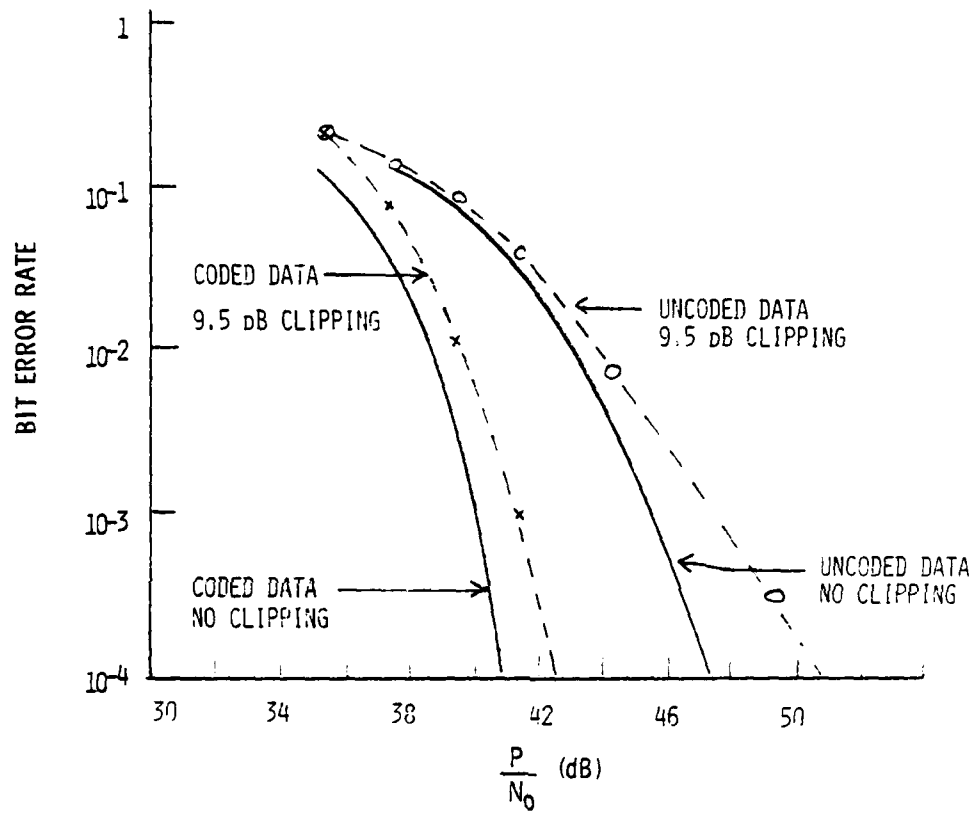


Fig. 8 — Bit error rate of coded and uncoded data, with and without peak clipping, for Gaussian channel

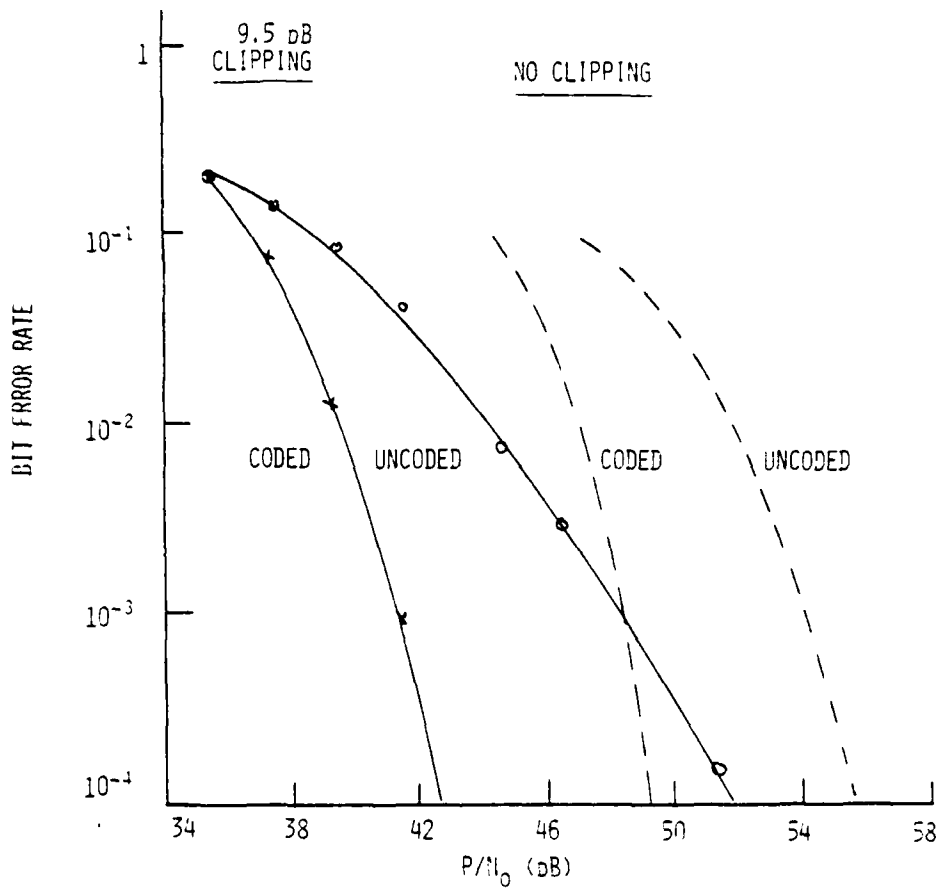


Fig. 9 — Performance with and without clipping for same peak power

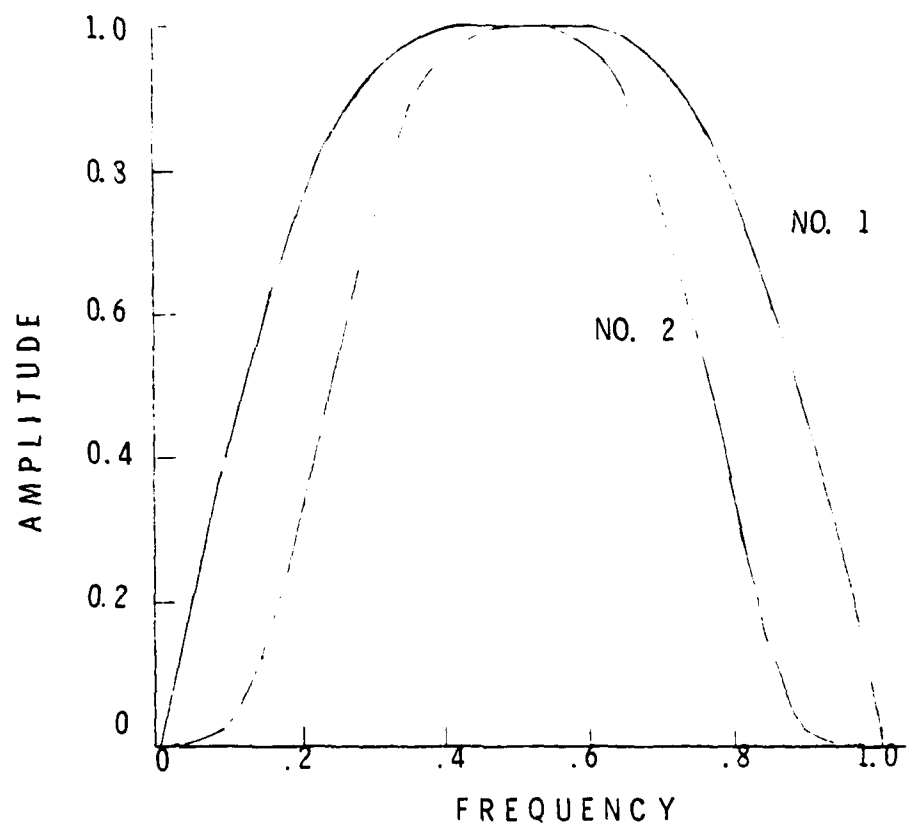


Fig. 10 — Frequency response of stress filters

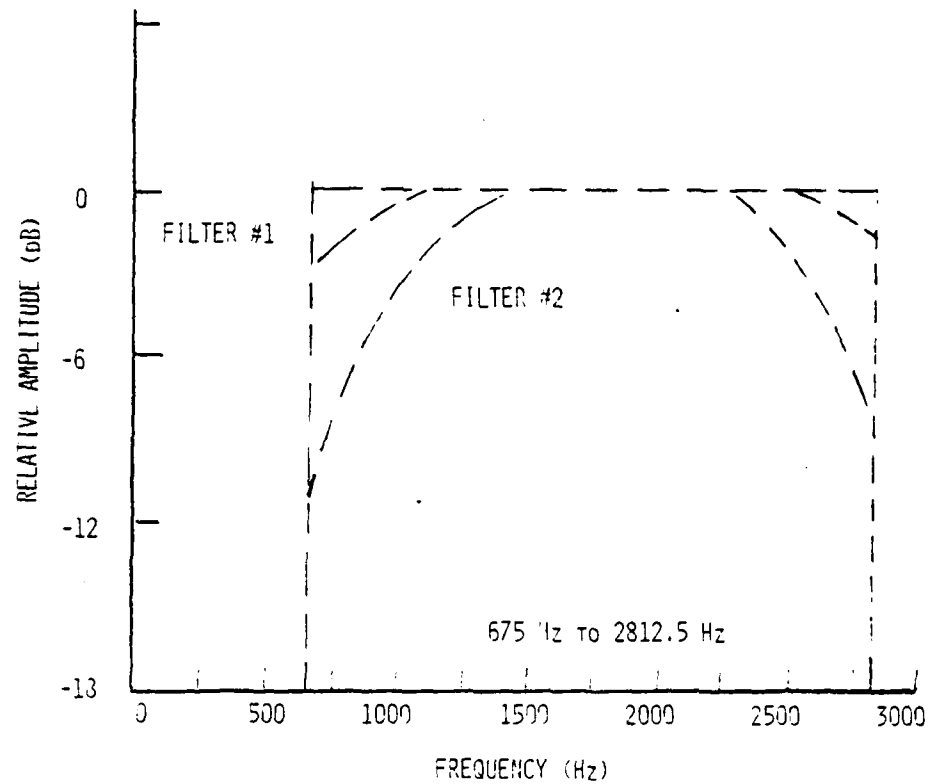


Fig. 11 — Effect of filtering on tone library number 1

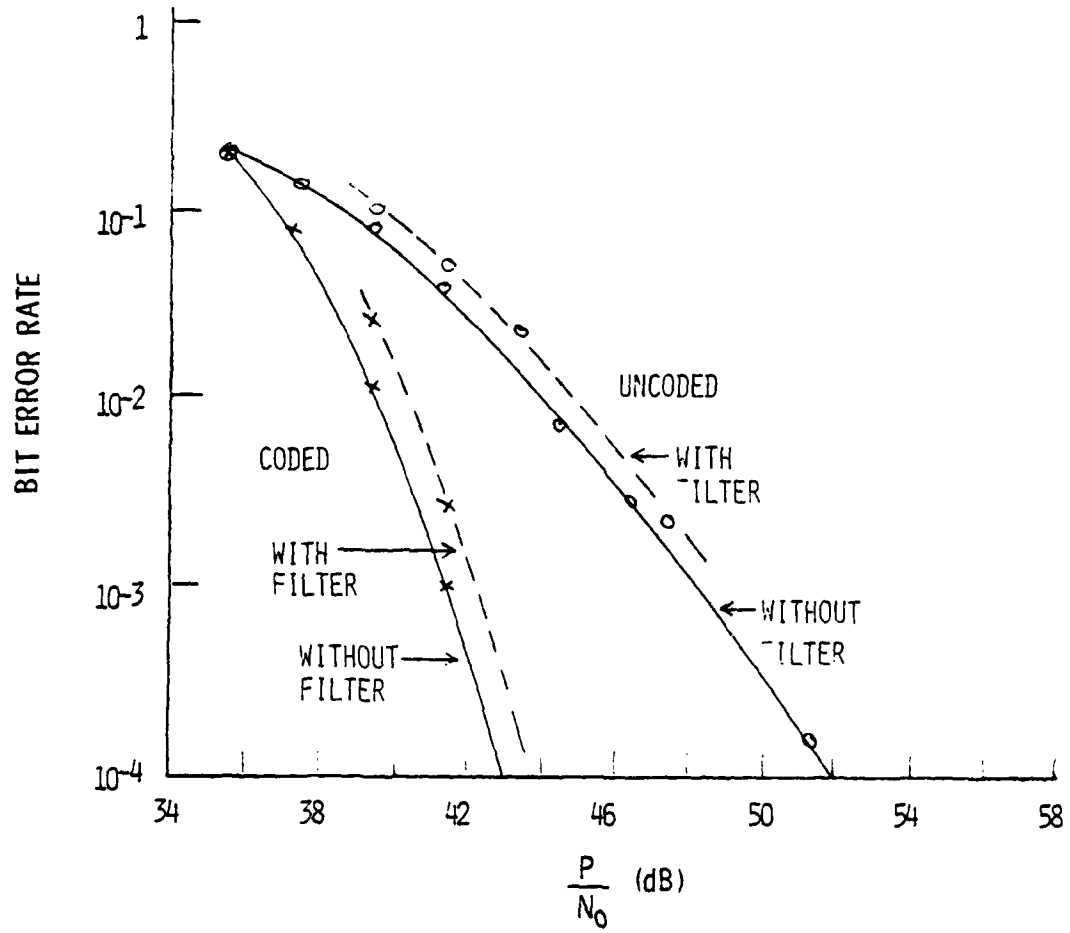


Fig. 12 — Performance with stress filter number 1

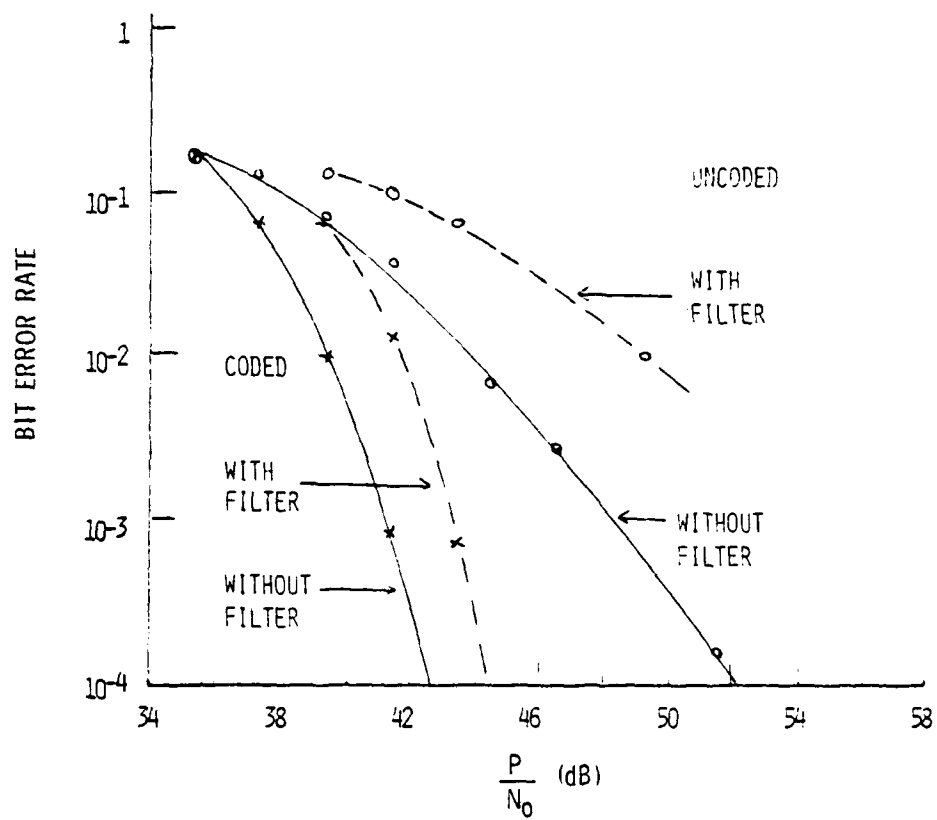


Fig. 13 — Performance with stress filter number 2

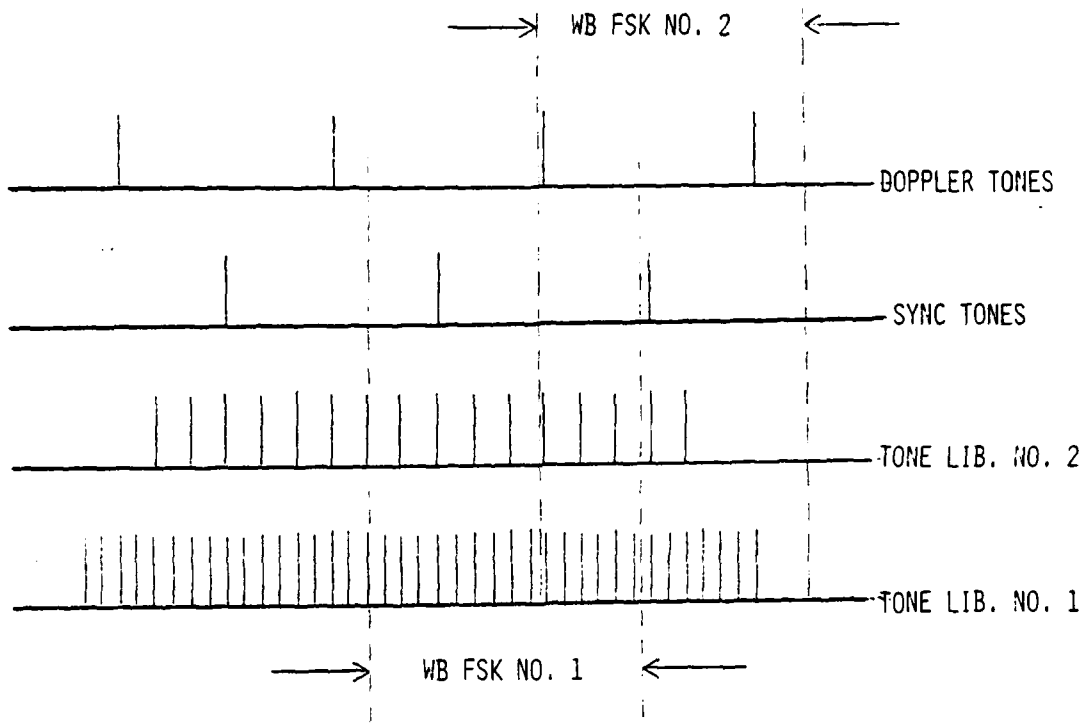


Fig. 14 — Relative location of WB FSK interference and modem tone assignments

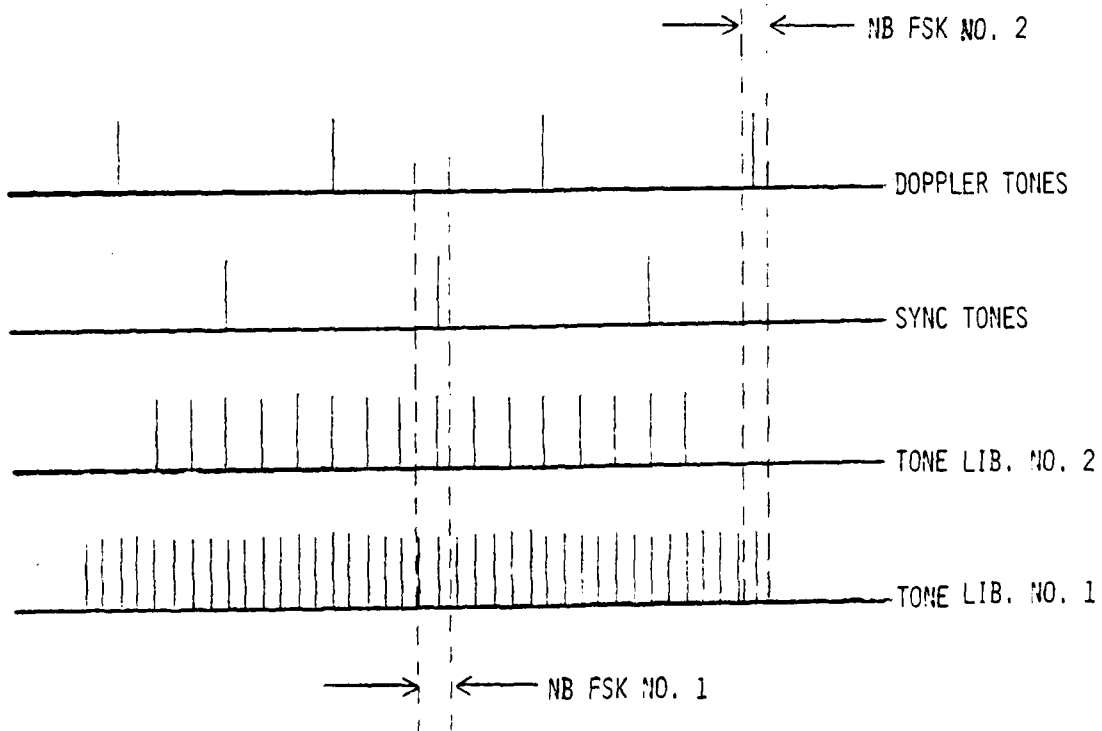


Fig. 15 — Relative location of NB FSK interference and modem tone assignments

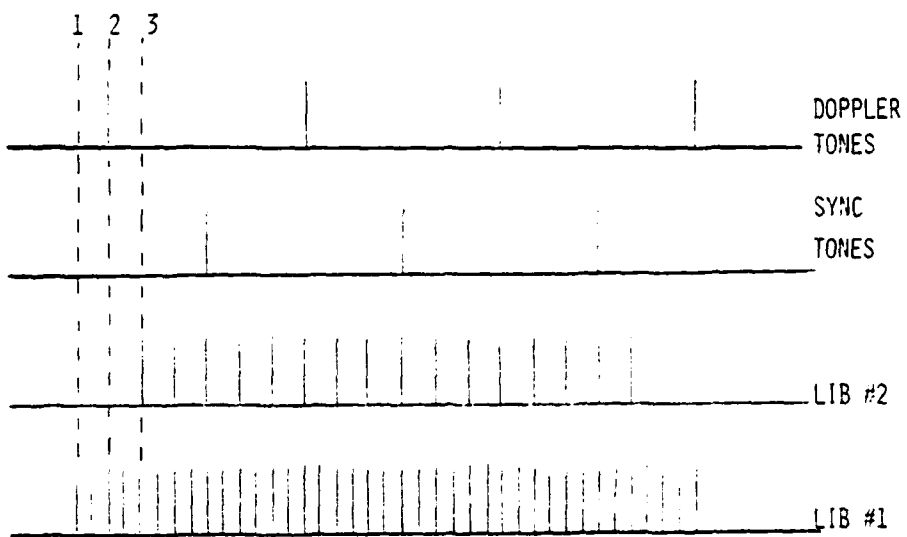


Fig. 16 —Relative location of CW tone interference and modem tone assignment

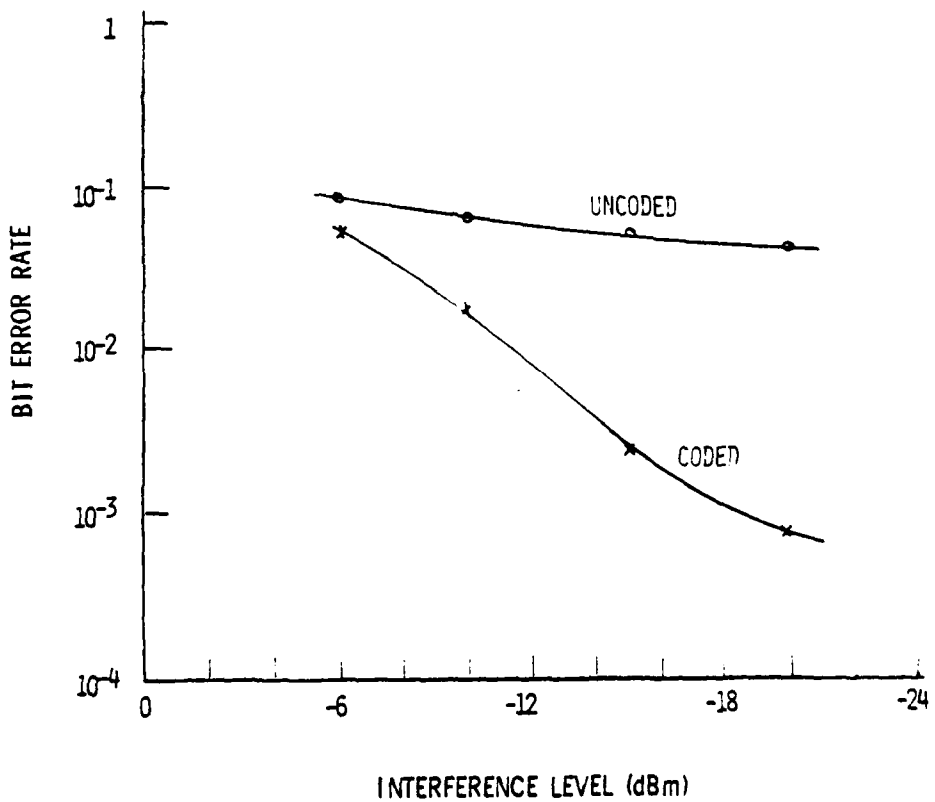


Fig. 17 — Interference by wideband FSK number 1,  
 $P/N_o = 42 \text{ dB}$

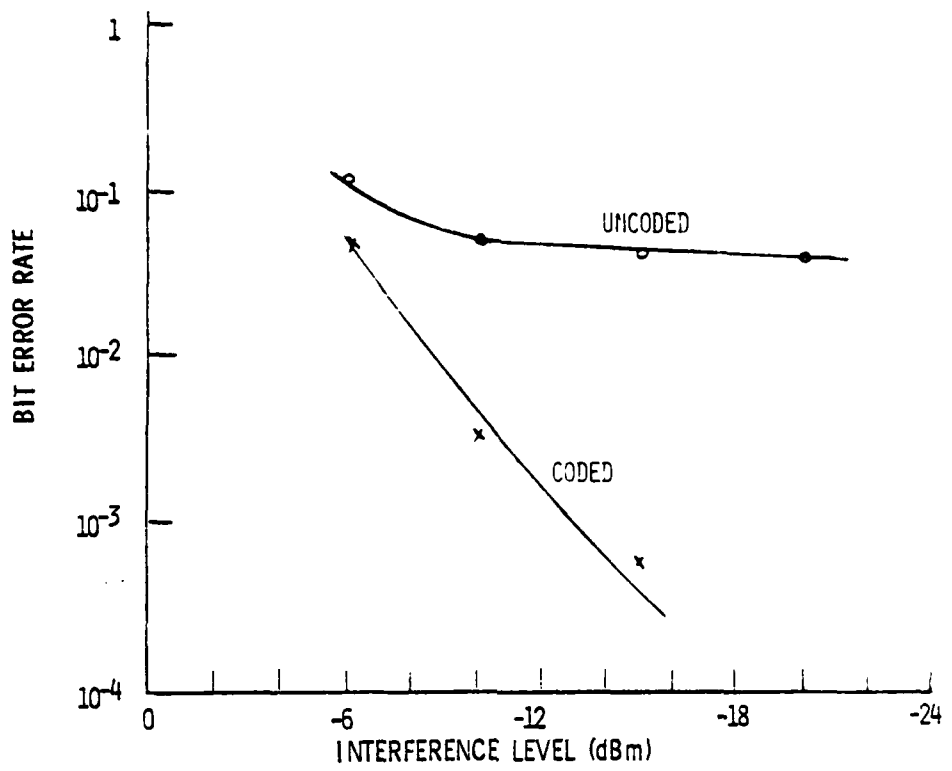


Fig. 18 — Interference by wideband FSK number 2,  
 $P/N_o = 42$  dB

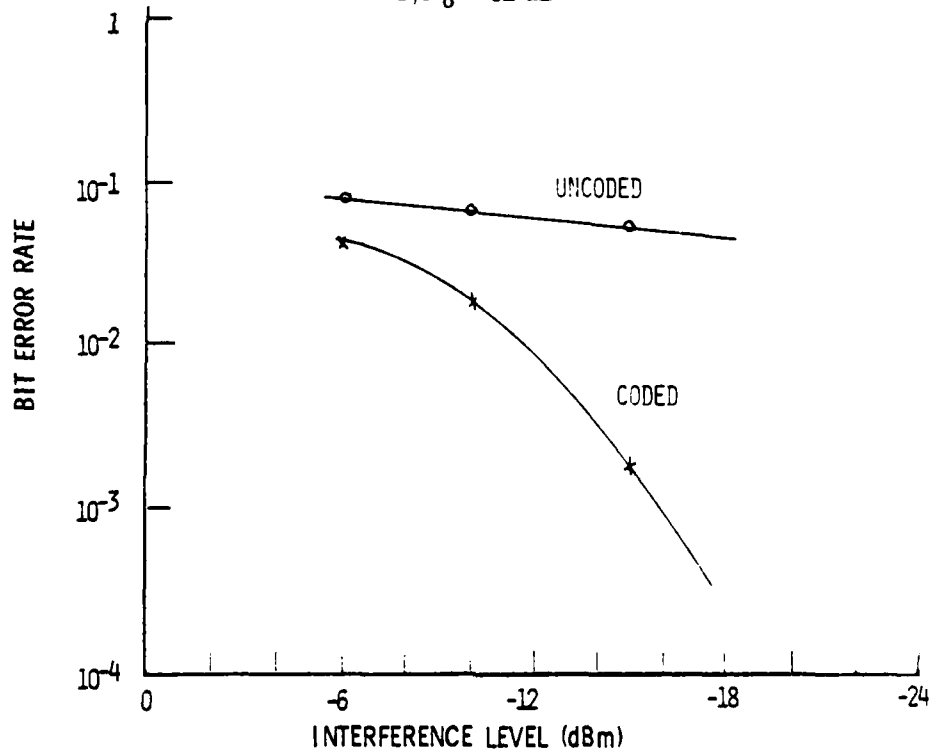


Fig. 19 — Interference by narrowband FSK number 1,  
 $P/N_o = 42$  dB

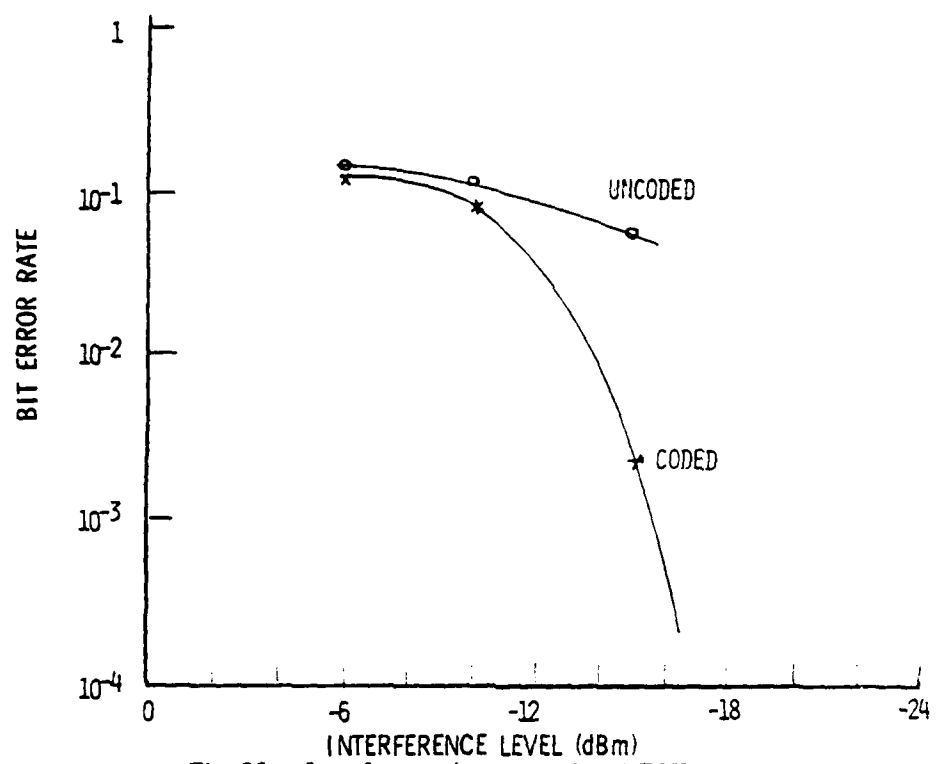


Fig. 20 — Interference by narrowband FSK number 2,  
 $P/N_o \approx 42$  dB

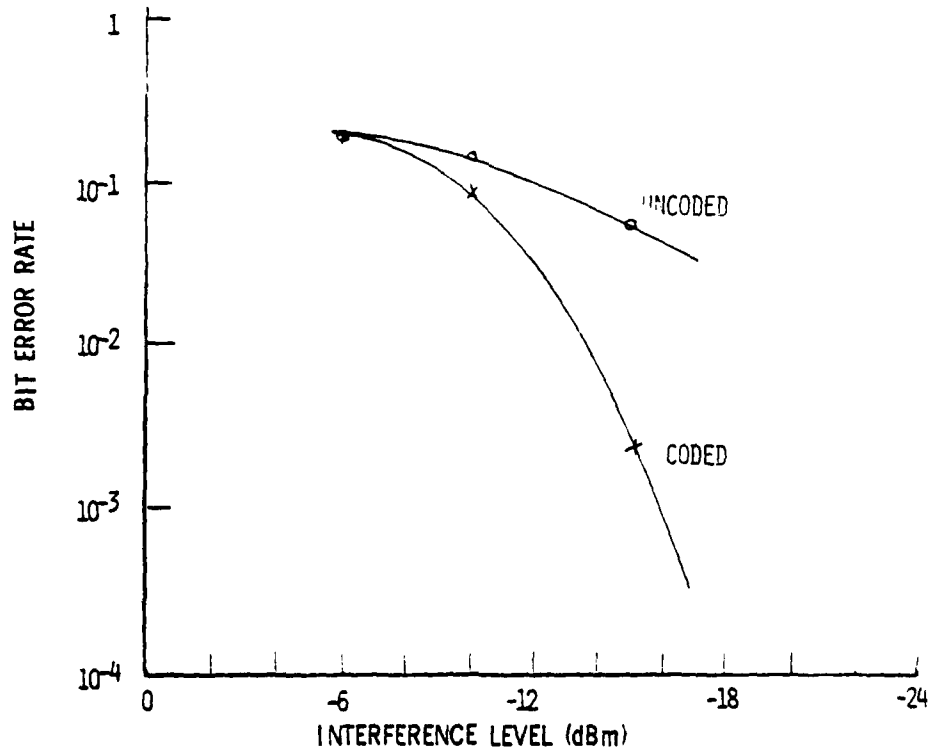


Fig. 21 — Interference by narrowband FSK number 3,  
 $P/N_o = 42$  dB

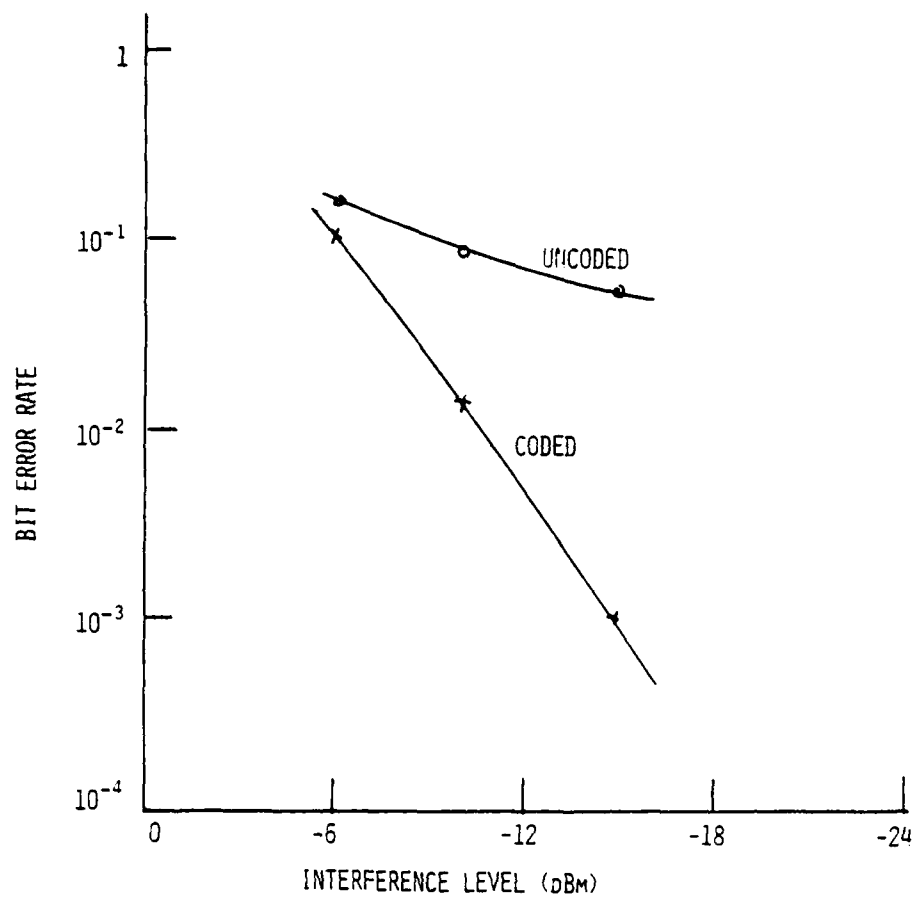


Fig. 22 — DPSK interference,  $P/N_o = 42$  dB

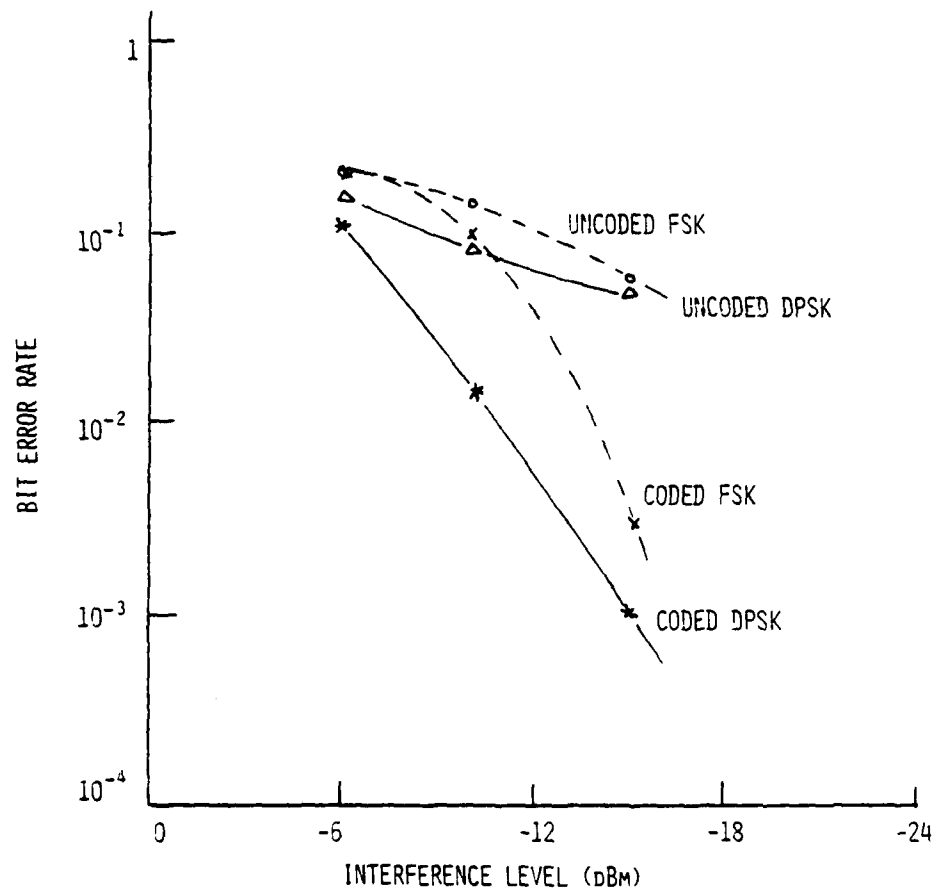


Fig. 23 — Comparison of effects of interference by either  
NB FSK number 3 or DPSK,  $P/N_o = 42$  dB

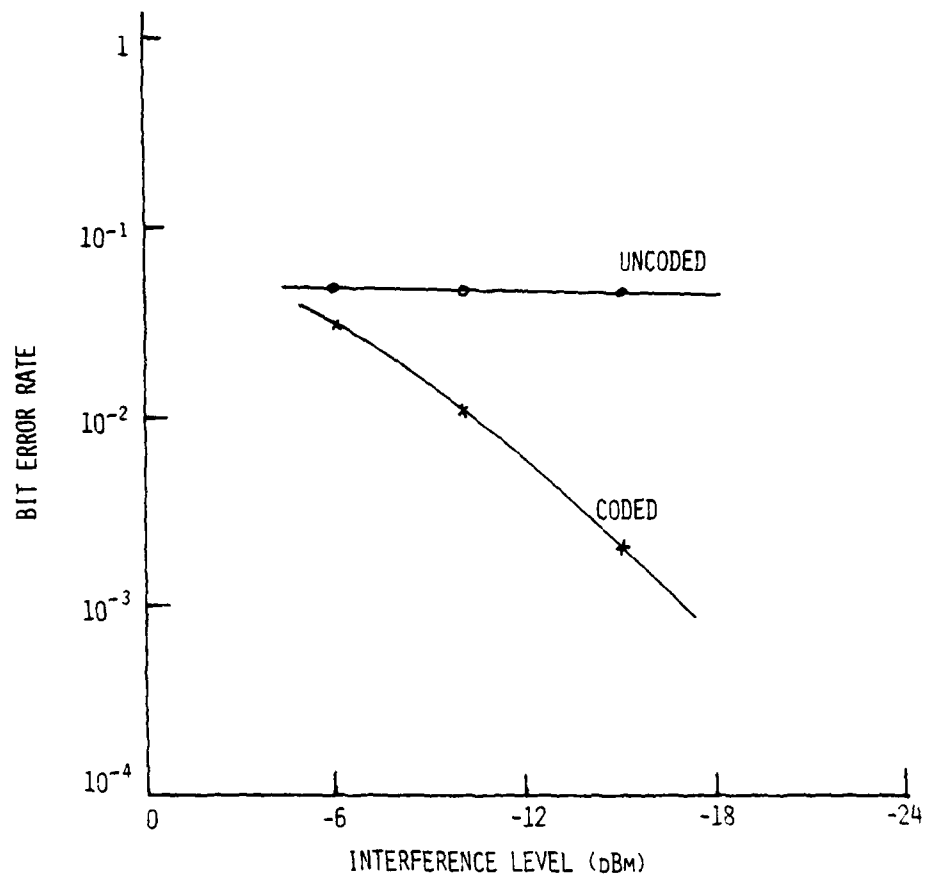


Fig. 24 — CW interference number 1,  
 $P/N_o = 42$  dB

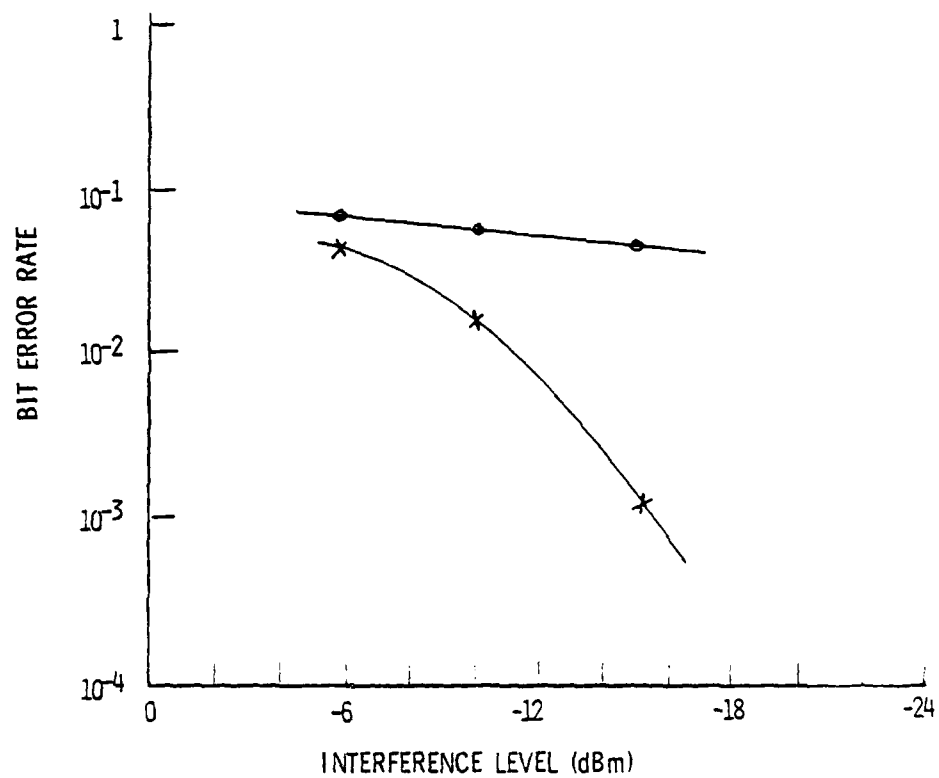


Fig. 25 — Interference by CW number 2,  
 $P/N_0 = 42$  dB

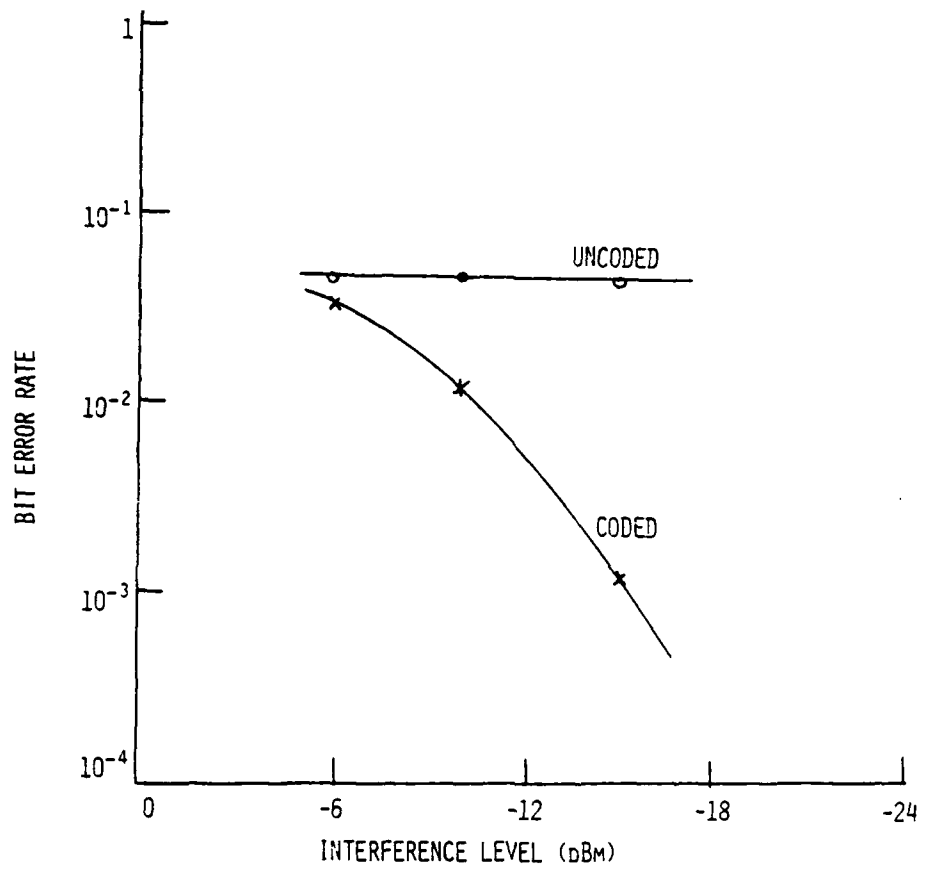


Fig. 26 — CW interference number 3,  
 $P/N_o = 42$  dB

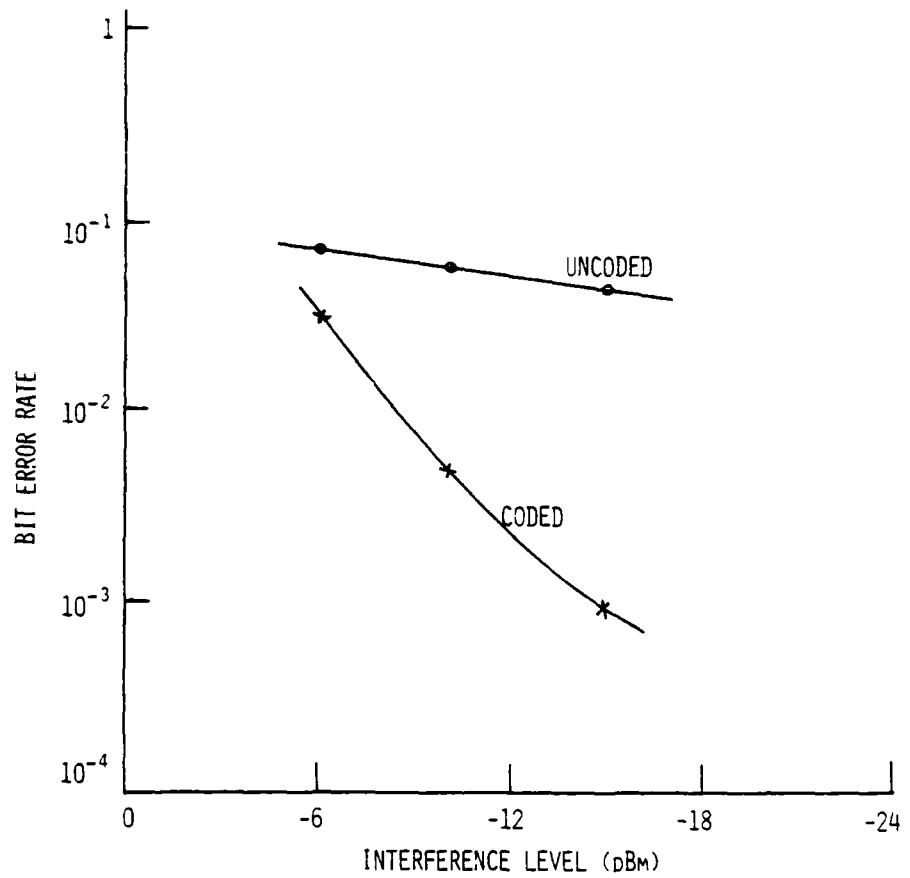


Fig. 27 — Swept tone interference,  
 $P/N_o = 42$  dB

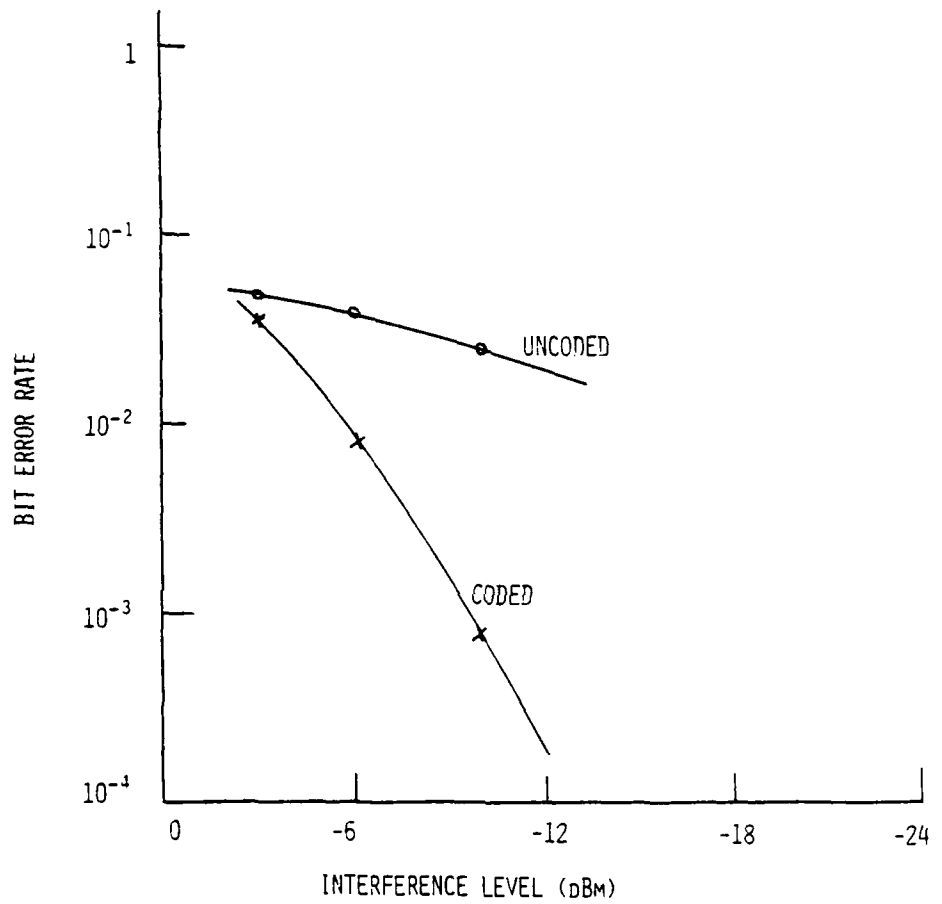


Fig. 28 — Swept tone interference,  
 $P/N_o = 49.4$  dB

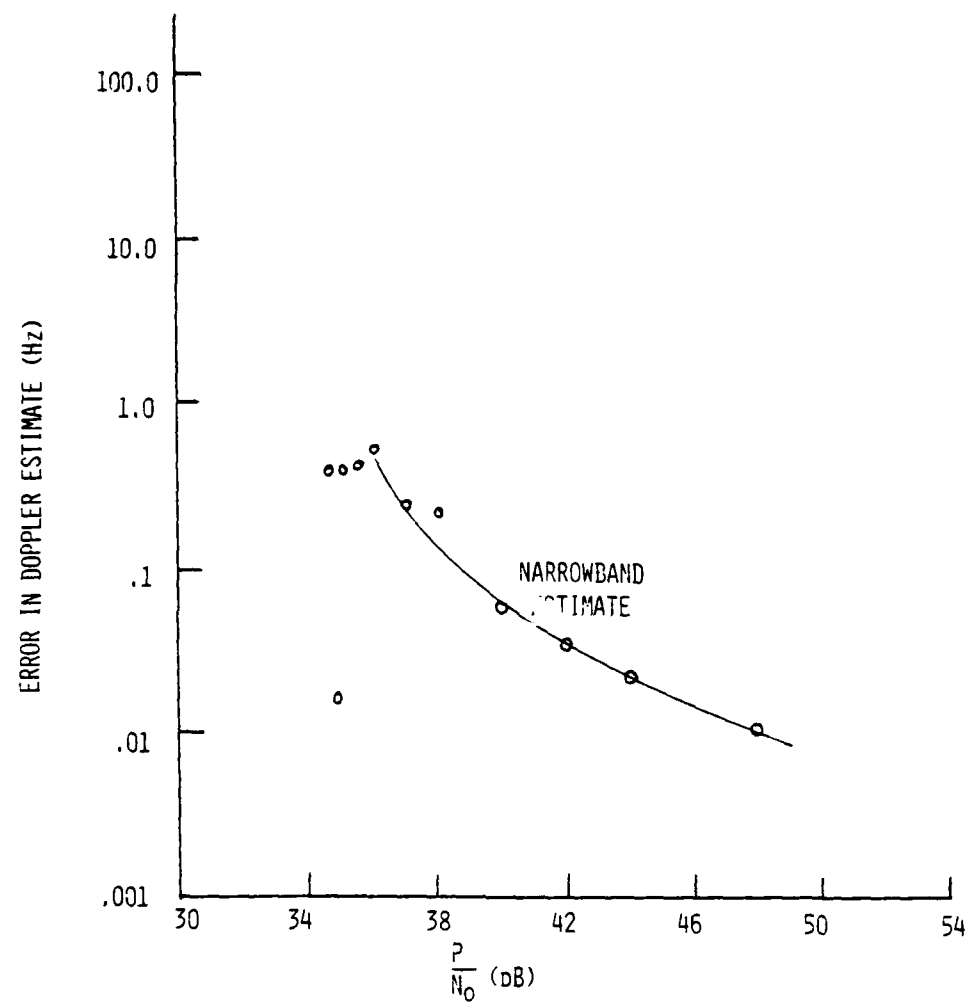


Fig. 29 — Doppler performance for frequency error of 0 Hz

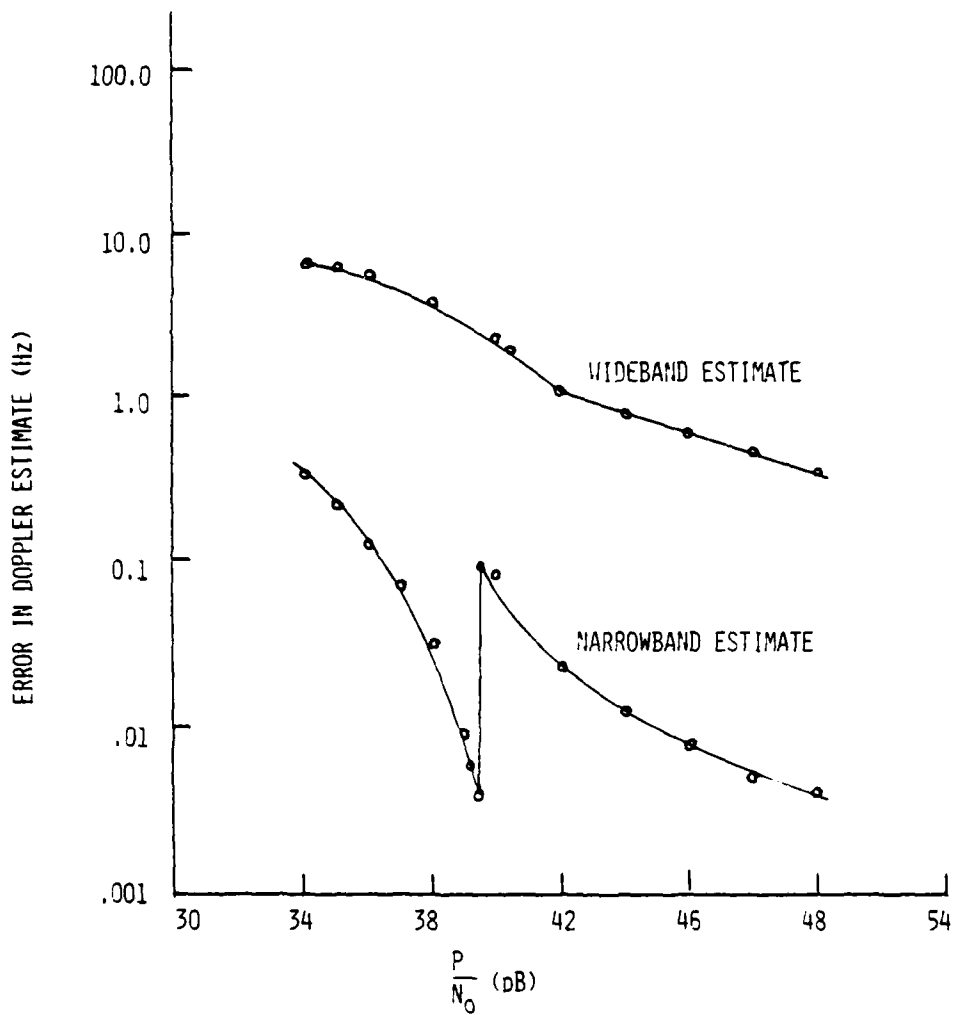


Fig. 30 — Doppler performance for frequency error of 50 Hz

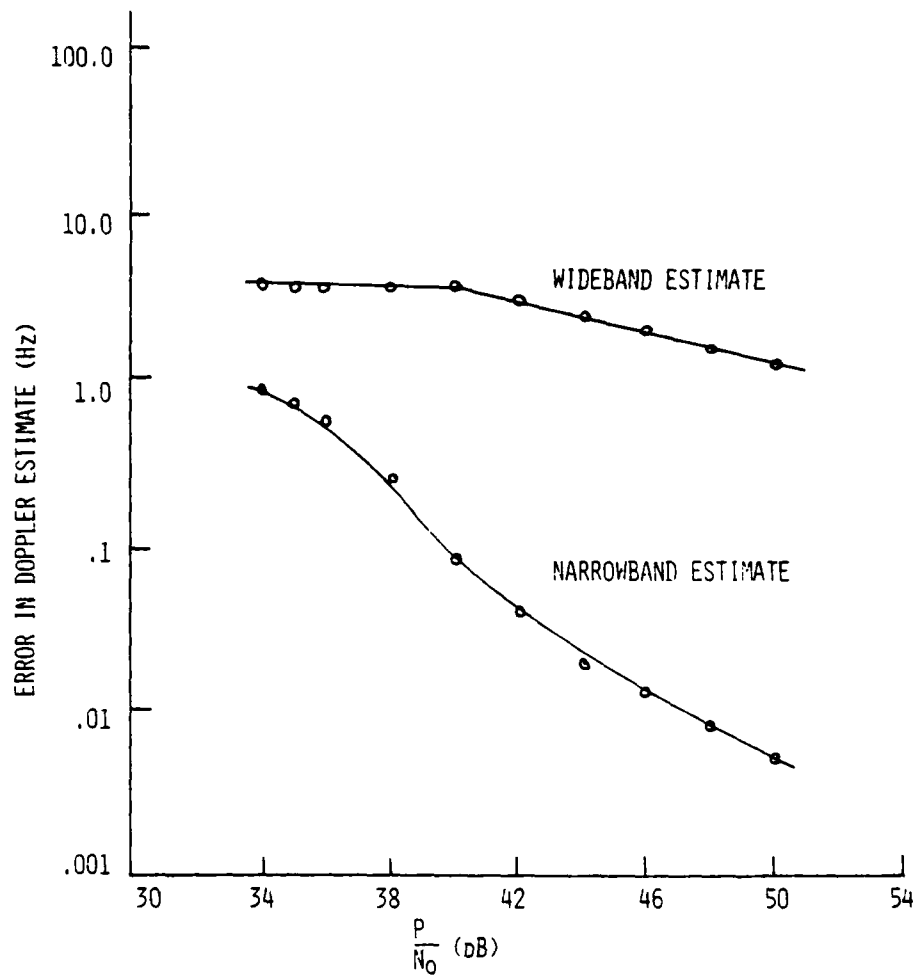


Fig. 31 — Doppler performance for frequency error of 62.5 Hz

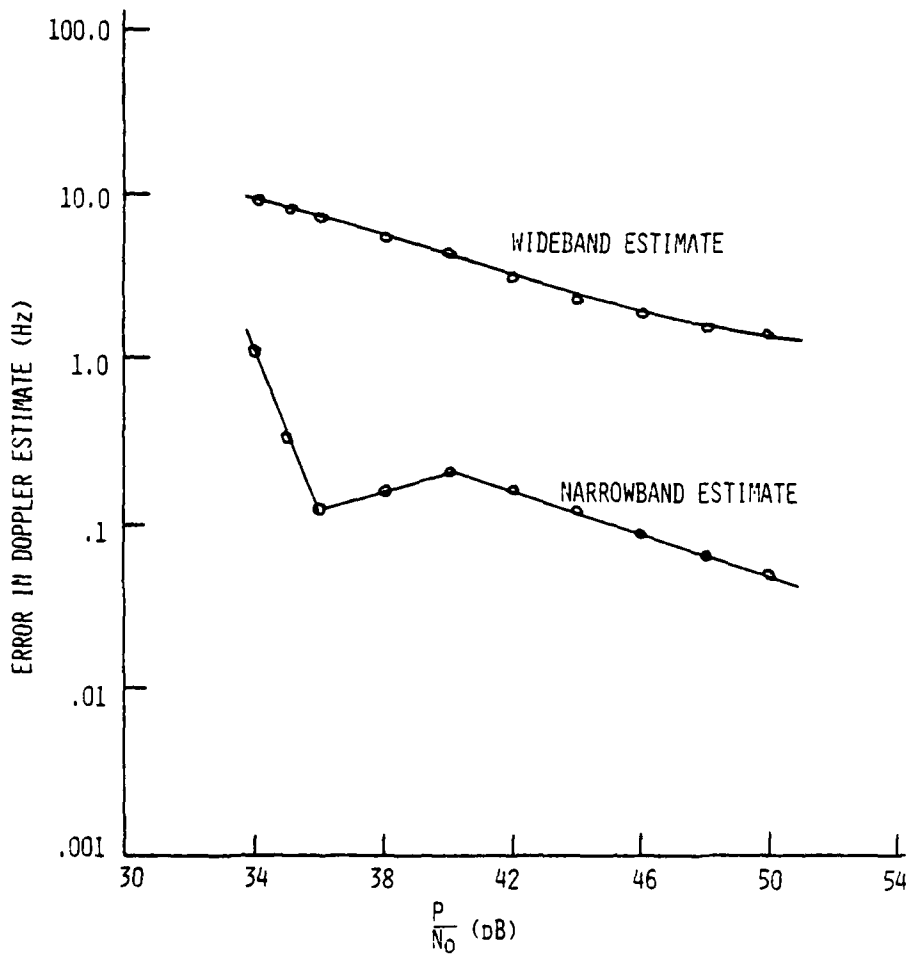


Fig. 32 — Doppler performance for frequency error of 75 Hz

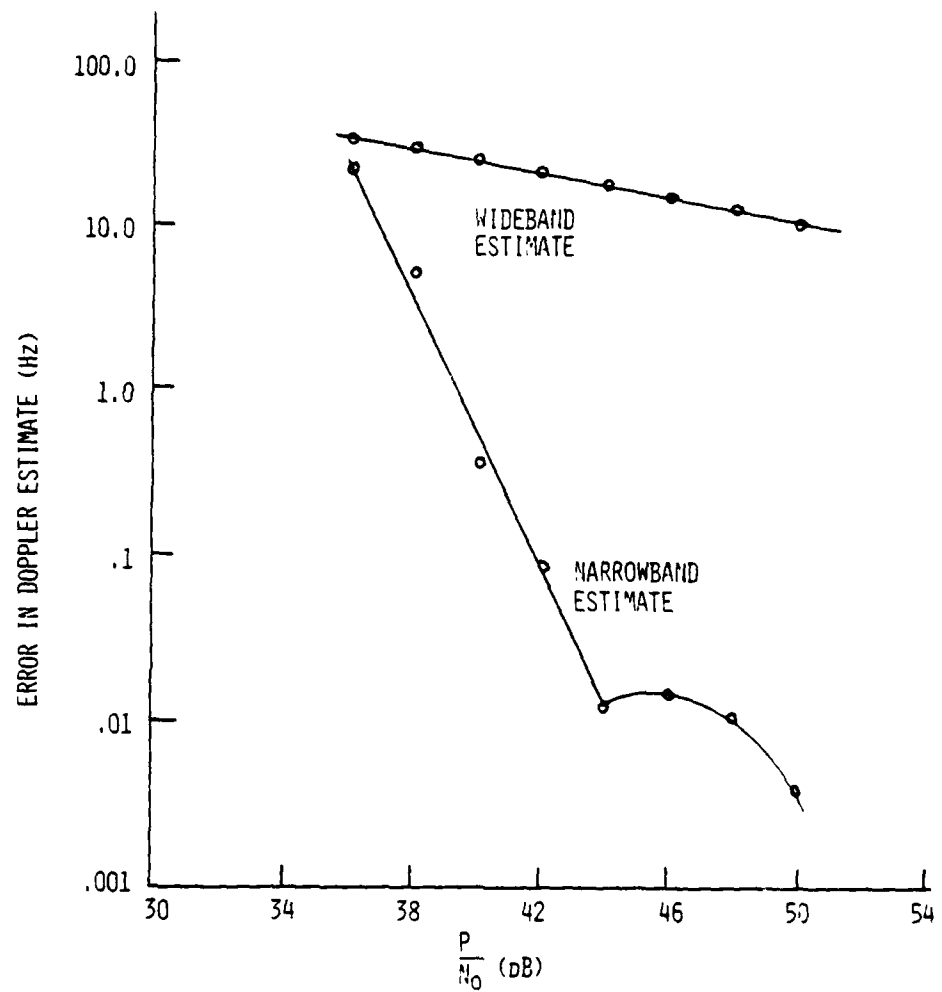


Fig. 33 — Doppler performance for frequency error of 112.5 Hz

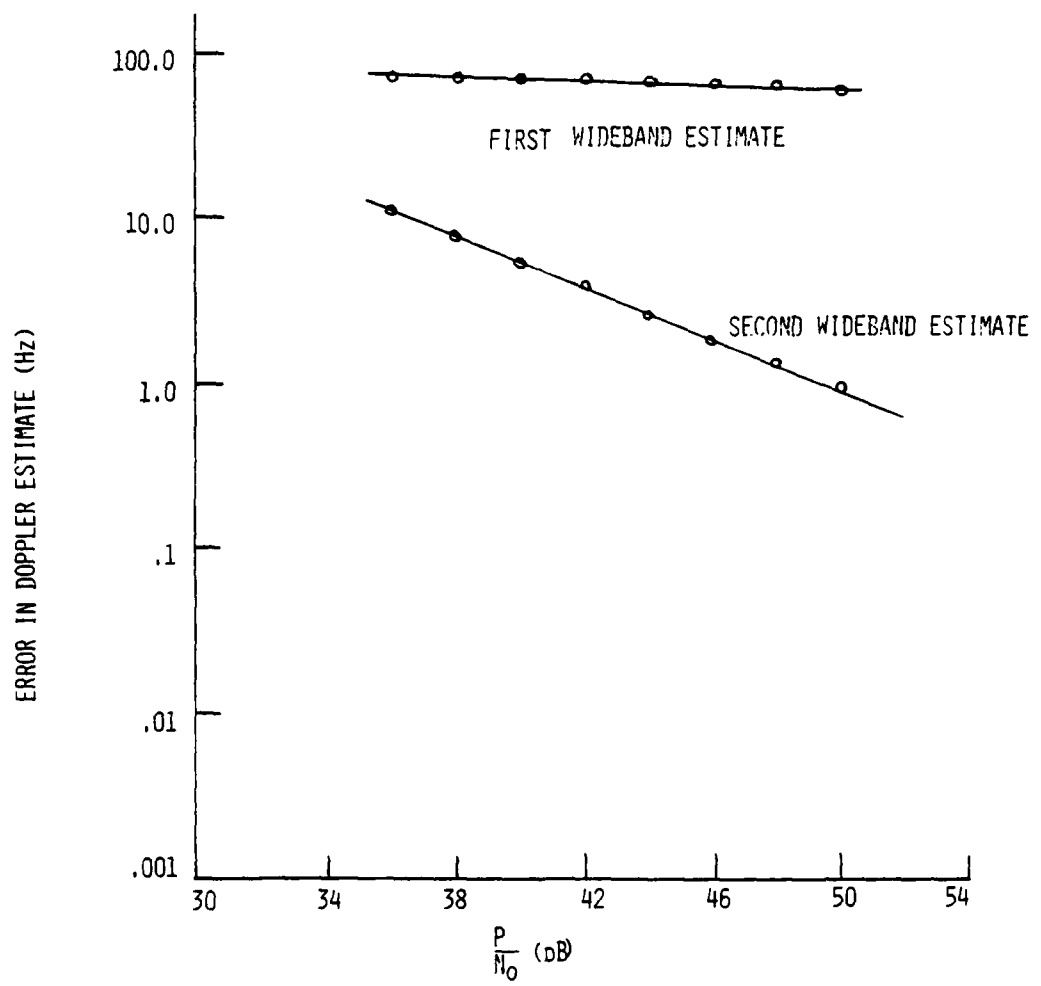


Fig. 34 — Doppler performance for frequency error of 150 Hz

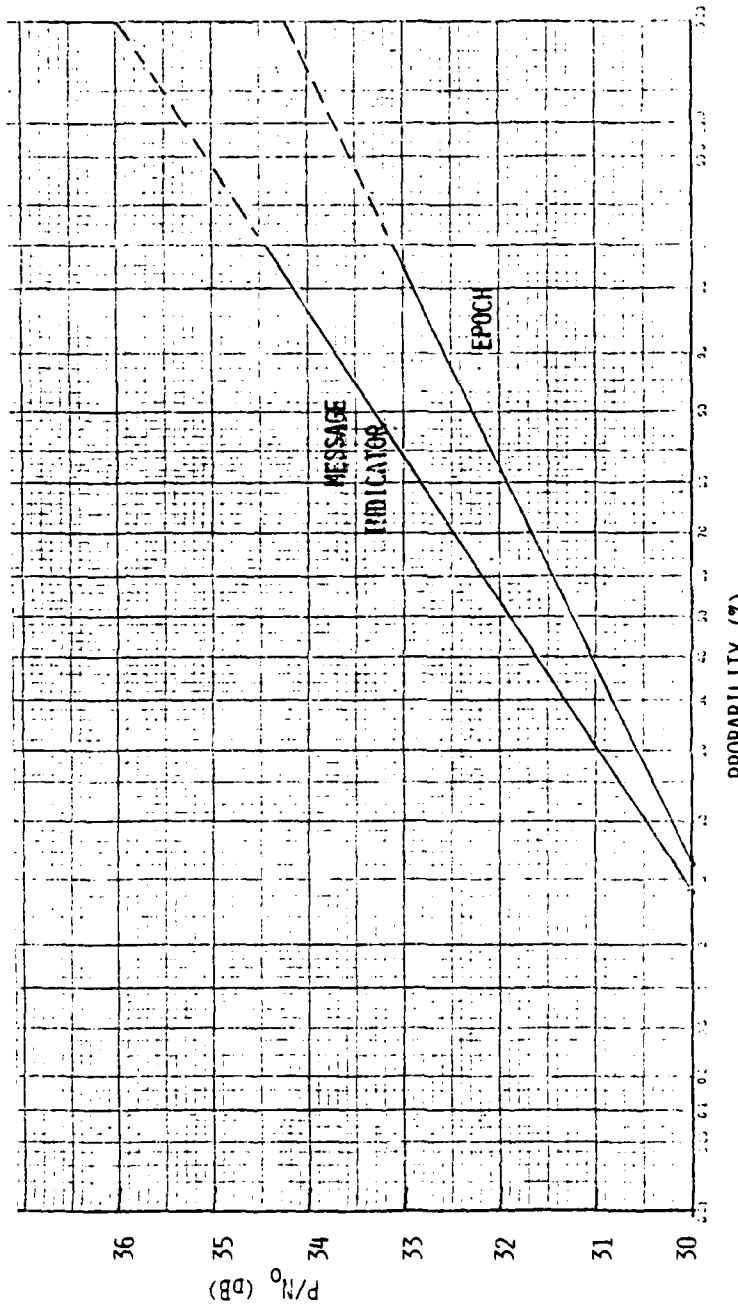


Fig. 35 – Probability of detecting a valid preamble

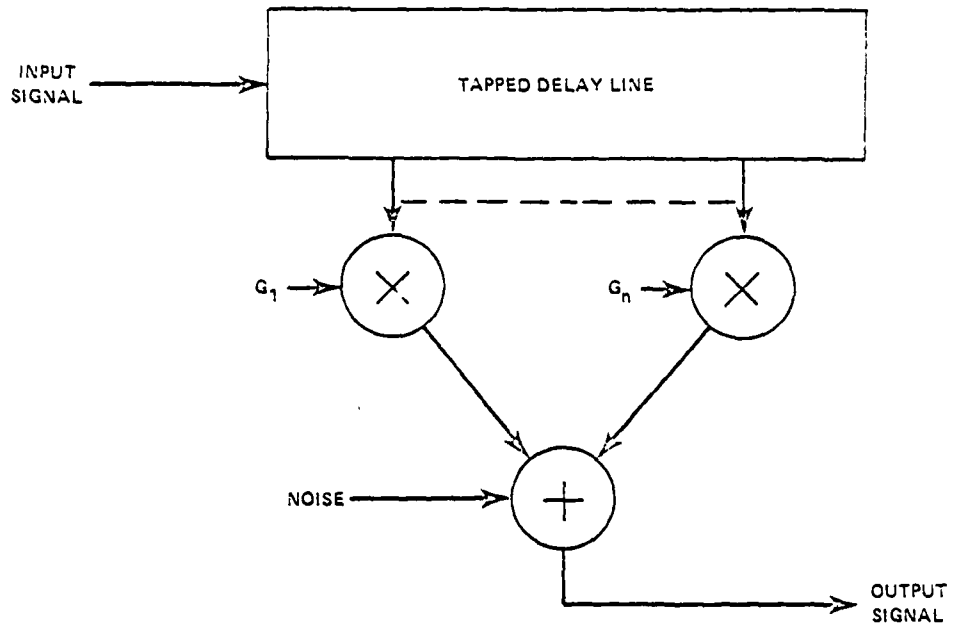


Fig. 36 — HF channel simulator

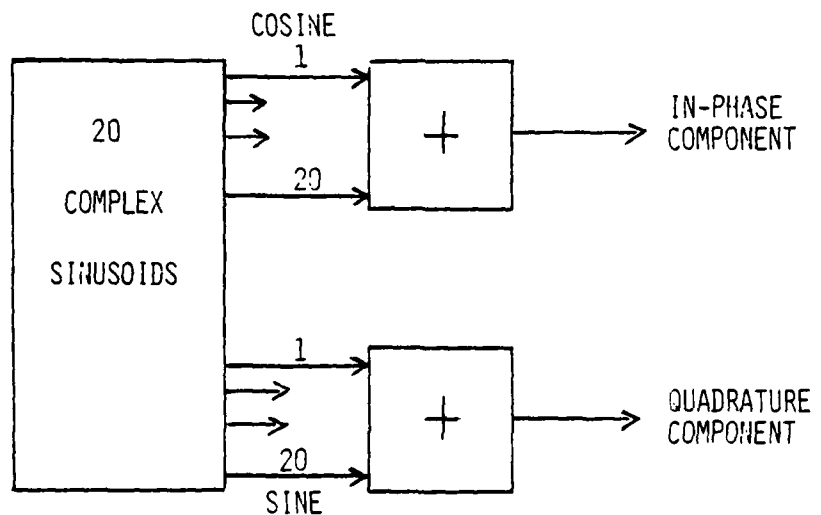


Fig. 37 — Generation of complex gain values for tapped delay line, software channel

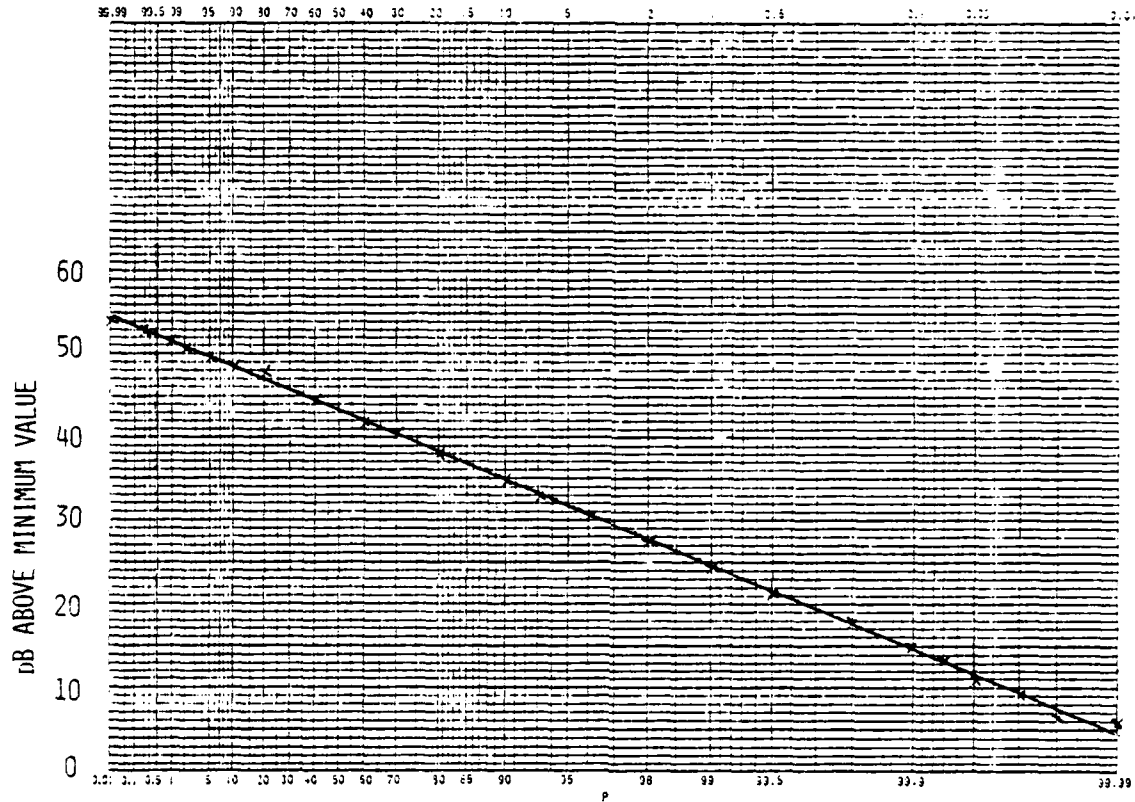


Fig. 38 — Cumulative amplitude distribution of fading path,  
generated by sum of 20 sinusoids with spread of  $\pm 1$  Hz  
(percentage of time the values are less than the ordinate (100-P))

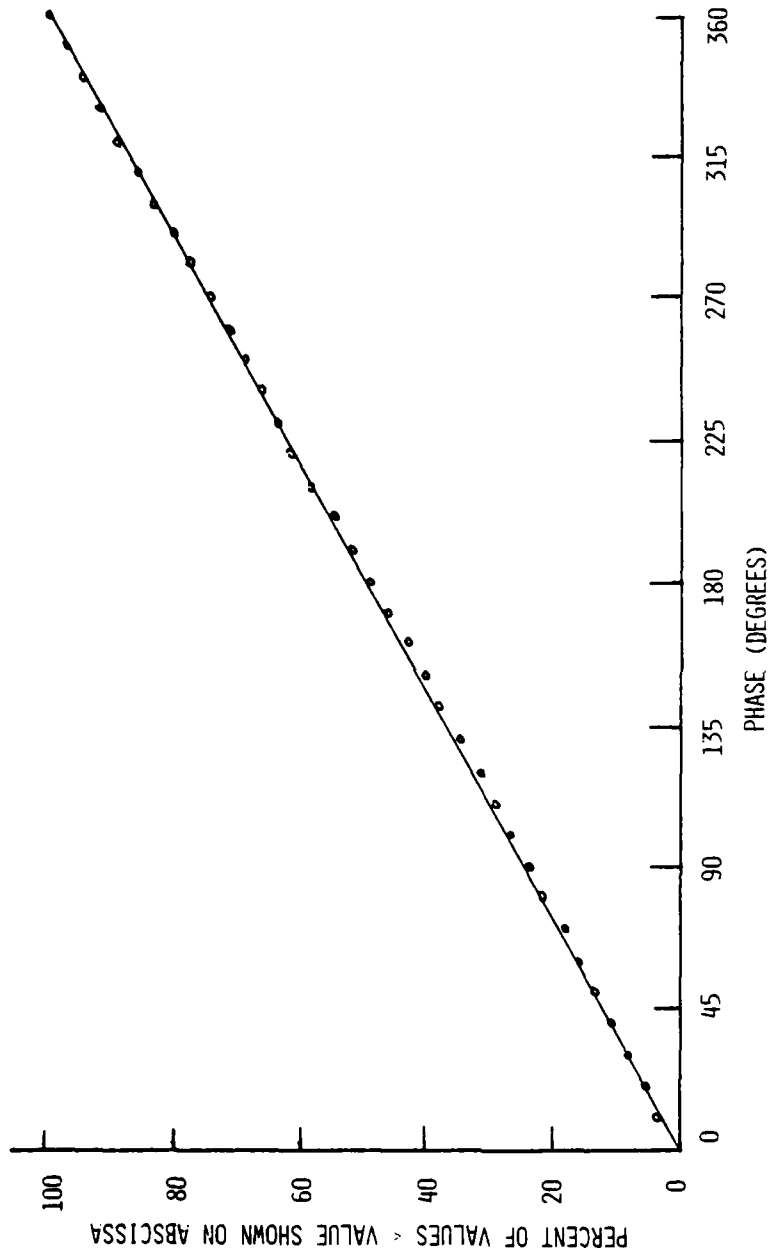


Fig. 39 — Cumulative distribution of phase of a fading signal, generated by sum of 20 sinusoids with spread of  $\pm 1$  Hz

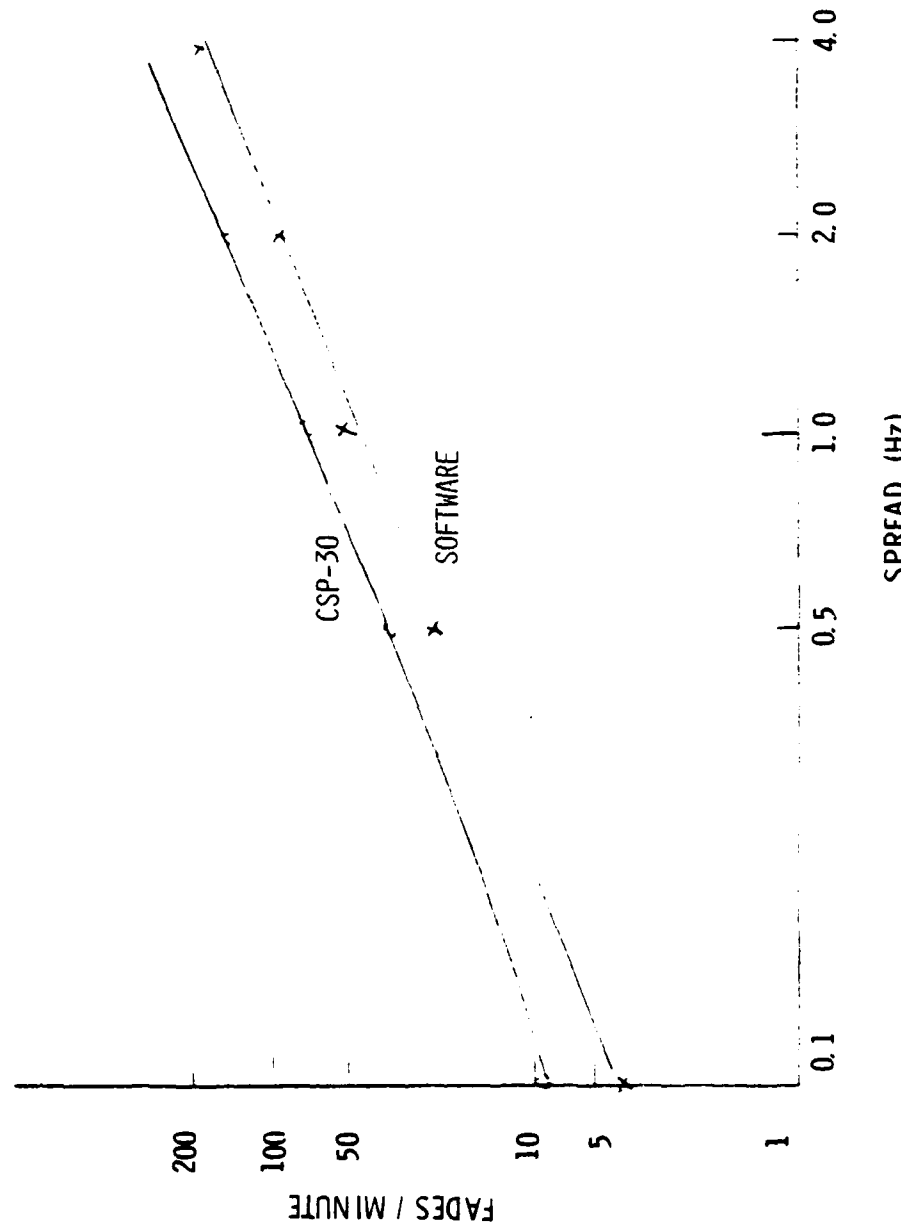


Fig. 40 — Fade rate vs frequency spread, one path,  
software channel and CSP-30

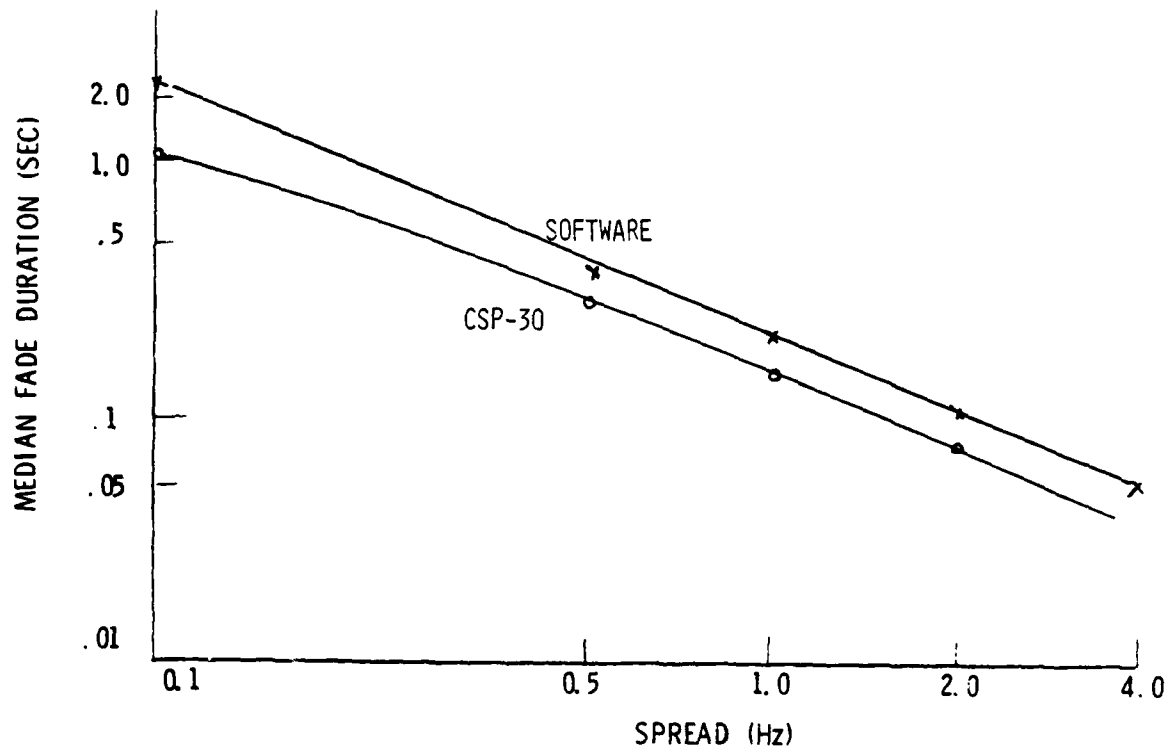


Fig. 41 — Median fade duration vs frequency spread,  
one path, software channel and CSP-30

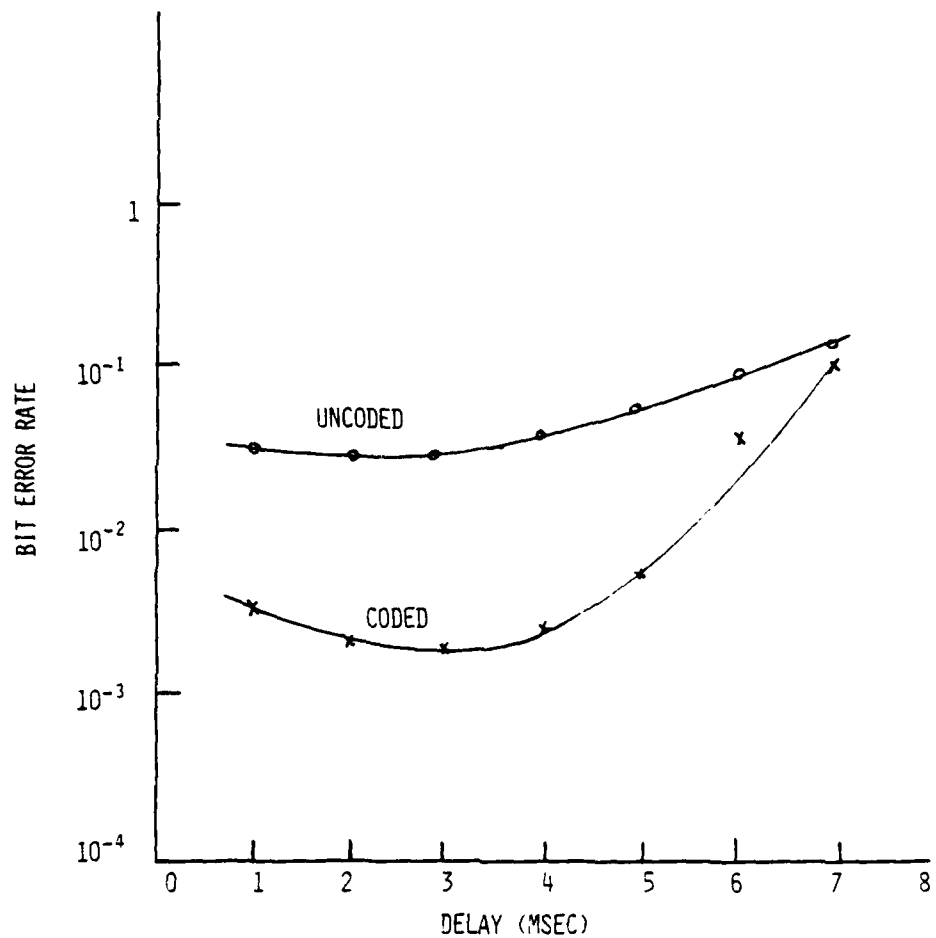


Fig. 42 — Two paths, 1 Hz spread,  $P/N_o = 49.4$  dB

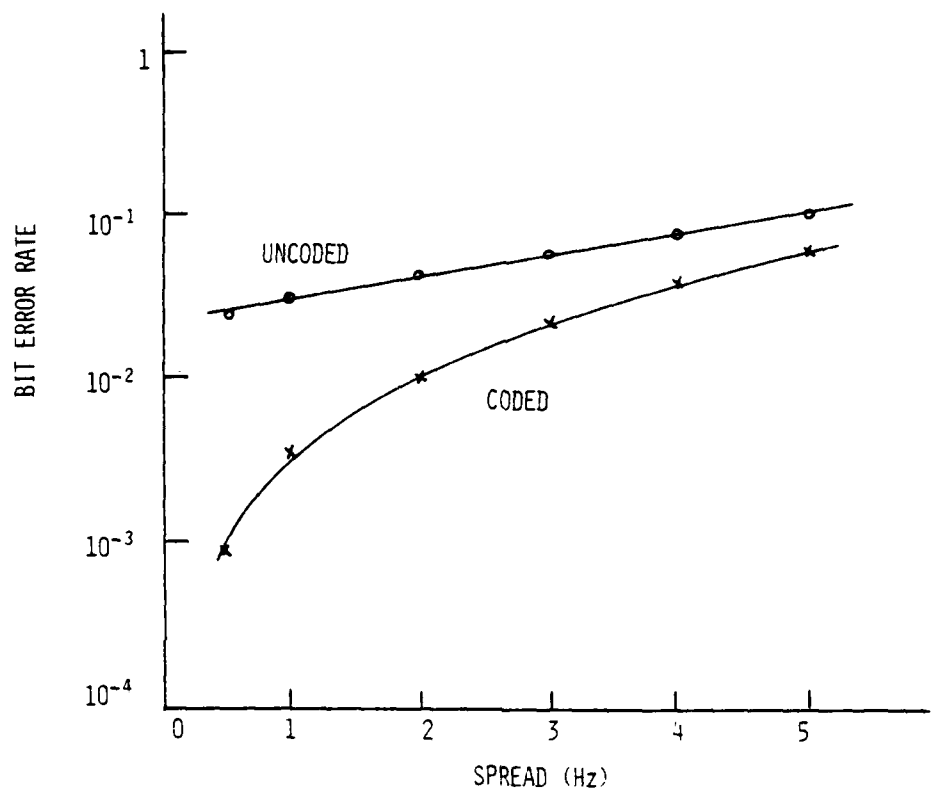


Fig. 43 — Two paths, 1 msec delay,  $P/N_0 = 49.4$  dB

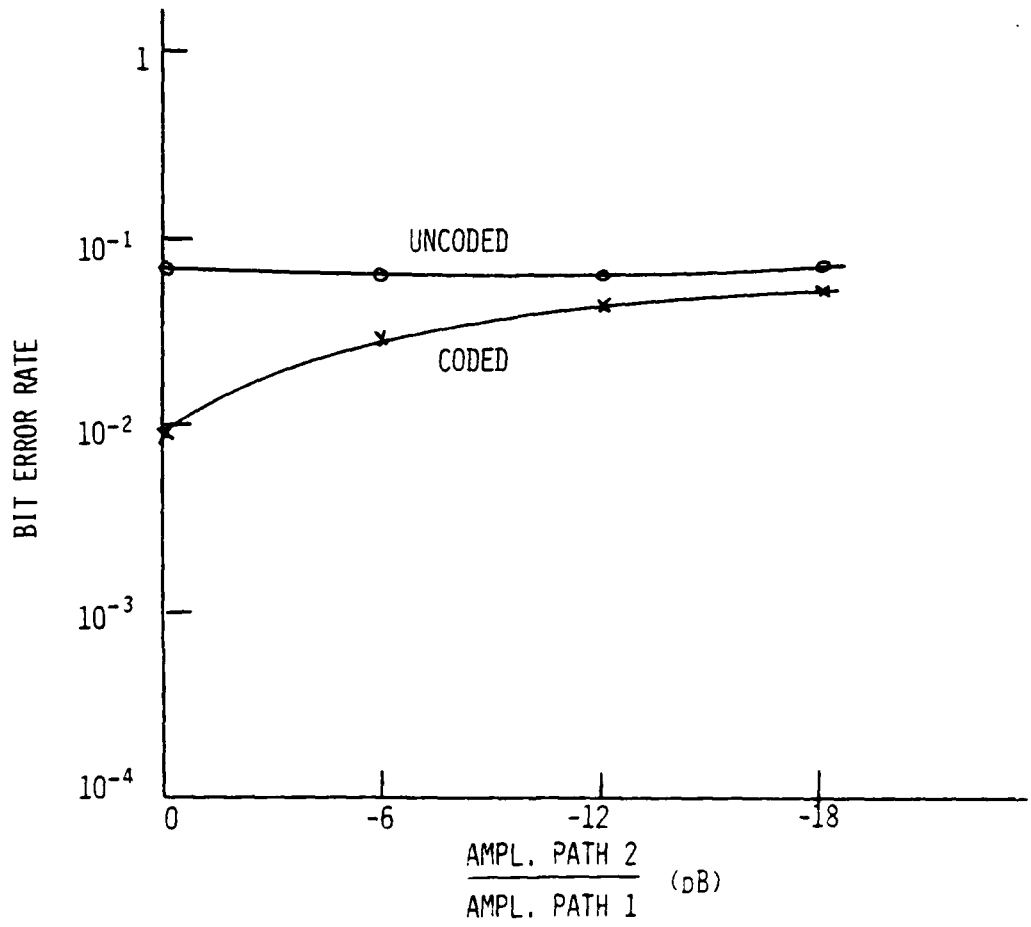


Fig. 44 — Bit error rate vs relative amplitude. Two paths of unequal amplitude, 1 Hz spread, 1 msec delay,  $P/N_0 = 49.4$  dB.

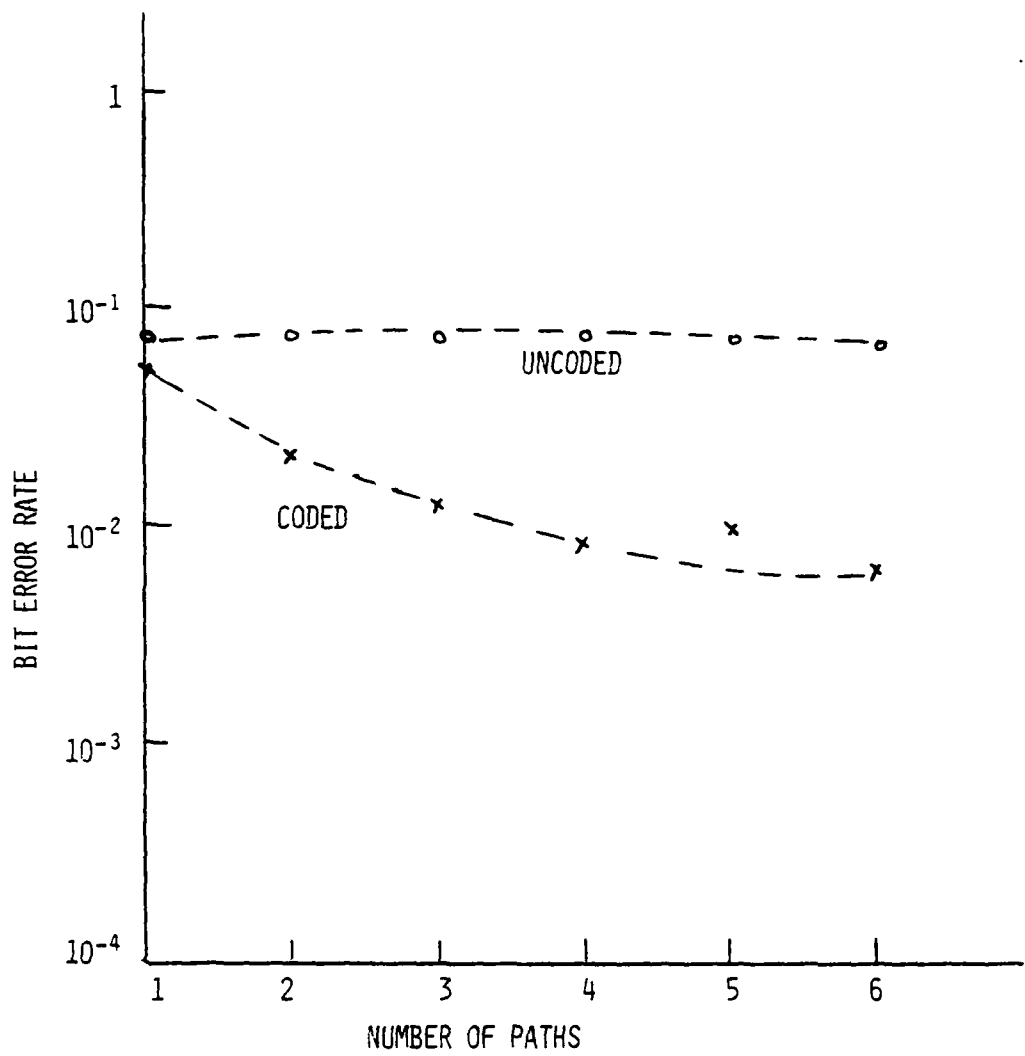


Fig. 45 — Bit error rate vs number of paths, equal amplitudes,  
 1 Hz spread,  $P/N_o = 44.4$  dB

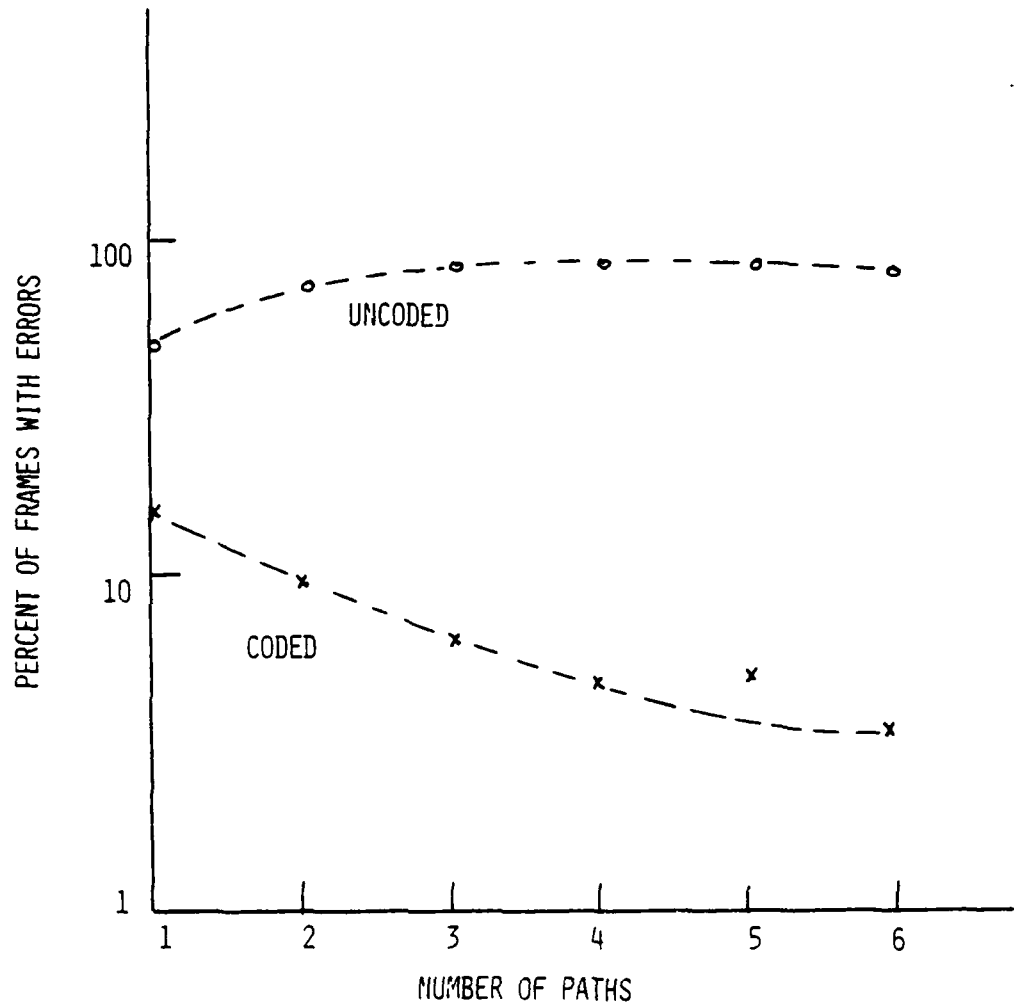


Fig. 46 — Percent of frames with errors vs number of paths,  
equal amplitudes, 1 Hz spread,  $P/N_o = 44.4$  dB

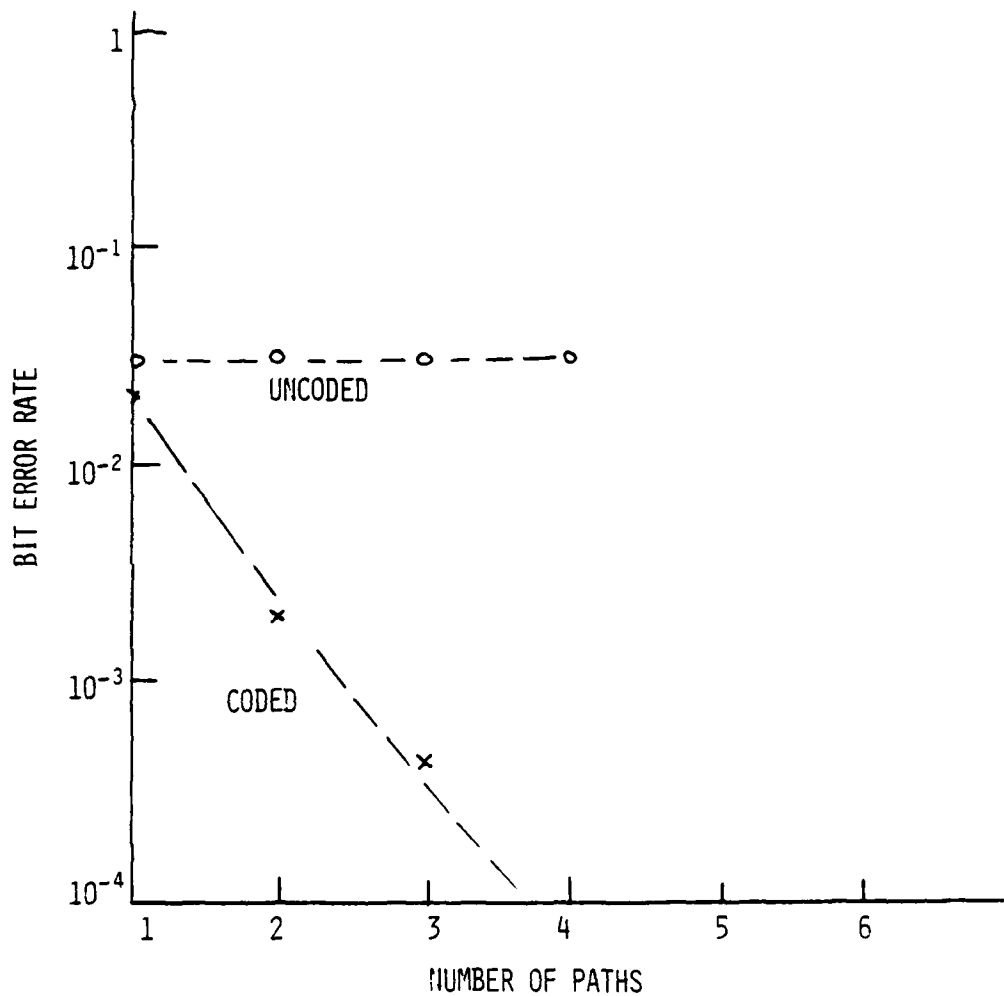


Fig. 47 — Bit error rate vs number of paths, equal amplitudes,  
1 Hz spread,  $P/N_0 = 49.4$  dB

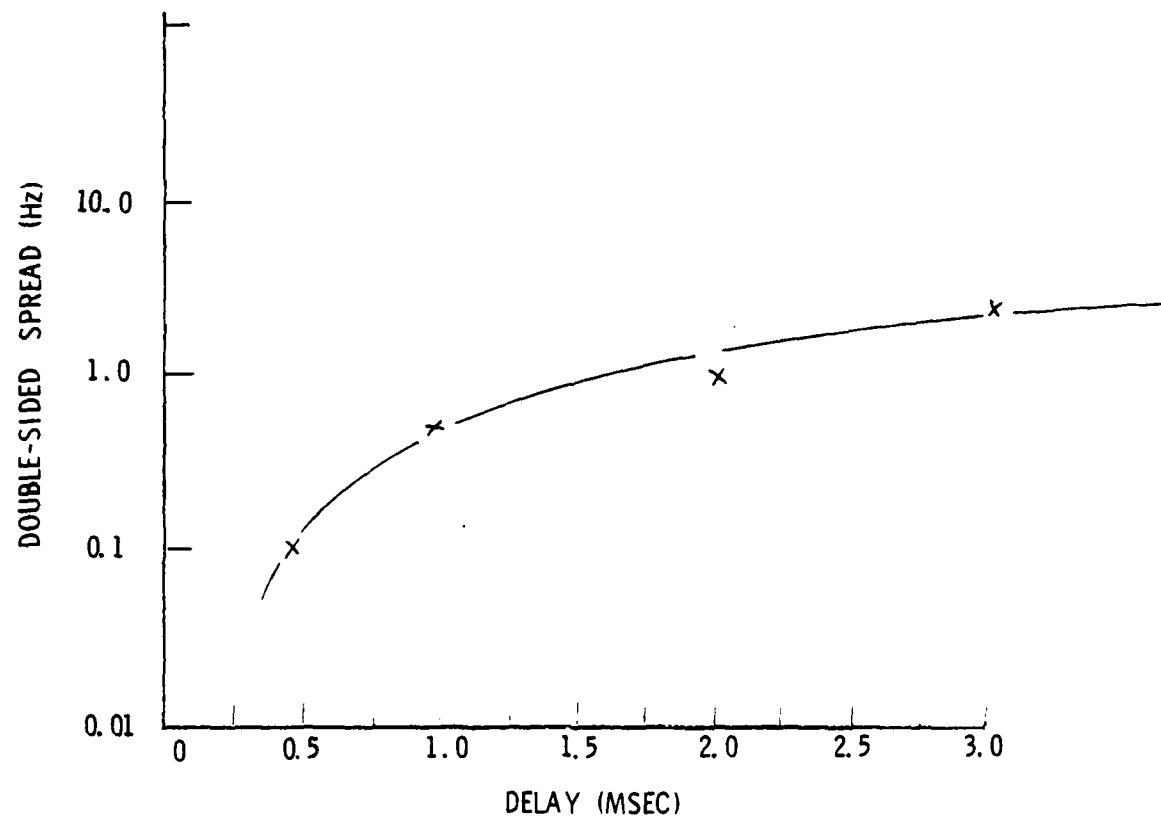


Fig. 48 — CCIR channel parameters

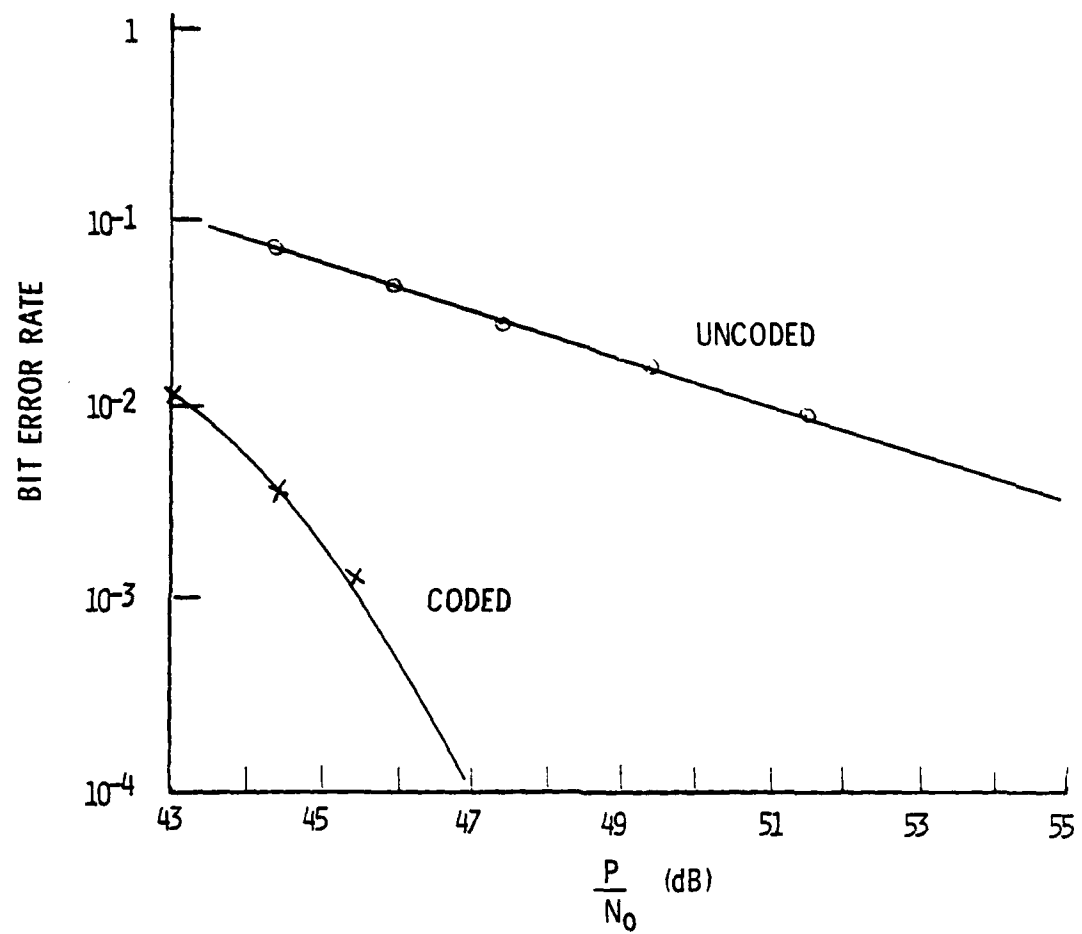


Fig. 49 — CCIR channel number 1

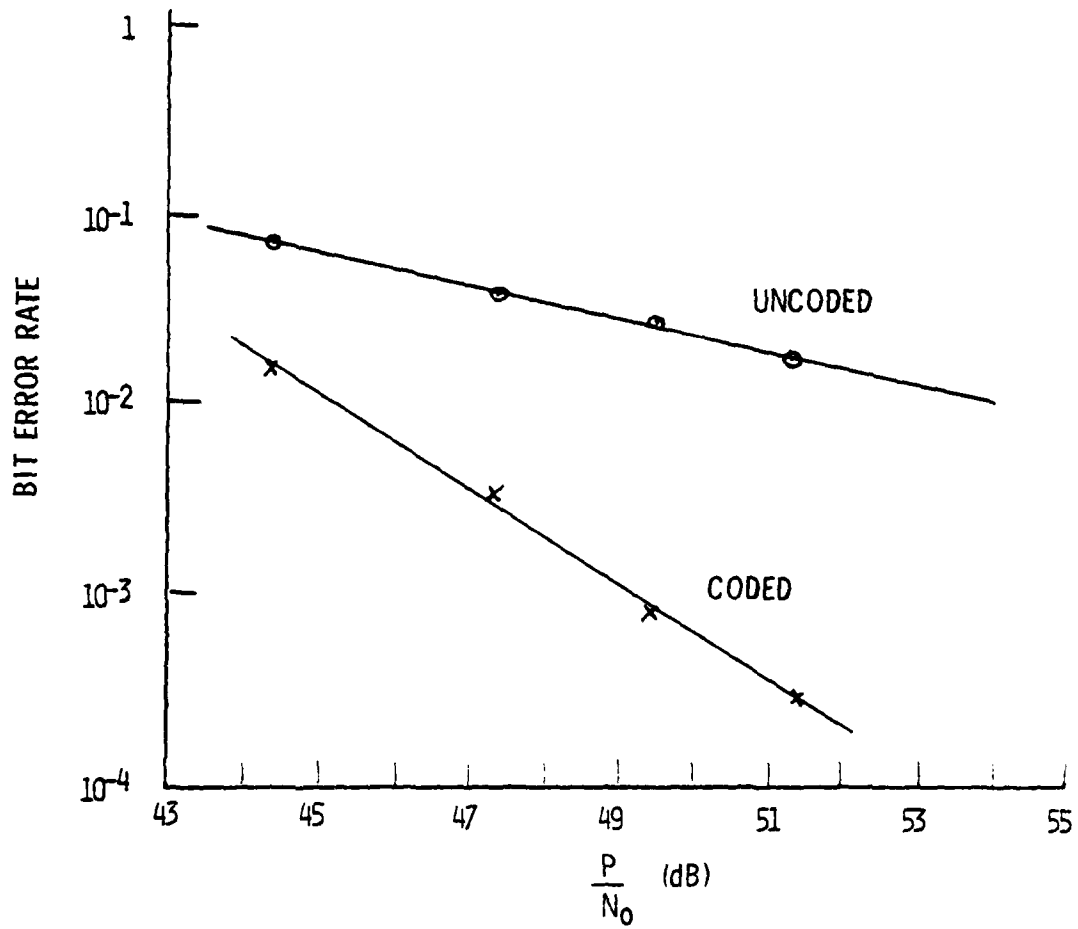


Fig. 50 - CCIR channel number 2

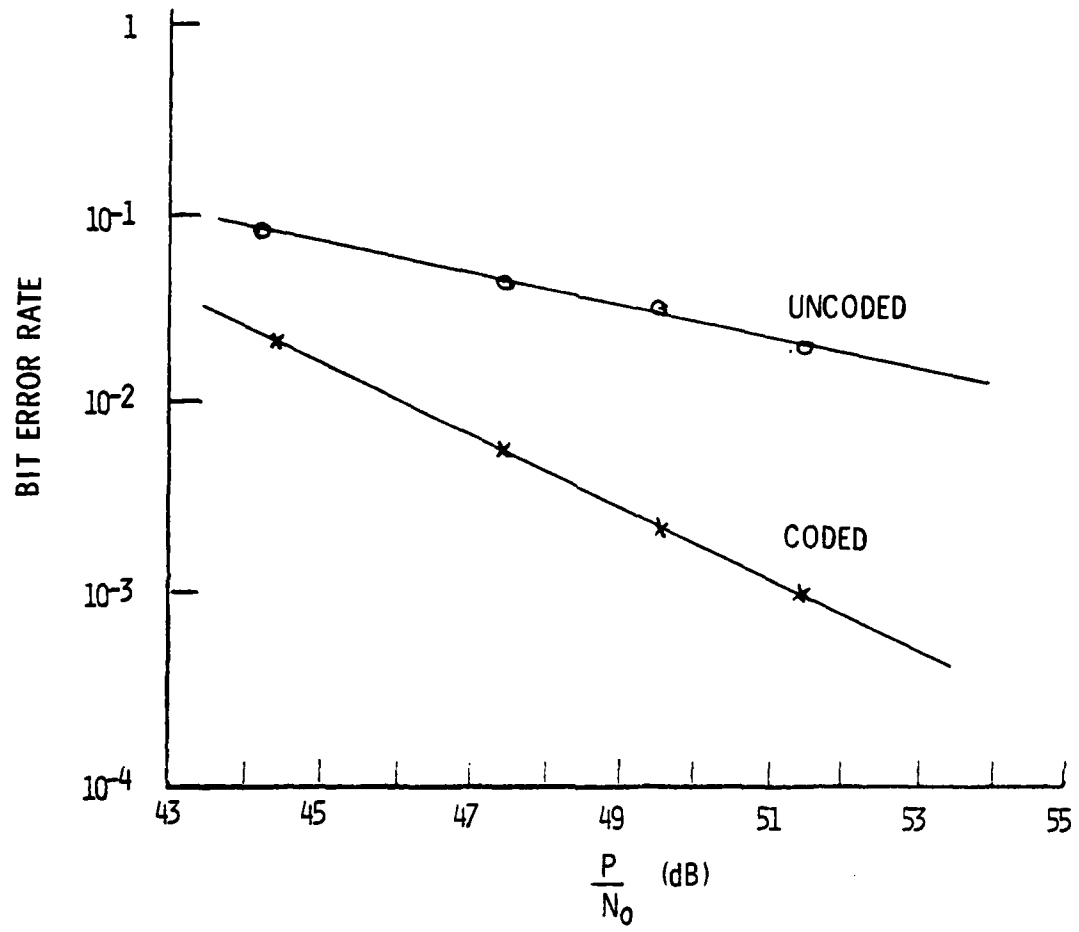


Fig. 51 — CCIR channel number 3

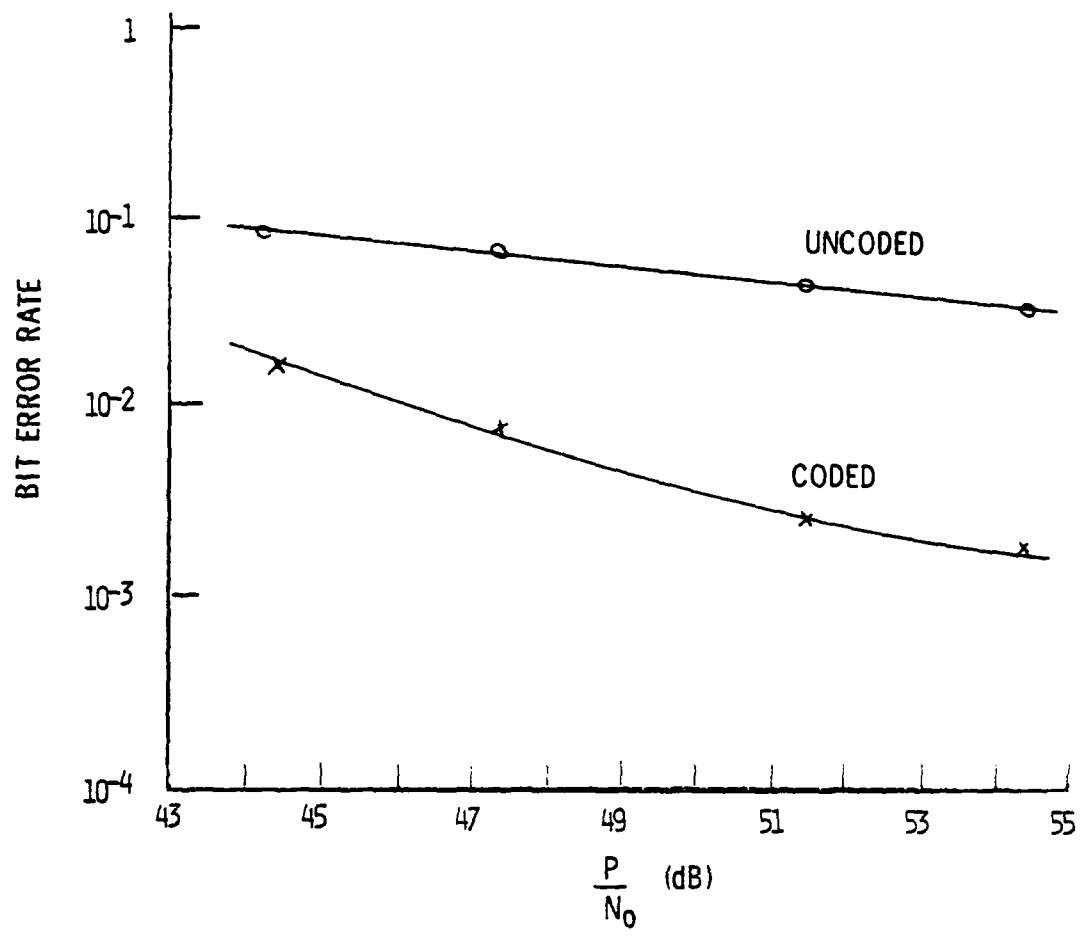


Fig. 52 — CCIR channel number 4

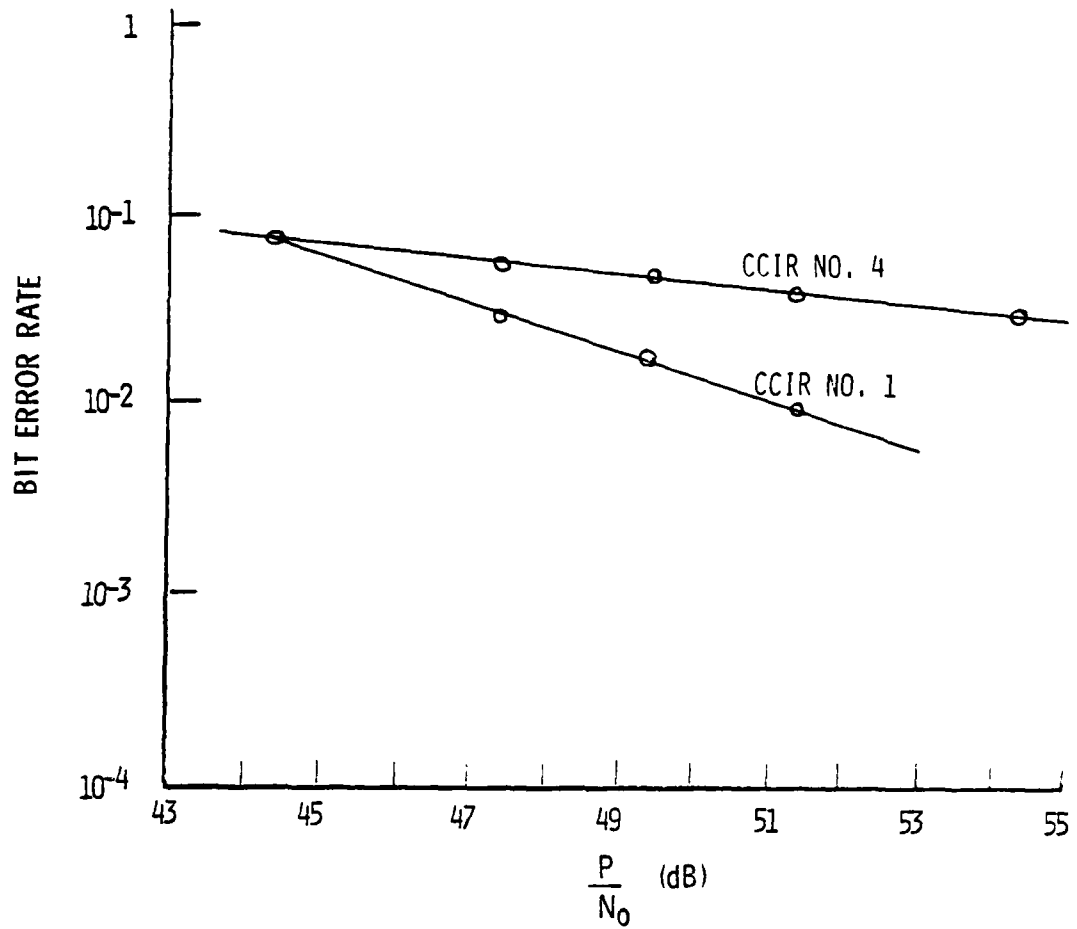


Fig. 53 — Comparison of CCIR number 1 and CCIR number 4 uncoded data

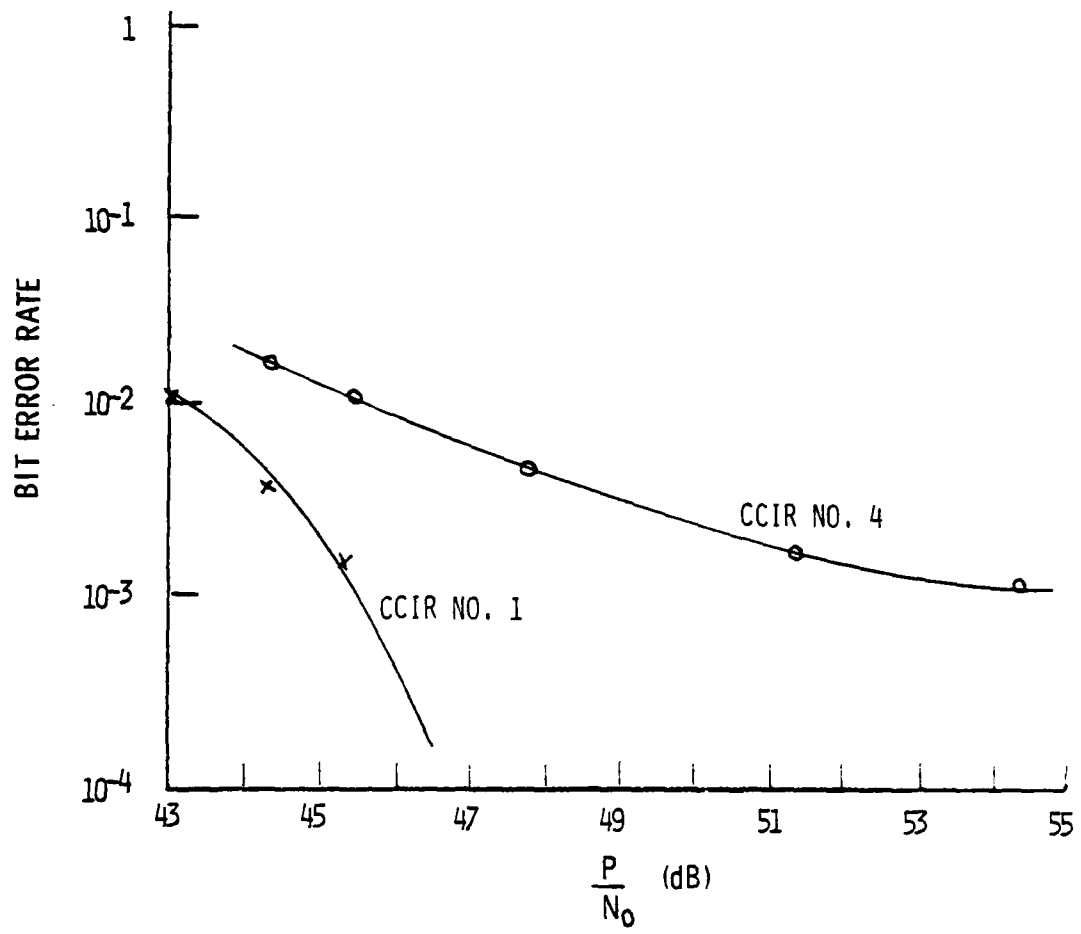


Fig. 54 — Comparison CCIR number 1 and CCIR number 4 coded data

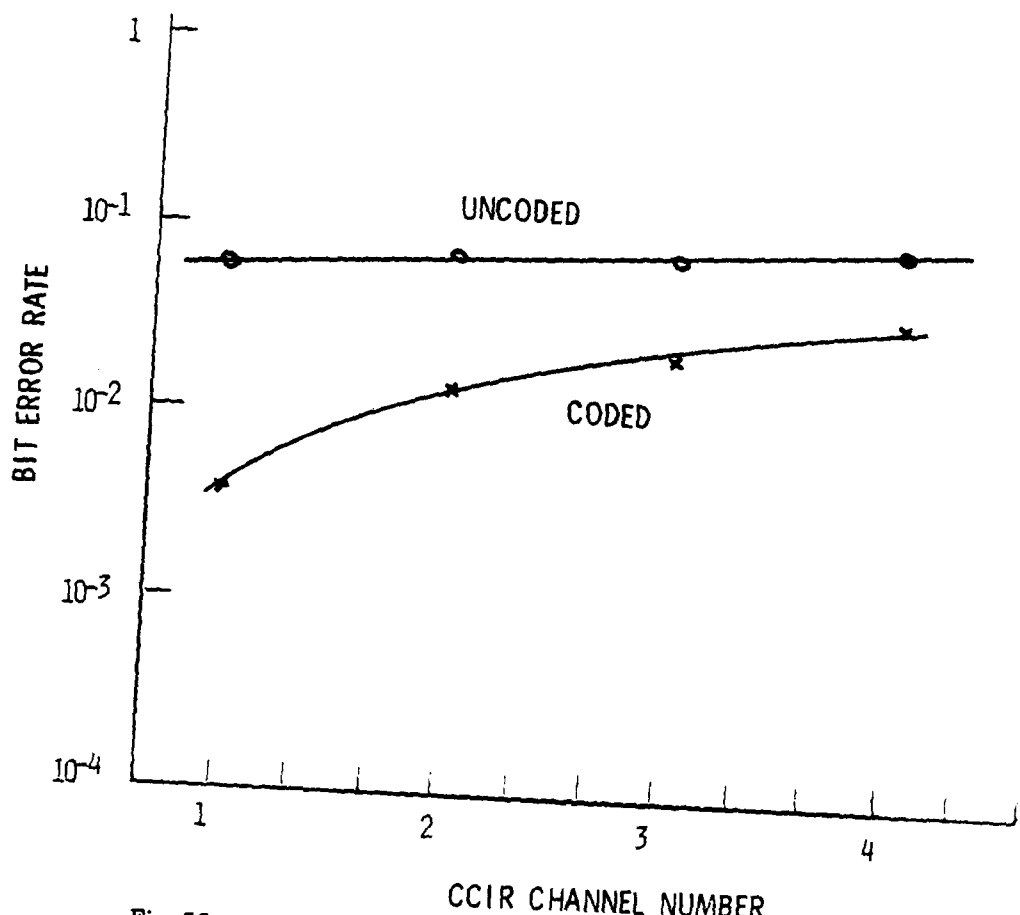


Fig. 55 — Comparison of four CCIR channels at  $P/N_o = 44.4$  dB

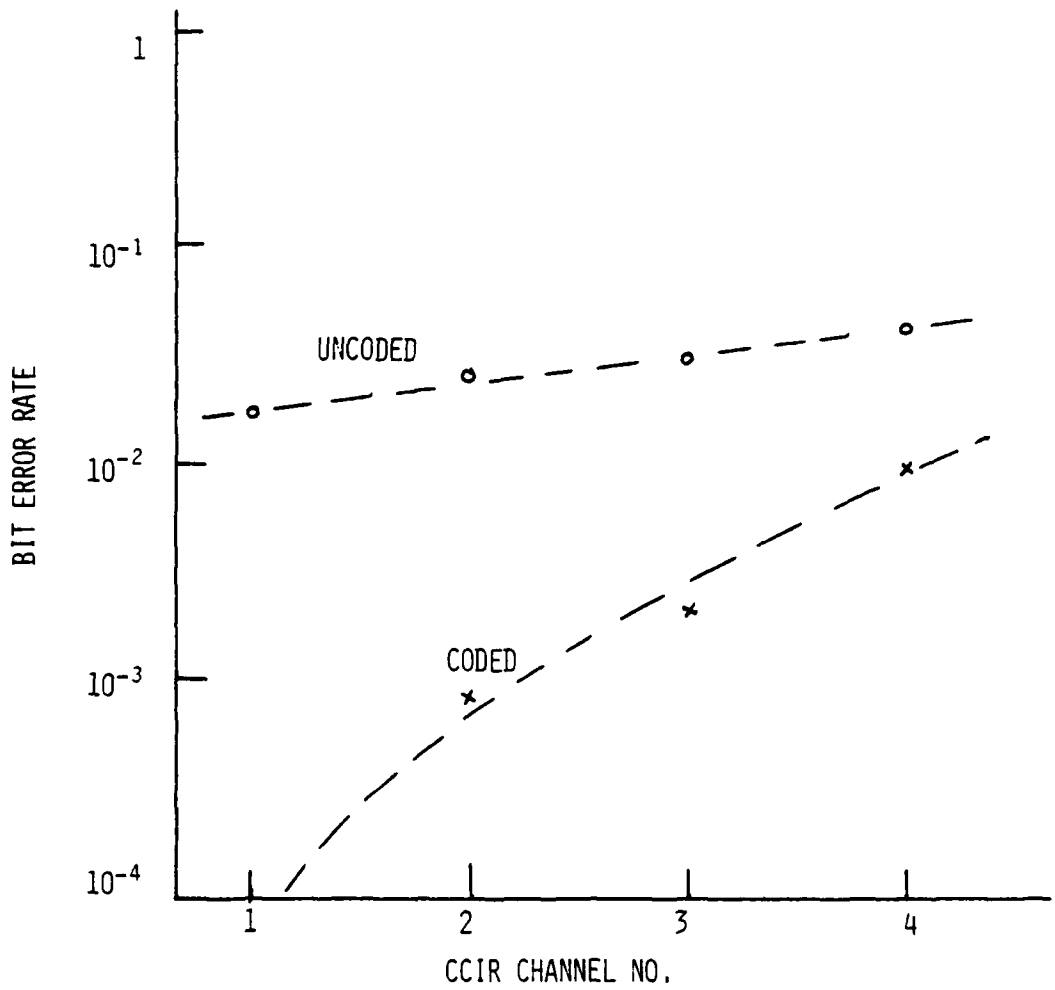


Fig. 56 — Comparison of four CCIR channels  
at  $P/N_o = 49.4$  dB

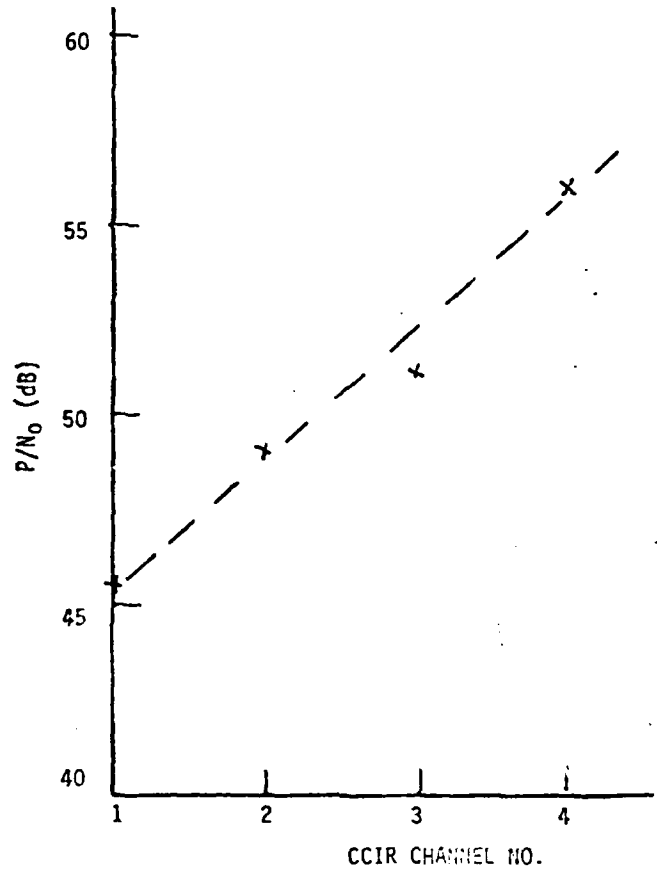


Fig. 57 —  $P/N_o$  vs CCIR channel number for coded bit error rate of  $1 \times 10^{-3}$

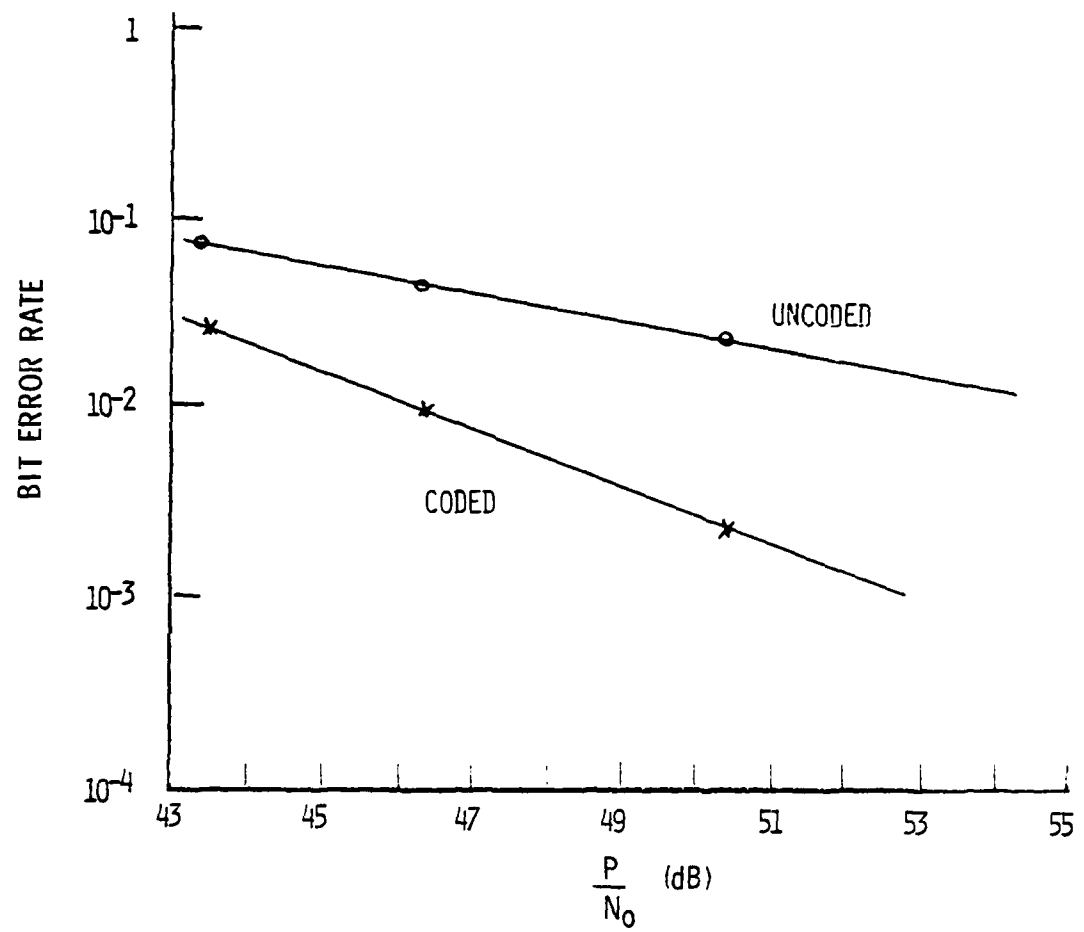


Fig. 58 — CNR 2-path model

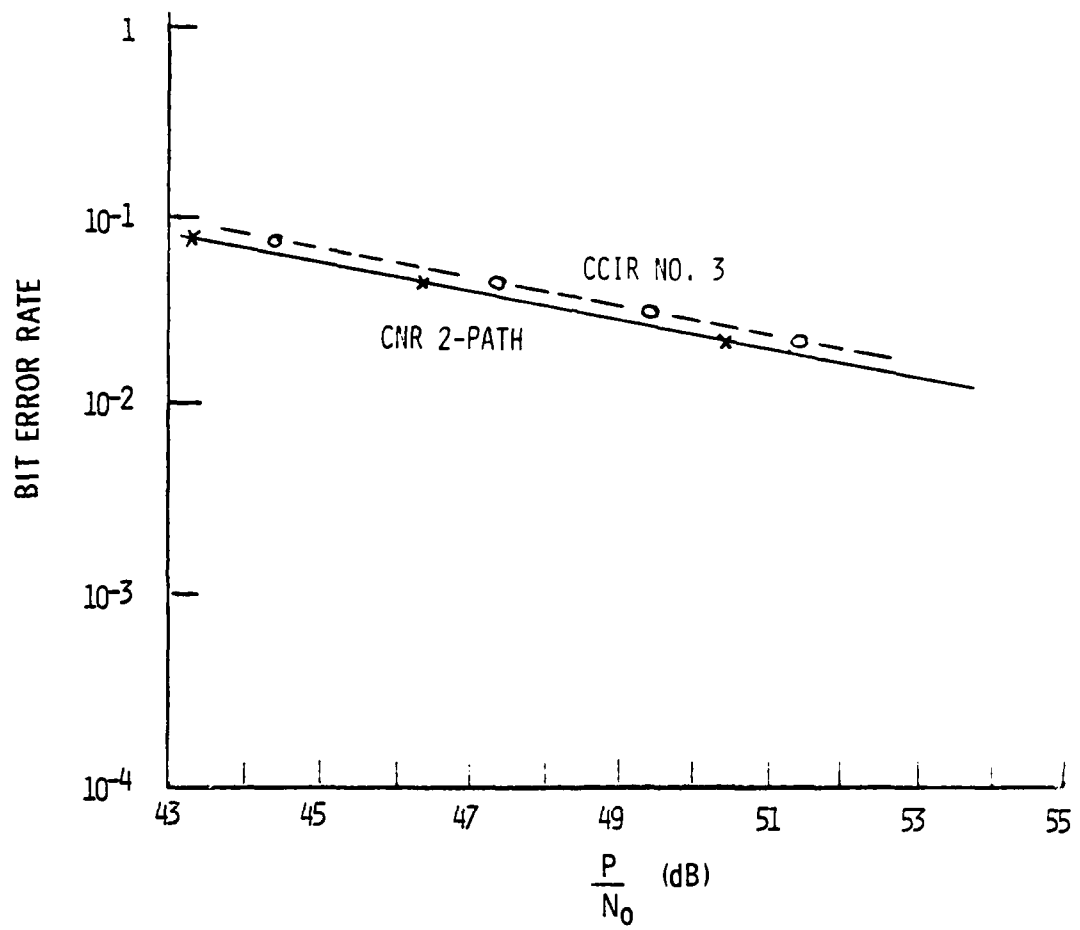


Fig. 59 -- Comparison of performance on two 2-path channel models, uncoded data

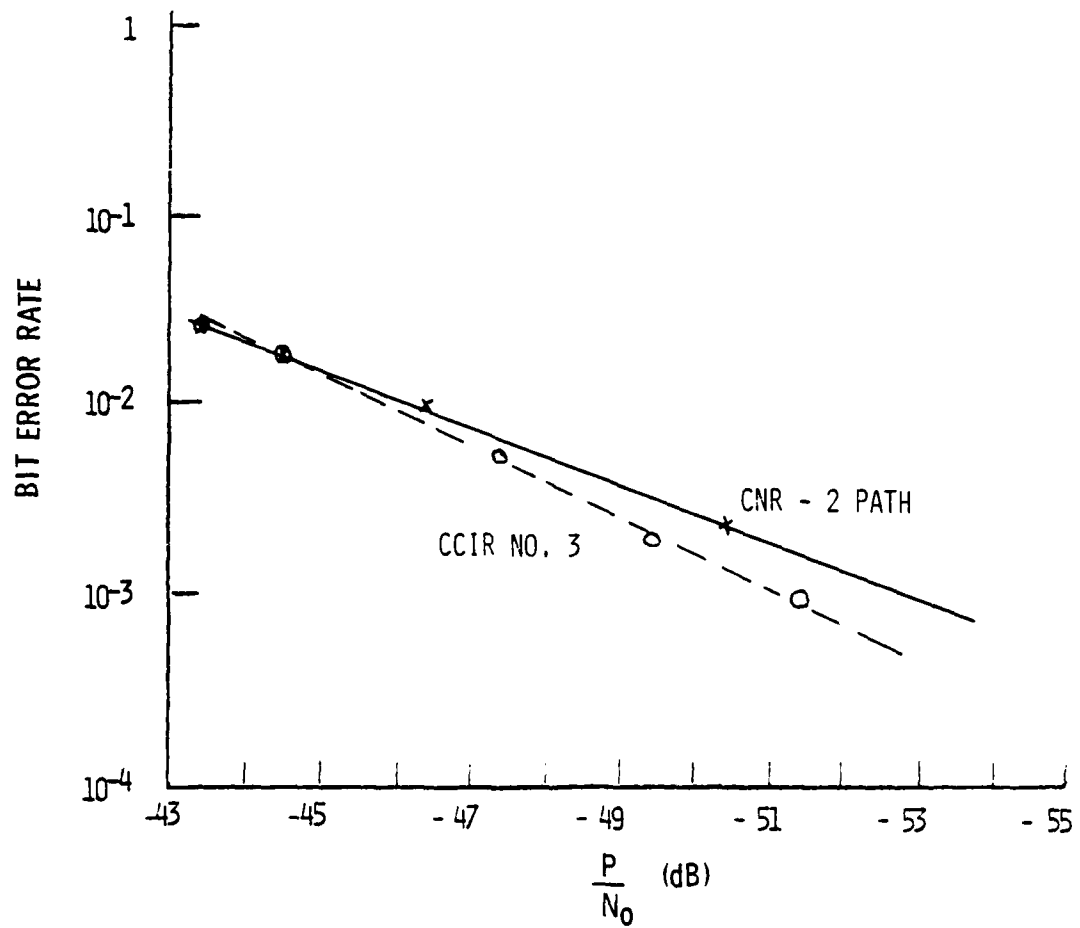


Fig. 60 — Comparison of performance on two 2-path channel models, coded data

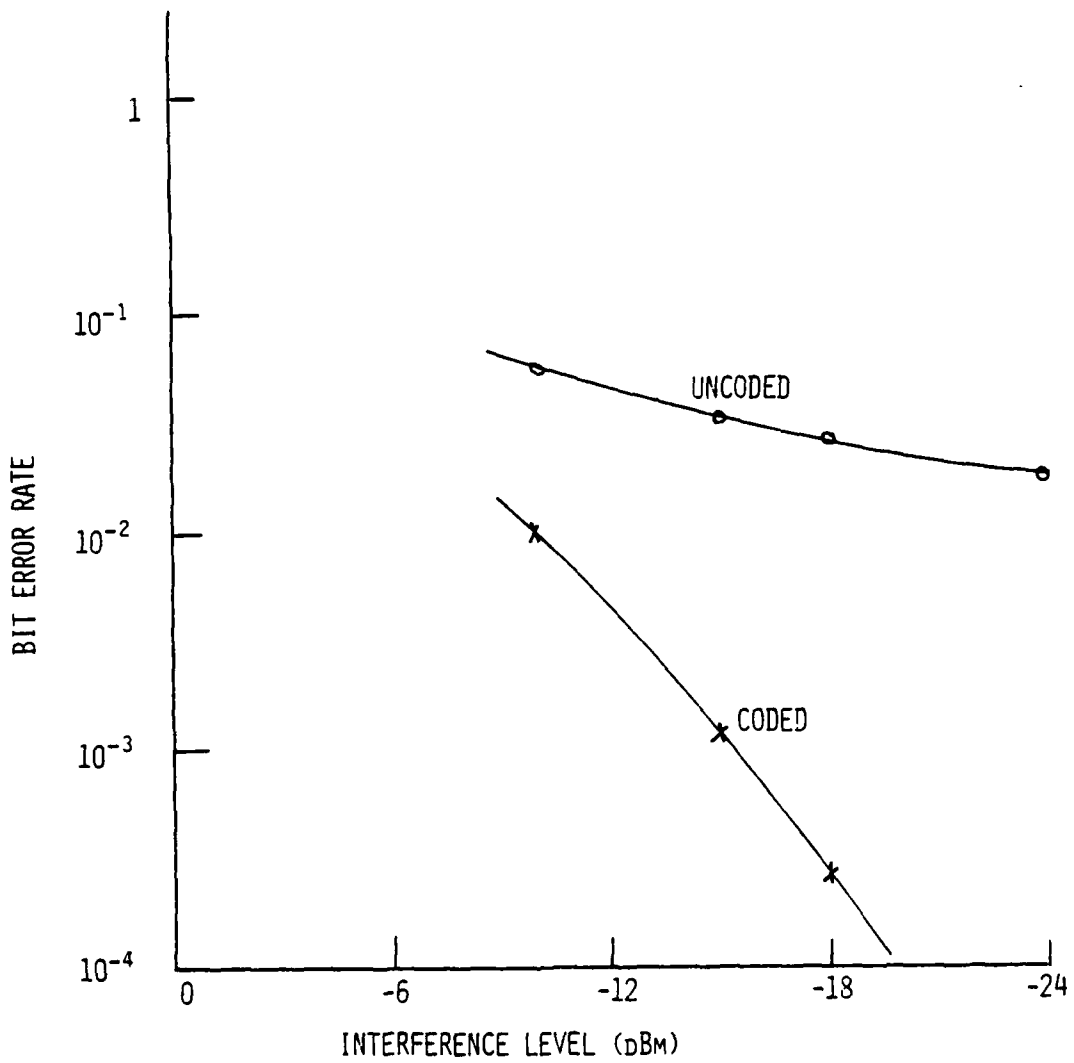


Fig. 61 — CCIR number 1, non-fading interference =  
WB FSK number 1,  $P/N_o = 49.4$  dB

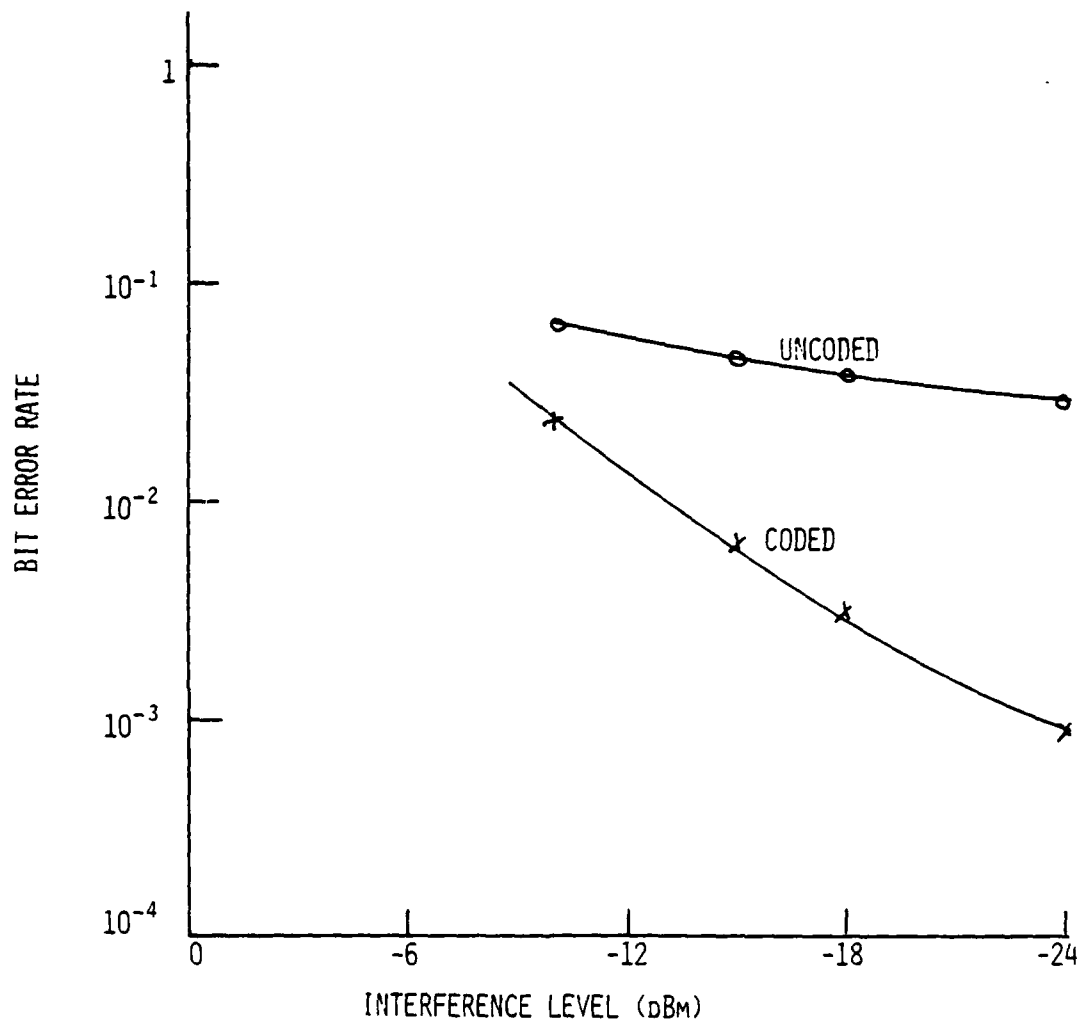


Fig. 62 — CCIR number 2, non-fading interference =  
WB FSK number 1,  $P/N_o = 49.4$  dB

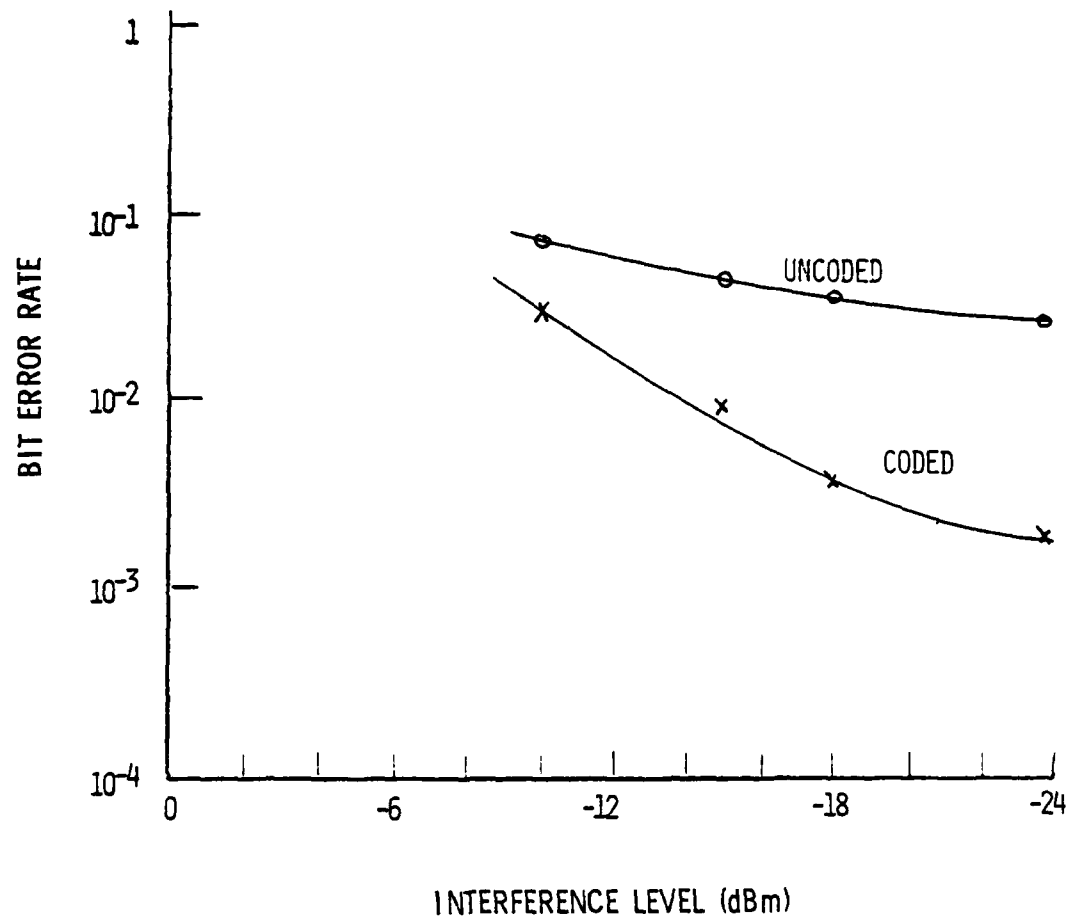


Fig. 63 — CCIR number 3, non-fading interference =  
WB FSK number 1,  $P/N_o = 49.4$  dB

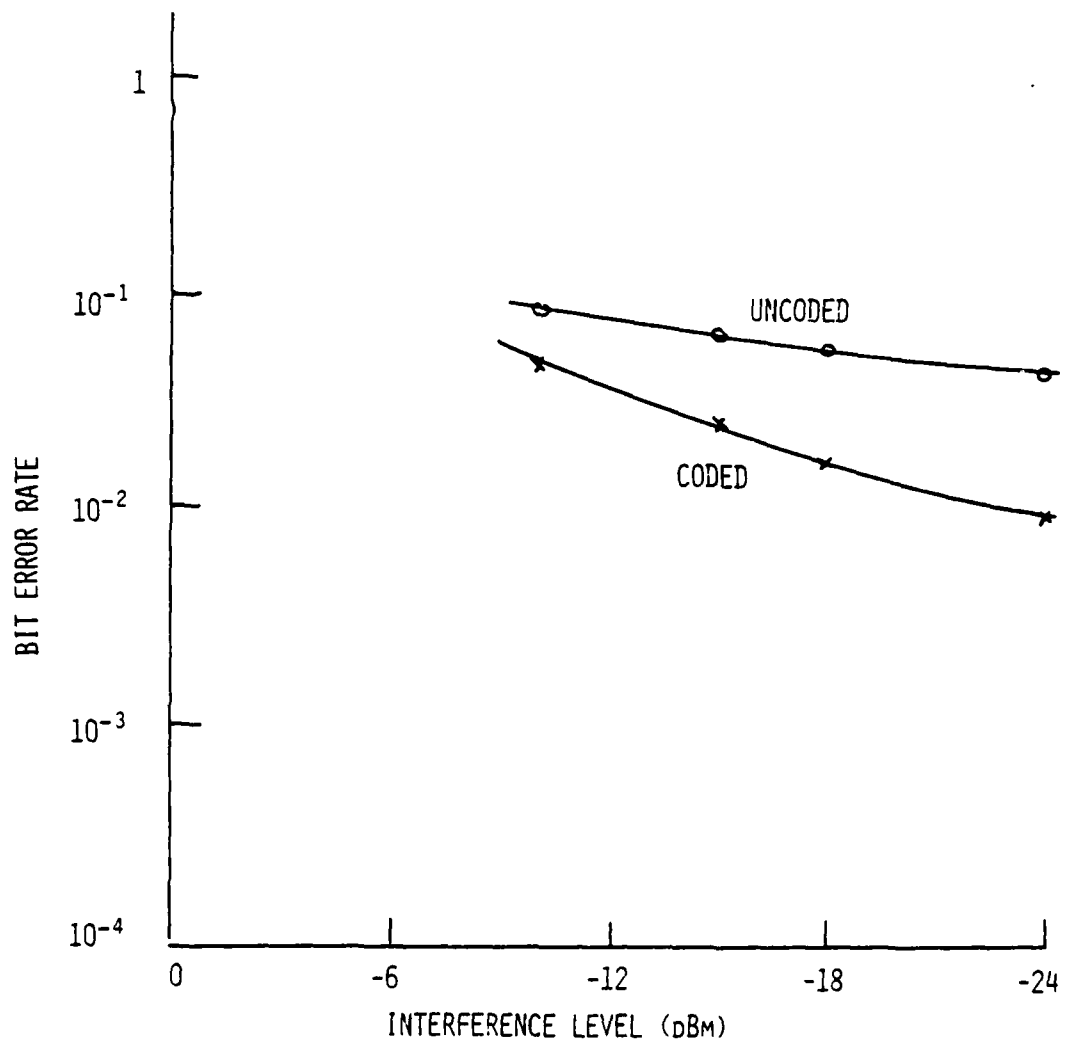


Fig. 64 — CCIR number 4, non-fading interference =  
WB FSK number 1,  $P/N_o = 49.4$  dB

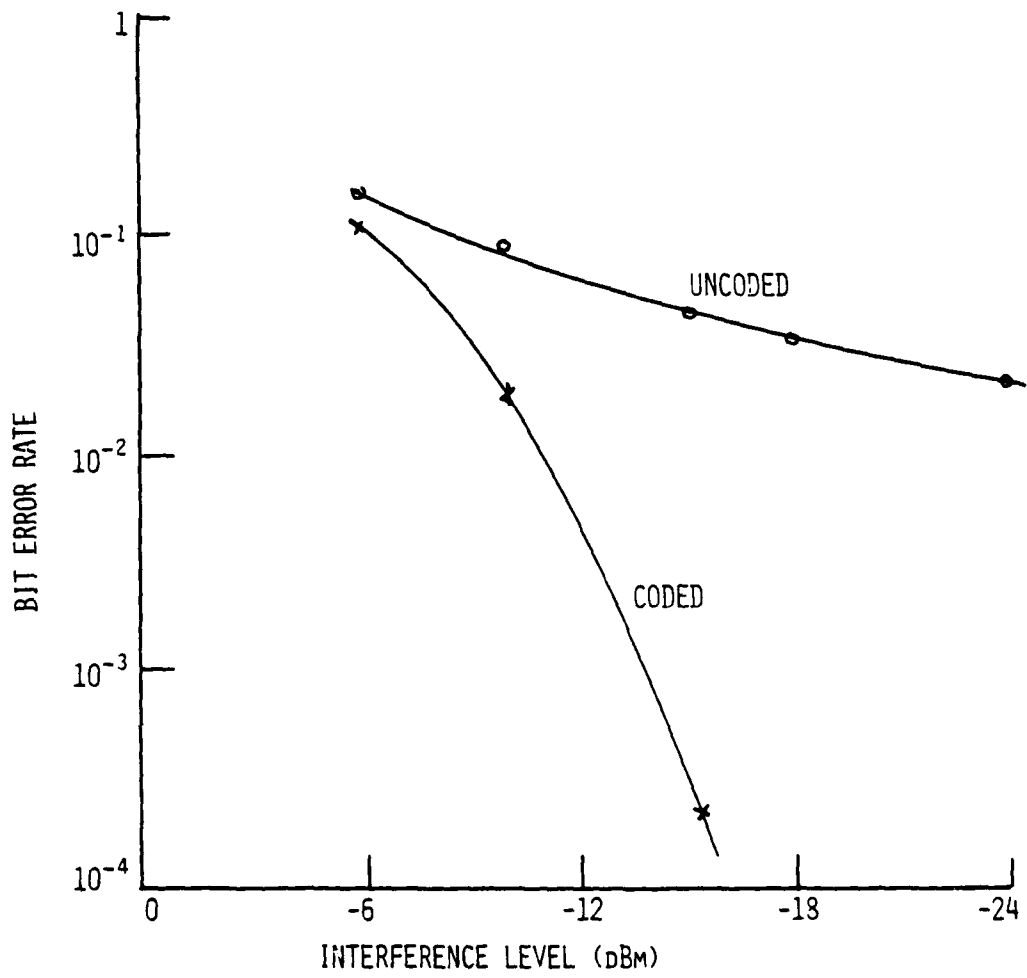


Fig. 65 — CCIR channel number 1, interference  
by DPSK,  $P/N_o = 49.4$  dB

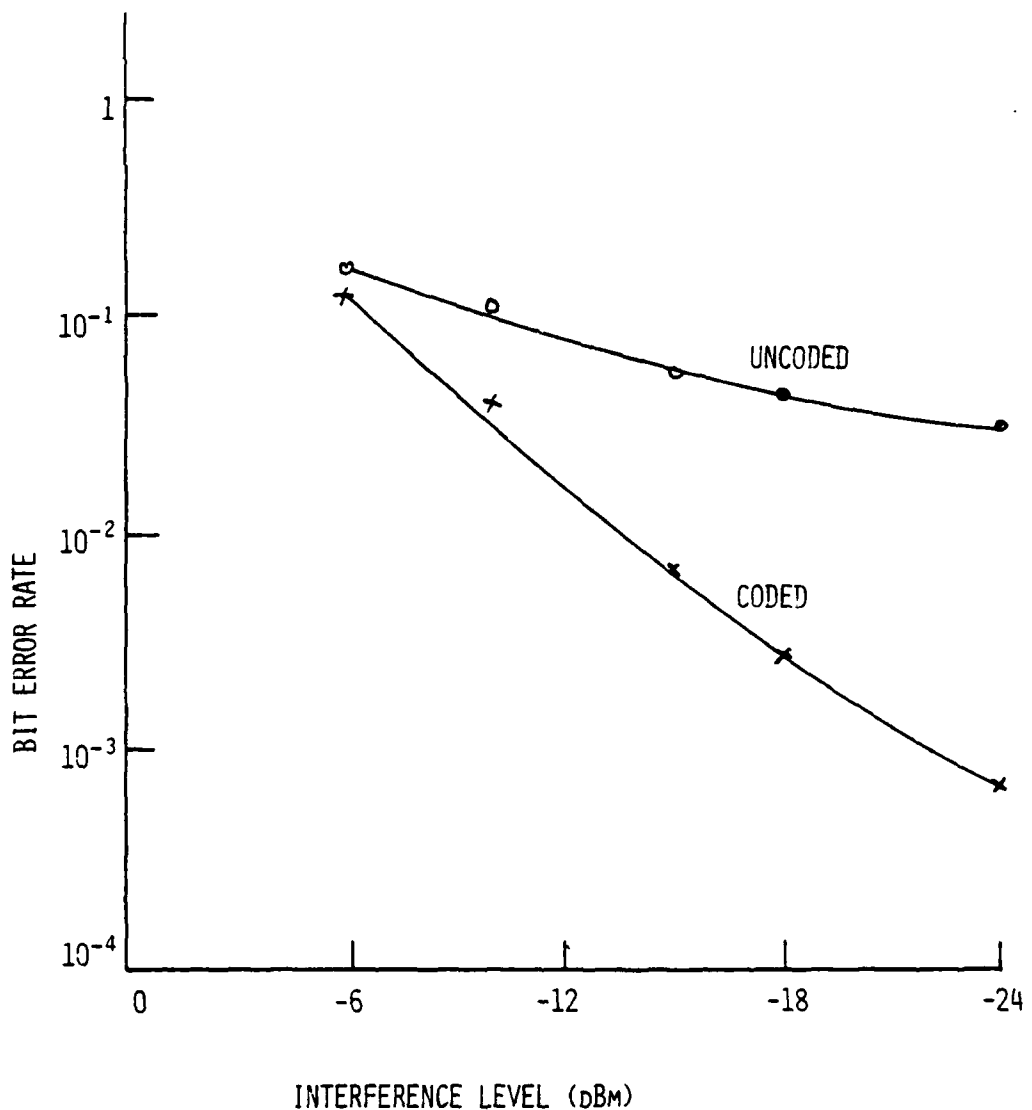


Fig. 66 — CCIR channel number 2, interference  
by DPSK,  $P/N_o = 49.4$  dB

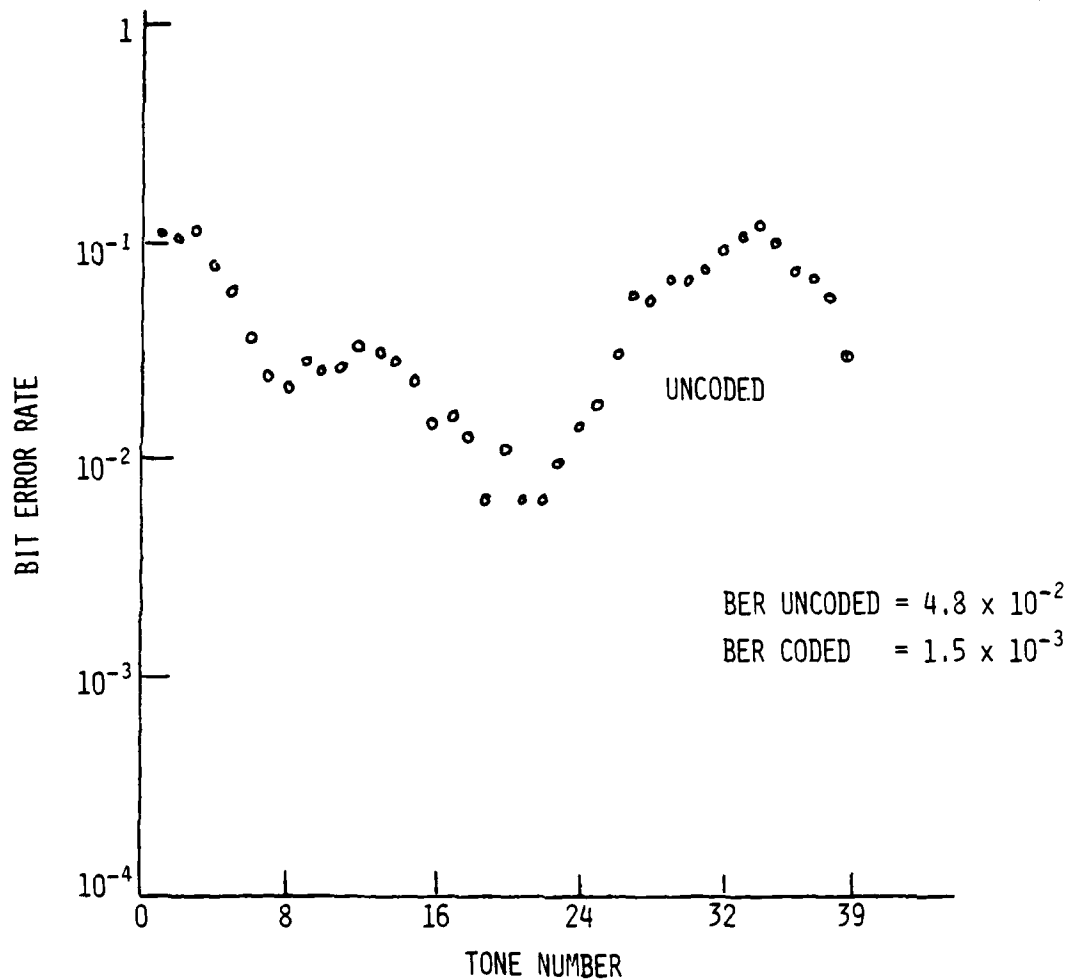


Fig. 67 — CCIR channel number 1, Fortran channel  
simulation,  $P/N_o = 45.4$  dB

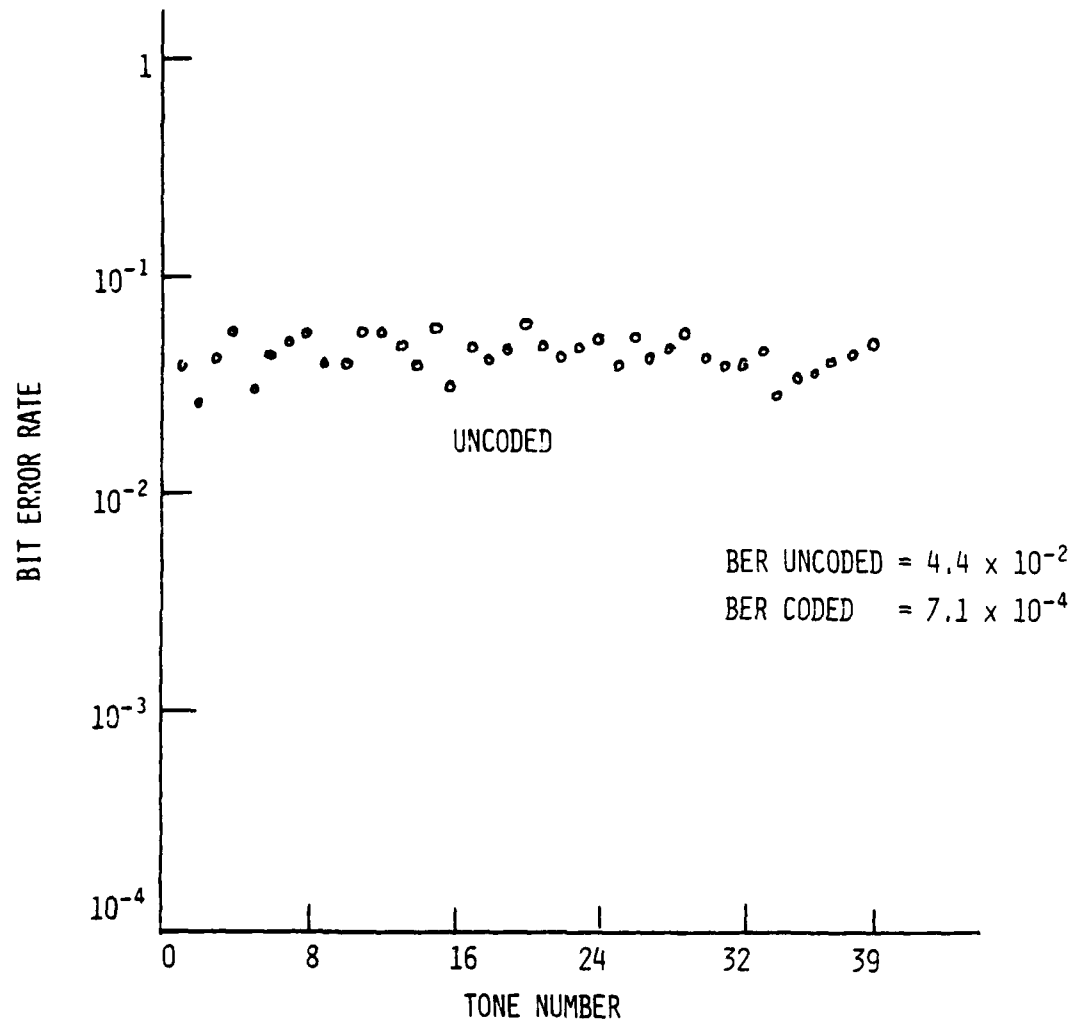


Fig. 68 — Modified CCIR channel number 1, 0.1 Hz mean frequency offset on one path, Fortran channel simulation,  $P/N_0 = 45.4$  dB

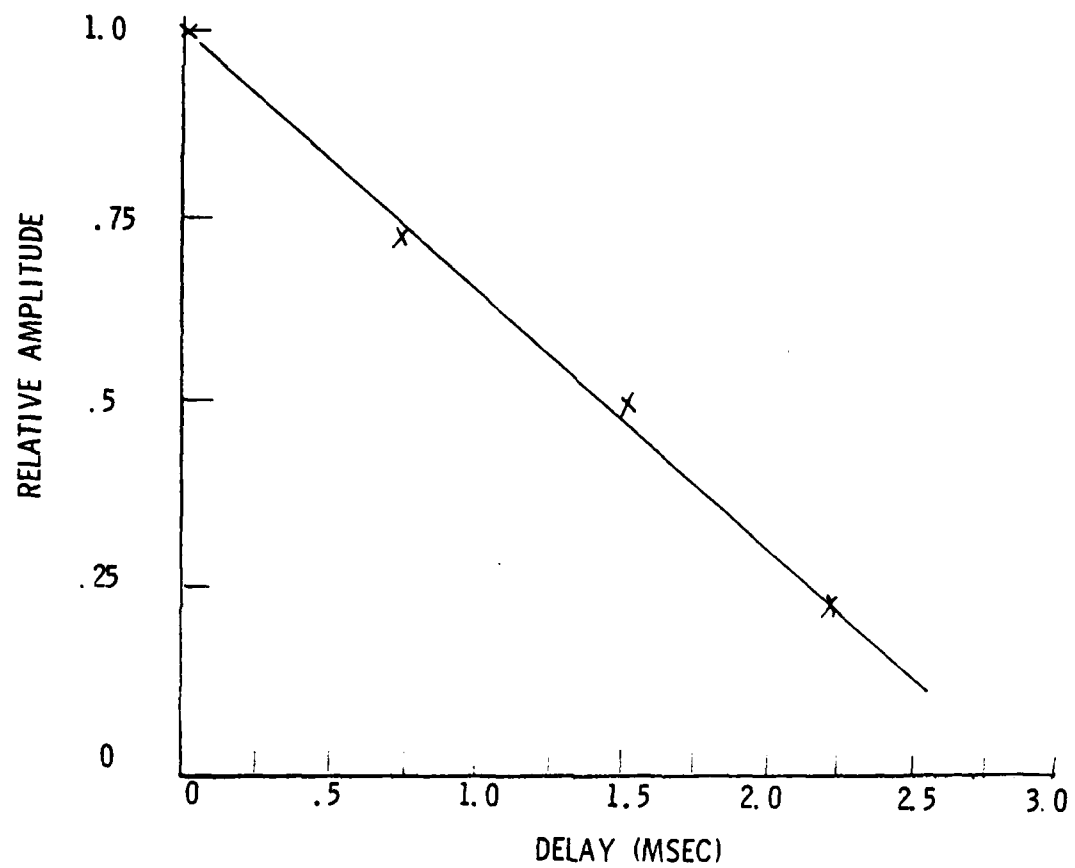


Fig. 69 — Consortium channel (relative amplitude vs delay)

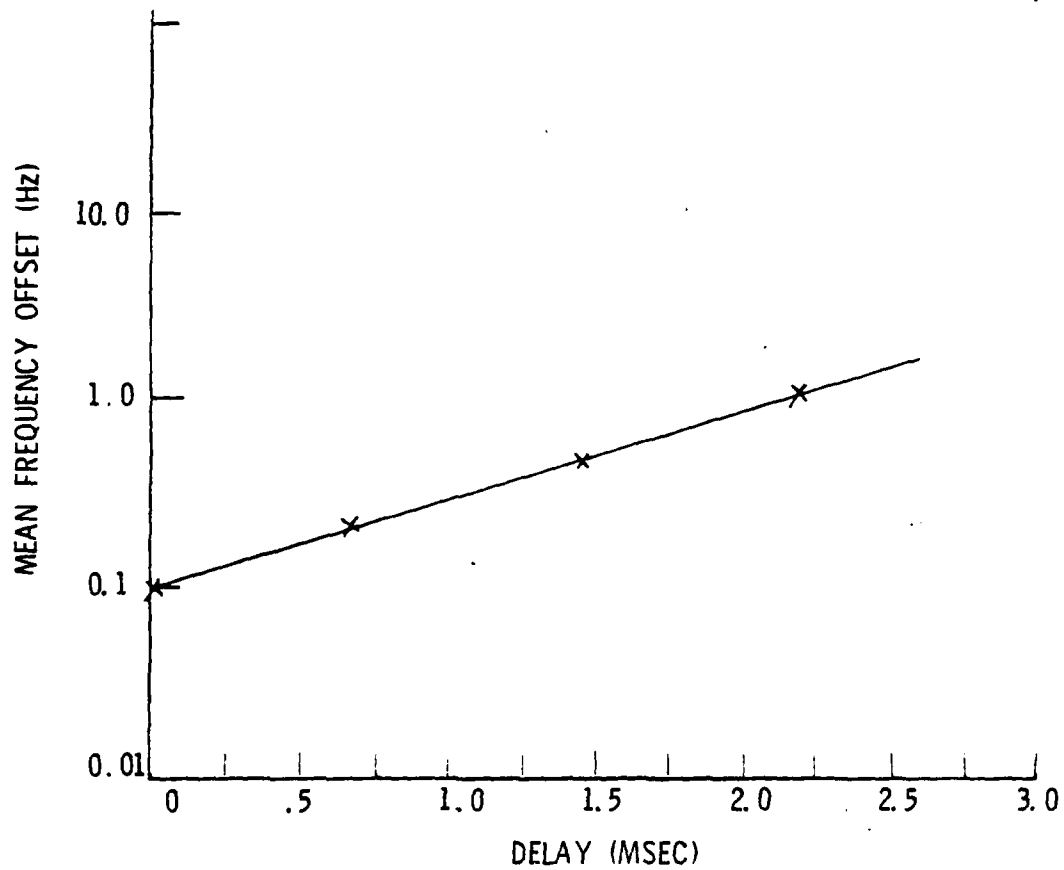


Fig. 70 — Consortium channel parameters (frequency offset vs delay)

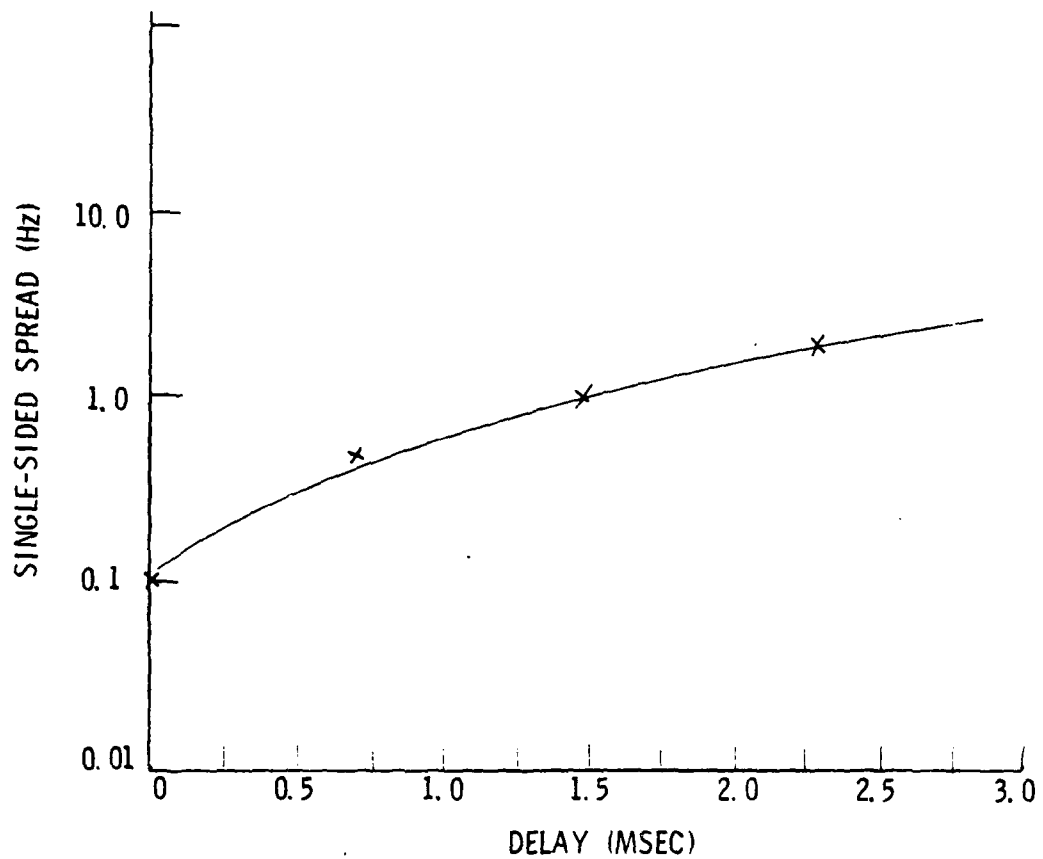


Fig. 71 — Consortium channel parameters (Doppler spread vs delay)

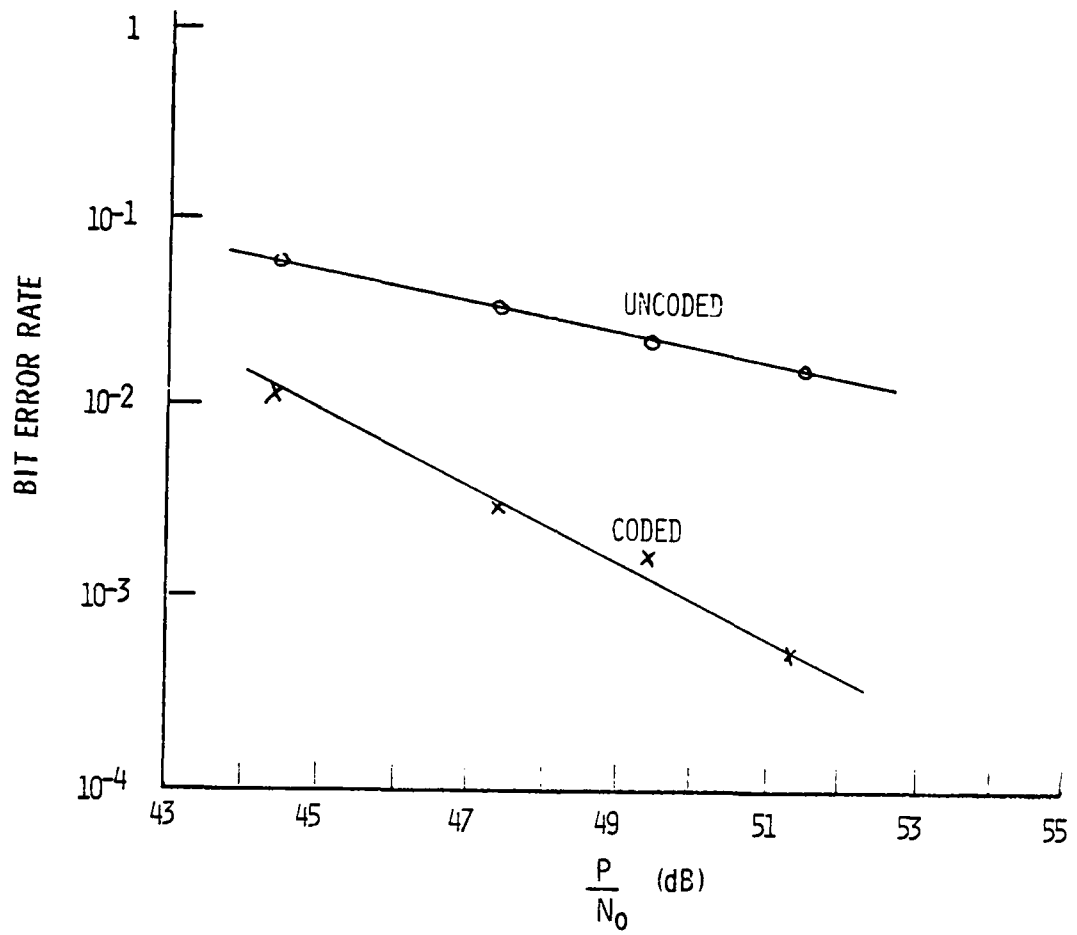


Fig. 72 — Bit error rate vs  $P/N_0$  for consortium channel

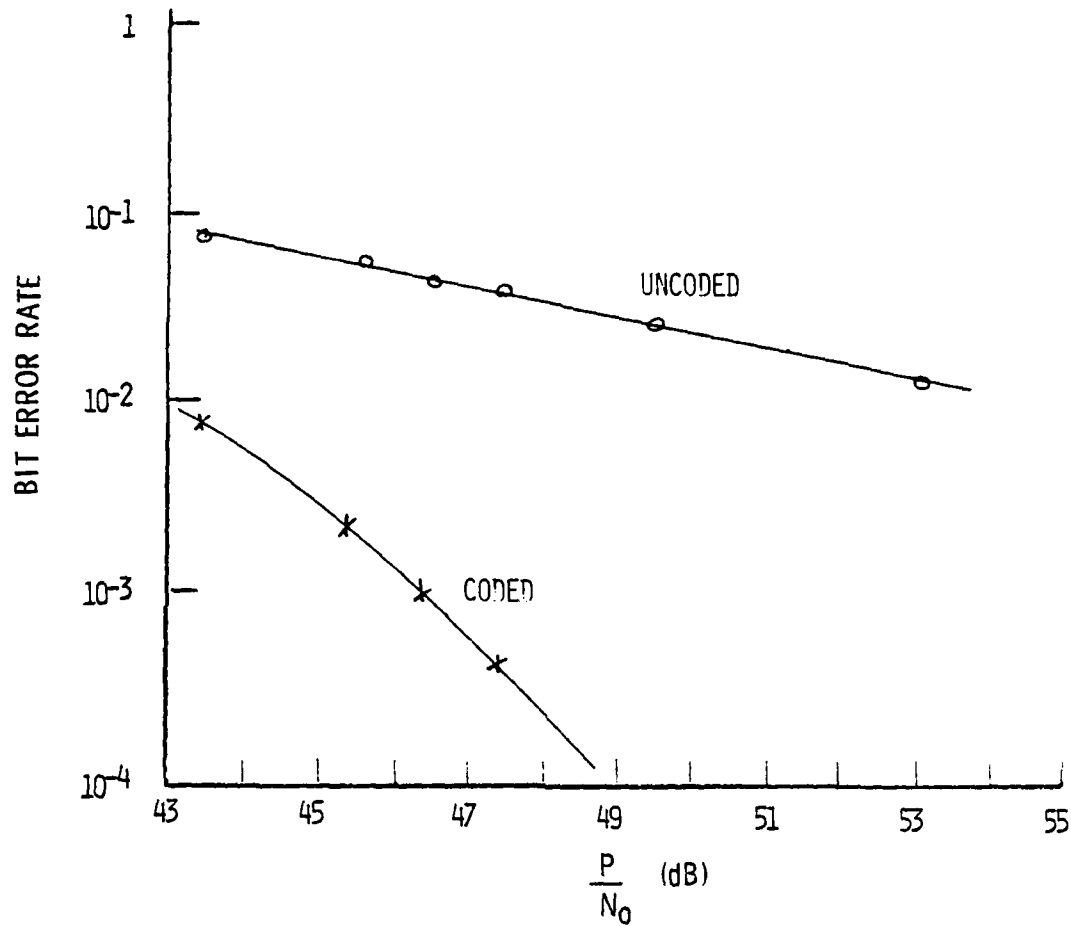


Fig. 73 — Bit error rate vs  $P/N_0$  for CNR 6-path model

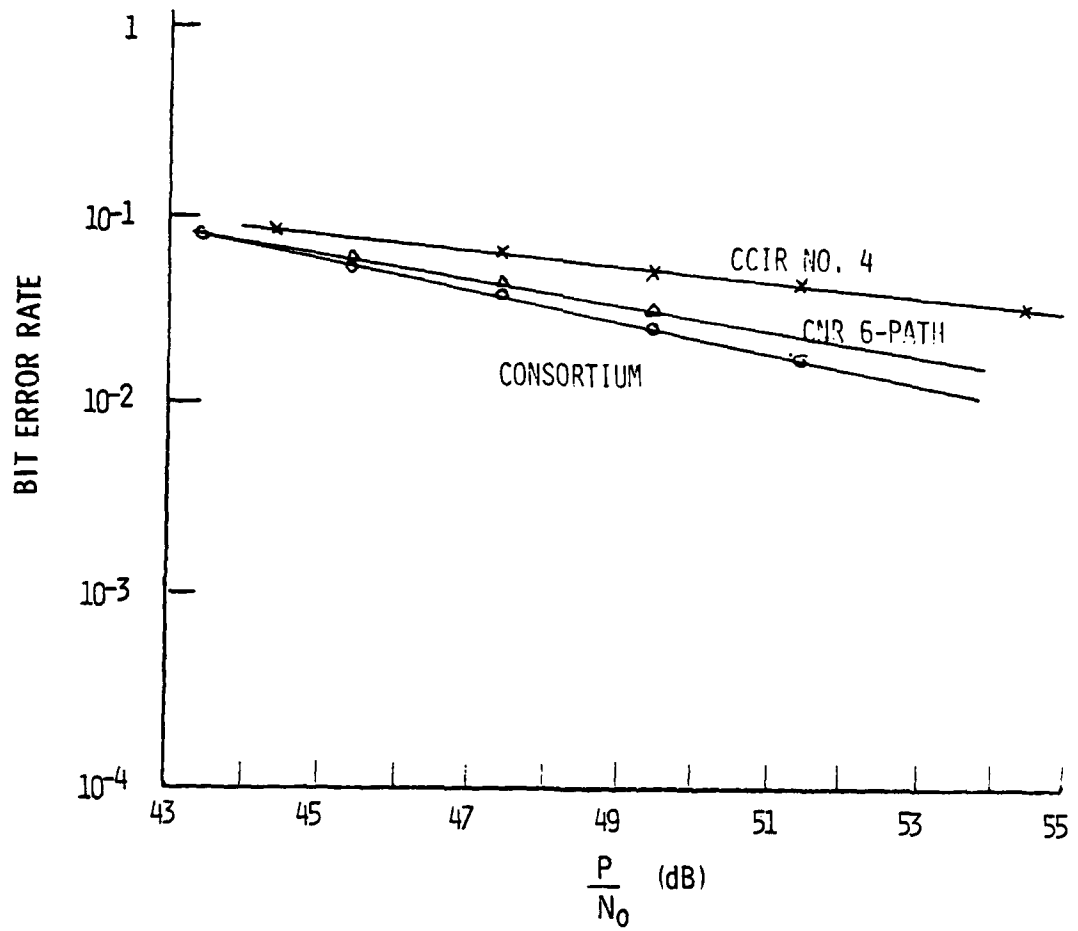


Fig. 74 — Comparison of performance on three channels, uncoded data

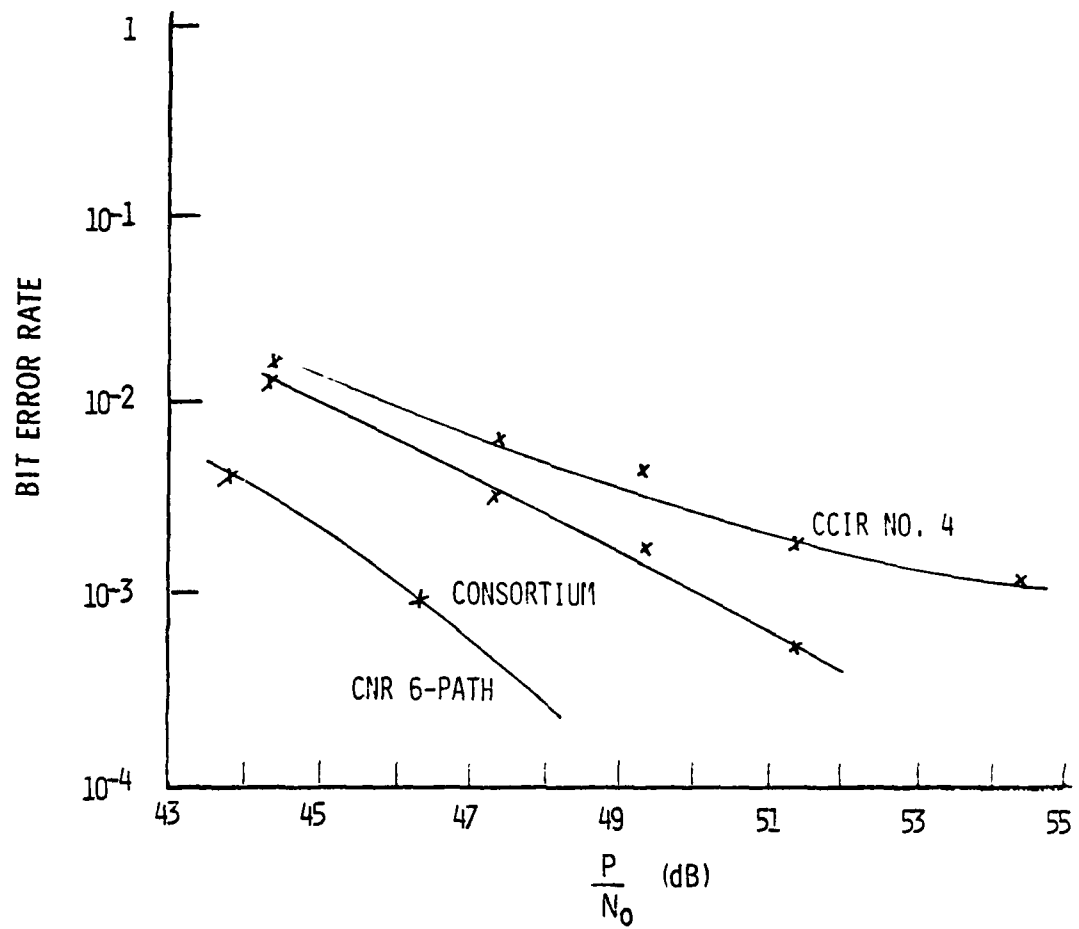


Fig. 75 — Comparison of performance on three channels, coded data

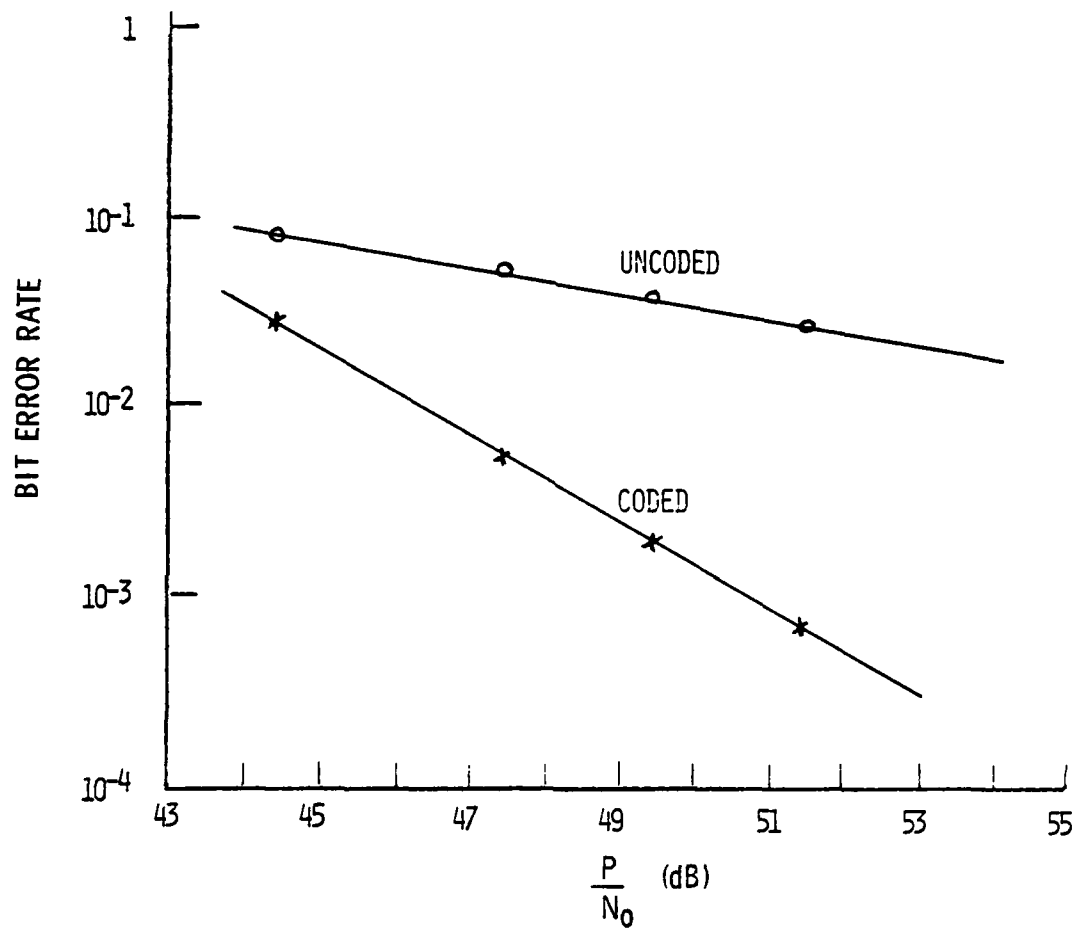


Fig. 76 — Bit error rate vs  $P/N_0$  for Rician channel

Table 1 — Amplitude Measurements on Output Signal  
Before Filtering vs. Clipping Level

CLIPPING LEVEL (dB)	MEASURE- MENT	SIGNAL LEVEL			
		DOPPLER TONES	SYNC TONES	MI 16 TONES	VOICE 39 TONES
0	RMS (dBm) PK/RMS (dB)	0 3.9	-0.1 4.1	-6.7 10.6	-9.1 13.0
8	RMS (dBm) PK/RMS (dB)			0 4.0	-1.7 5.7
9.5	RMS (dBm) PK/RMS (dB)				-0.6 4.6

Table 2 — Amplitude and Phase Response of Stress Filters

RELATIVE FREQ.	FILTER NO. 1		FILTER NO. 2	
	AMPL.	PHASE	AMPL.	PHASE
0.00	.000	0	.001	180.
0.05	.218	78.45	.002	-52.69
0.10	.422	67.07	.031	-92.26
0.15	.603	56.00	.131	-136.12
0.20	.750	45.43	.316	-178.33
0.25	.860	35.54	.547	142.12
0.30	.934	26.51	.759	106.02
0.35	.975	18.50	.904	73.97
0.40	.994	11.54	.974	46.14
0.45	.999	5.50	.996	21.99
0.50	1.000	0.00	.9995	0.00
0.55	.999	-5.50	.996	-21.99
0.60	.994	-11.54	.974	-46.14
0.65	.975	-18.50	.904	-73.97
0.70	.934	-26.51	.759	-106.02
0.75	.860	-35.54	.547	-142.12
0.80	.750	-45.43	.316	-178.33
0.85	.603	-56.00	.131	-136.12
0.90	.422	-67.07	.031	-92.26
0.95	.218	-78.45	.002	-52.69
1.00	.000	-79.65	.001	180.00

Table 3 — Example of Random Tone Selection  
for Spread of 1 Hz

NO.	FREQ. (Hz)	NO.	FREQ. (Hz)
1	-0.951	11	0.079
2	-0.878	12	0.169
3	-0.790	13	0.277
4	-0.638	14	0.381
5	-0.594	15	0.420
6	-0.404	16	0.599
7	-0.353	17	0.633
8	-0.261	18	0.763
9	-0.129	19	0.802
10	-0.048	20	0.994

Table 4 — Comparison of Fade Rate on Channel  
Simulation with CCIR Standards

DOPPLER SPREAD (Hz)	FADES/MINUTE	
	SIMULATION	CCIR
0.1	4.2	4
0.5	23.8	22
1.0	45.6	44
2.0	92.3	88

Table 5 — CCIR Channel Models  
Two Paths with Equal Amplitudes and Equal Doppler Spreads

MODEL NO.	DELAY (MSEC)	SPREAD (Hz)	NRL SINGLE-SIDED SPREAD
1	0.5	0.1	0.05
2	1.0	0.5	0.25
3	2.0	1.0	0.5
4	3.0	2.0	1.0

Table 6 — U.S. Consortium Channel Model

PATH NO.	DELAY (MSEC)	RELATIVE AMPL.	MEAN FREQ. OFFSET (Hz)	SINGLE-SIDED DOPPLER SPREAD (Hz)
1	0	1.0	0.1	0.1
2	0.7	0.7	0.2	0.5
3	1.5	0.5	0.5	1.0
4	2.2	0.25	1.0	2.0

Table 7 — Combined Skywave and Groundwave

PATH NO.	DELAY (MSEC)	RELATIVE AMPL.	MEAN FREQ. OFFSET (Hz)	SINGLE-SIDED DOPPLER SPREAD (Hz)
1	0	0.5	0	0
2	2.2	1.0	0	1.0

